THE UNIVERSITY OF HULL

Development of Zirconium-89 Chelators for Use in Positron Emission Tomography Imaging

being a Thesis submitted for the Degree of Doctor of Philosophy in the University of Hull

by

Boon-Uma Jowanaridhi

November 2017

Abstract

Positron emission tomography (PET) is used for non-invasive high sensitivity molecular imaging to diagnose diseases, to follow biological processes or to monitor treatment response. Immuno-PET is an imaging technique used to improve the visualisation of a target site by combining the high sensitivity of PET with the specificity of monoclonal antibodies (mAbs). Due to the relatively slow pharmacokinetics of antibodies, the half-life of the radioisotope and the stability of radioisotope attachment are key factors in the development of immuno-PET imaging agents. Zirconium-89 is an excellent candidate to be the immuno-PET radionuclide of choice as it decays with a half-life of 78.41 hours.

DFO (acyclic structure) is the most common chelator used to bind to [^{89}Zr]Zr(IV) for imaging applications. However, it has been reported that the [^{89}Zr]ZrDFO-mAb conjugate showed decomplexation and significant uptake of radioactivity in bones. The bone uptake of free [^{89}Zr]Zr(IV) results in increased radiation dose to the bone marrow and a decrease in target-to-background ratio. Therefore, the development of a more suitable chelator for [^{89}Zr]Zr(IV) is of high interest to biomedical researchers.

The tetraazamacrocycle cyclen was functionalised with three different pendant arms; phosphonic acid, phosphinic acid and picolinic acid, to offer at least eight binding sites for Zr(IV) to form complexes with the metal ion either "in cavity" or "out of cavity". A preliminary study of [^{89}Zr]Zr(IV) radiolabelling of compounds **1**, **5** and **9** was performed in acetate buffer at pH 7, with [^{89}Zr]zirconium(IV) oxalate incubated at 95^{o}C for 2 hours to obtain 5.0%, 6.1% and 8.4% labelling yields respectively. Labelling with [^{89}Zr]zirconium(IV) chloride was performed either in water or acetate buffer to form [^{89}Zr]Zr**9** in a 49.3% labelling yield when using 0.5 MBq of [^{89}Zr]Zr(IV) in 0.2 M acetate buffer at pH 6 incubated at 95^{o}C for 2 hours but achieving this yield required a higher concentration of the chelator. Extended picolinic acid arm chelators were synthesised with both cyclen and cyclam backbones. Compounds **16** and **20** were synthesised and labelled with [^{89}Zr]zirconium(IV) chloride. Unexpectedly [^{89}Zr]Zr**9** gives higher radiolabelling yields than [^{89}Zr]Zr**16** and [^{89}Zr]Zr**20**. It was possible that **16** and **20** formed lower stability complexes with Zr(IV) with a higher chelator to metal ratio than the anticipated 1:1 ratio, and so the chelators are not octadentate.

Novel macrocycle-linked DFO chelators were designed as the linear chelator DFO rapidly forms a complex with Zr(IV) at ambient temperature and then the metal could transfer to the

cyclic ring giving a higher stability thermodynamic product (the “in-cavity” complex). Compounds **21**, **22** and **23** were synthesized and labelled with [^{89}Zr]Zr(IV). The labelled compounds were stable in 100-fold excess EDTA and fetal bovine serum but did not show any clear improvement over DFO.

Risk Assessment

All experiments were carried out in accordance with the University of Hull's Health and Safety guidelines. A full COSHH and risk assessment was carried out for each new experiment, signed by the undertaking student, supervisor (Prof. S. J. Archibald) and the departmental safety officer (Dr T. McCreedy) before any practical work started. The COSHH forms carry the reference numbers BUJSJA1 to BUJSJA12.

Radiochemistry experiments were assessed using the PET Research Facility Risk Assessment Form**,** signed by the undertaking student, supervisor (Prof. S. J. Archibald) and the radiation protection supervisor (Dr C. Cawthorne) before radiochemical experiments were carried out, with the forms carrying the reference numbers BJ-Zr-01 to BJ-Zr-02.

Acknowledgement

First of all I would like to thank Thailand Institute of Nuclear Technology and the Royal Thai Government for providing me the scholarship without which this great opportunity would not have been possible. I would also like to thank my supervisor Prof. Steve J Archibald for his scientific ideas, supervision and encouragement given to me over the last four years. This work would not have been completed without all his support and valuable advice.

I would like to express my thanks to Dr Johanna Seemann, Dr Benjamin P Burke, Dr Juozas Domarkas and Dr Ping He who have discussed my work with me, made suggestions and helped me throughout my study. Thanks also goes to the technical staff in the chemistry department for helping me to obtain analytical data.

All members of the Archibald group also deserve thanks for their academic support and friendship, but special thanks go to Rhiannon Lee, Zainab Al-Ali, Hayley Bignell and Tahani Alresheedi for their care, patiently listening to me, laughing with me and cheering me up.

A massive thanks goes to Dr Bongkot Ngamsom, who has always offered kind words of advice.

I am very grateful to Howard Jopp for being there, being so understanding when thesis writing took priority, and taking my mind off stressful situations. I would also like to say thanks for everything you have done for me.

Finally I would like to thank my family, especially my wonderful dad, mum and grandma, for their unconditional love and keeping me motivated when things were tough.

Abbreviations

β^+	Positron
µg	Microgram
µL	Microlitre
µM	Micromolar
µmol	Micromole
δ	Chemical shift
BFC	Bifunctional chelator
br	Broad signal
CT	Computed tomography
d	Doublet
DCM	Dichloromethane
DMF	N,N'-Dimethylformamide
DMSO	Dimethyl sulfoxide
DOTA	1,4,7,10-Tetraazacyclododecane-1,4,7,10-tetraacetic acid
DOTP	1,4,7,10-Tetraazacyclododecane-1,4,7,10-tetra(methylenephosphonic acid)
DOTPI	1,4,7,10-Tetraazacyclododecane-1,4,7,10-tetrakis[methyl(2-carboxyethyl) phosphinic acid]
DTPA	Diethylene triamine pentaacetic acid
EC	Electron capture
EDTA	Ethylenediaminetetraacetic acid
ESI	Electrospray ionisation
FDA	Food and drug administration
g	Gram
HPLC	High performance liquid chromatography
HRMS	High resolution mass spectrometry
keV	Kilo electron volt
KI	Potassium iodide
M	Molar
mAb	Monoclonal antibody
mg	Milligram
mM	Millimolar
mmol	Millimole

MS	Mass spectrometry
NMR	Nuclear magnetic resonance
NHS	N-hydroxy succinimide
PBS	Phosphate buffer solution
PET	Positron emission tomography
RCY	Radiochemical yield
rt	Room temperature
s	Singlet
SPECT	Single photon emission computed tomography
$t_{1/2}$	Half-life
TEA	Triethylamine
TFA	Trifluoroacetic acid
THF	Tetrahydrofuran
TLC	Thin layer chromatography

List of Figures

List of Schemes

List of Tables

Table of Contents

Chapter 1

Introduction

1. Introduction

1.1. Medical imaging

Medical imaging encompasses a number of non-invasive modalities that can be used for clinical diagnosis and disease monitoring. It includes nuclear medicine techniques such as single photon emission computed tomography (SPECT) and positron emission tomography (PET), and other radiological methods such as x-ray and computed tomography (CT), as well as non-ionising radiation techniques such as magnetic resonance imaging (MRI) and ultrasound.

Nuclear medicine is a discipline that uses radiopharmaceuticals to diagnose and treat disease. Radiopharmaceuticals are administered orally or via intravenous injection. Subsequently the radiation emitted is detected by an external detector. For x-ray and ultrasound techniques, the radiation is applied externally and passes through the body to create images by attenuation. Advantages and disadvantages of various medical imaging techniques are shown in Figure 1.[1, 2] The wide range of applications in nuclear medicine covers oncology, cardiology, orthopedics, rheumatology and neurology.

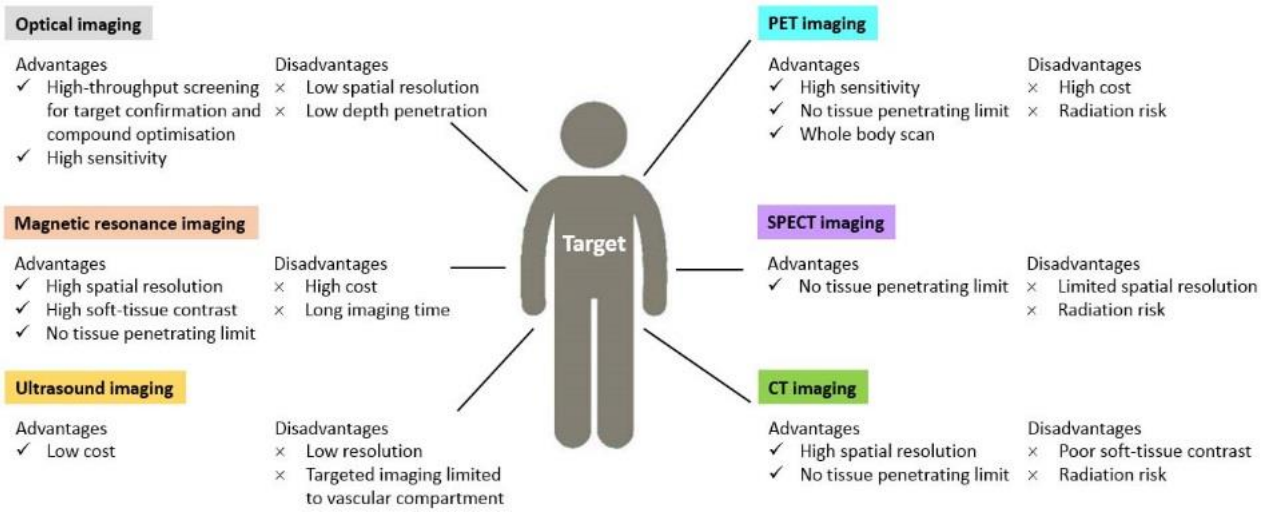

Figure 1 - A summary of advantages and disadvantages of medical imaging modalities.

1.1.1. Computed tomography (CT)

Computed tomography is a digitally supported radiology technique, which was developed to overcome the limitation of visualisation from conventional x-ray imaging.[3] It measures the attenuation of x-rays passing through the patient at different angles and reconstructs cross-sectional images of the body from these x-ray images, see Figure 2. This

technique provides anatomical images of parts of the body, the contrast of which is much better than that of traditional x-ray photography.

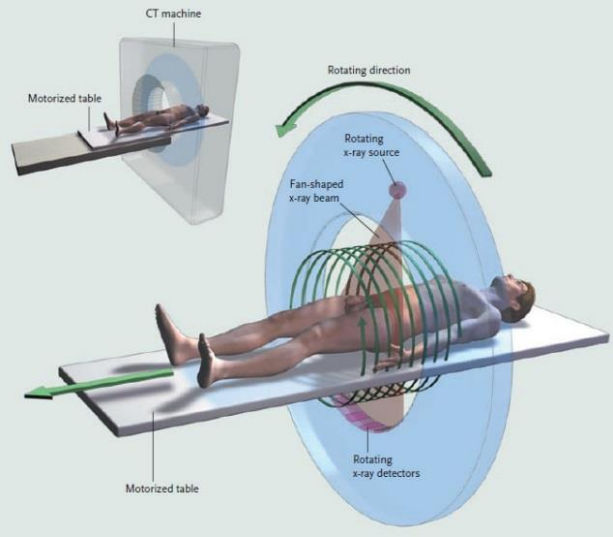

Figure 2 - The basic principles of CT scanning reproduced from W Brenner, D. J. *et al.*, New England Journal of Medicine, 2007.[4]

1.1.2. Magnetic resonance imaging (MRI)

Magnetic resonance imaging is widely used clinically to image tissues and provide anatomical information. It takes advantage of the magnetic properties of hydrogen atoms in the body when a magnetic field is applied. Therefore, MRI can be used in anatomical imaging (for organs such as breast, heart, lungs, kidney, liver, colon, gall bladder), for cardiovascular imaging, musculoskeletal imaging of both spine, joint and soft tissues, oncology for diagnosis and follow up on therapy, as well as functional imaging such as measurement of blood flow in vessels.[5]

1.1.3. Single photon emission computed tomography (SPECT)

Single photon emission computed tomography is an imaging technique that relies on detected gamma rays from gamma emitting radioisotopes. It was developed from planar imaging (2D) by using multiple angles of a gamma camera to reconstruct a 3D view. Moreover, combining the functional imaging from SPECT and the anatomic imaging from CT has shown benefit in clinical situations.[6]

SPECT/CT is used in many routine clinical applications. For example, in cardiology, ^{201}Th and ^{99m}Tc labelled sestamibi are used to evaluate myocardial blood flow.[7, 8] In oncology,

^{111}In-capromab pendetide is used to identify sites of metastatic disease from prostate cancer.[9] In addition, ^{188}Re-HEDP is used for treatment of painful bone metastases.[10]

A variety of radionuclides can be used in SPECT. The most commonly used is ^{99m}Tc. ^{99m}Tc has ideal characteristics as it releases 142 keV gamma rays with a half-life of 6.02 hours. Its half-life is long enough for radiolabelling procedures to be carried out and the gamma energy is suitable for use in nuclear medicine.[11] Moreover, ^{99m}Tc is produced by a ^{99}Mo/^{99m}Tc generator and compounds used for ^{99m}Tc-radiopharmaceuticals are usually in a form of lyophilised kit, which is easy for formulation of ^{99m}Tc compounds in hospital radiopharmacies.[12] There are many radiopharmaceuticals used with ^{99m}Tc; for example, DTPA and MAG3 are used to determine kidney function, MDP is used for bone scans, MAA is used for lung perfusion imaging, and ECD is used for brain imaging. ^{111}In is also widely used in SPECT. As it has a half-life of 2.8 days, ^{111}In is useful for labelled antibody SPECT imaging.[13]

1.1.4. Positron emission tomography (PET)

Positron emission tomography is a non-invasive imaging technique that detects a pair of annihilation photons produced by a positron encountering an electron. PET is similar to SPECT in terms of using radioactive tracers and detecting emitted radiation. However, radioactive materials used in PET emit positrons which travel a distance of a few millimetres before annihilation, which depends on photon energy and density of the surroundings.[14] Annihilation with electrons generates two photons with an energy of 511 keV at *ca.* 180 degree to each other, see Figure 3.[15] The detector will detect these photons coincidently allowing electronic collimation, whereas SPECT requires a physical collimator that will reduce sensitivity.

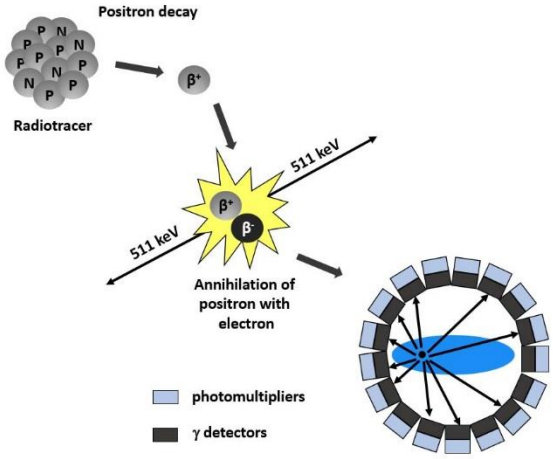

Figure 3 - Physical principles underlying PET imaging.

The sensitivity of PET is relatively high, with only 10^{-11} - 10^{-12} mol/L of radiotracer required for detection.[16] The required use of a collimator in SPECT causes the lower detection efficiency.

Multimodal imaging using PET has been designed and established in clinical applications.[17] The combination of PET and CT is used to acquire both accurate structure and function in a single scan, see Figure 4.

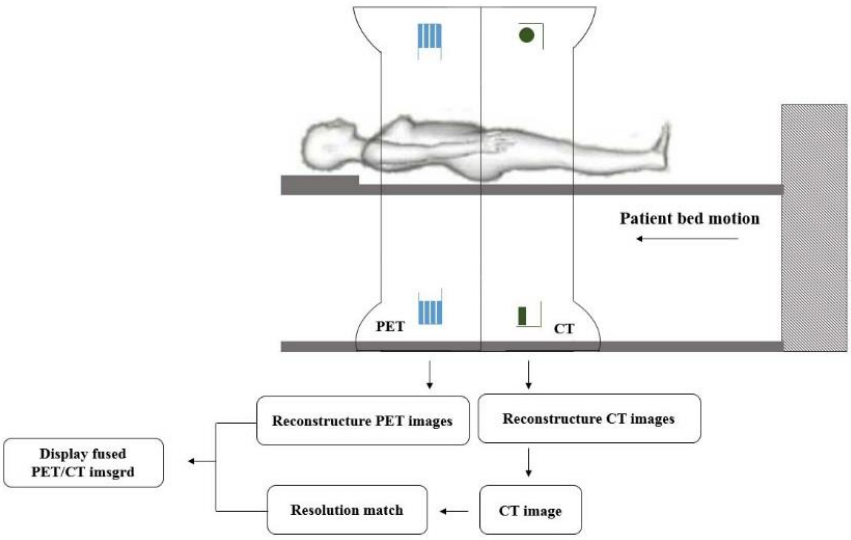

Figure 4 - Schematic of PET-CT scanner and imaging process.

To reduce the radiation dose to patients, improve the low contrast of soft tissues in CT and offer an alternative to the lower spatial resolution of PET (between 1.5 and 2 mm in clinical scanners), the combination of PET with MRI has been created.[18,19] For example, a hybrid PET/MRI scan can be performed to detect and localise brown adipose tissue (BAT), which is a kind of soft tissue that is a promising therapeutic target against obesity.[20]

The common radioisotopes used in PET are shown in Table 1. In general, radionuclides used in PET have a short half-life and are produced by cyclotron (such as ^{18}F); therefore, a cyclotron needs to be located close to the PET scanner site.[21] ^{18}F is produced by accelerated proton bombardment of ^{18}O enriched water. It decays with a half-life of 110 minutes by positron emission (97%) and electron capture (3%). ^{18}F-labelled fluorodeoxyglucose (FDG), which is a glucose analogue, is widely used in many applications in cardiology, neurology, and oncology.[22] Moreover ^{18}F-labelled plasma membrane biogenic monoamine transporters; dopamine transporter (DAT), serotonin transporter (SERT), and norepinephrine transporter

(NET), are used to diagnose psychiatric disorders, such as depression, Parkinson's disease (PD), and attention deficit hyperactivity disorder (ADHD).[23]

The radioisotopes produced using a generator, such as ^{68}Ga, overcome the limitation of the infrastructure needed for cyclotron-produced radioisotopes. It is produced and separated from the parent isotope, ^{68}Ge, via a ^{68}Ge/^{68}Ga generator. The half-life of ^{68}Ge is 271 days which allows storage and use of one generator for about a year.[24] The advantages of the generator system has made ^{68}Ga a popular radionuclide used in neuroendocrine tumour imaging with ^{68}Ga-NOTATOC, ^{68}Ga-DOTATATE and ^{68}Ga-DOTATOC.[25]

Table 1 - Properties of some common isotopes used in PET.[26-28]

Radionuclide	Production method	Half-life	Decay characteristics
^{11}C	Cyclotron, ^{14}N(p,α)^{11}C	20.3 min	β^+ (100%)
^{13}N	Cyclotron, ^{16}O(p,α)^{13}N	9.97 min	β^+ (100%)
^{15}O	Cyclotron, ^{14}N(d,n)^{15}O	2.04 min	β^+ (100%)
^{18}F	Cyclotron, ^{18}O(p,n)^{18}F	110 min	β^+ (97%)
			EC (3%)
^{44}Sc	^{44}Ti/^{44}Sc generator	3.9 h	β^+ (94%)
			EC (6%)
^{64}Cu	Cyclotron, ^{64}Ni(p,n)^{64}Cu	12.7 h	β^+ (19%)
			β^- (40%)
			EC (41%)
^{68}Ga	^{68}Ge/^{68}Ga generator	68 min	β^+ (90%)
			EC (10%)
^{86}Y	Cyclotron, ^{86}Sr(p,n)^{86}Y	14.7 h	β^+ (33%)
			EC (66%)
^{89}Zr	Cyclotron, ^{89}Y(p,n)^{89}Zr or	78.4 h	β^+ (23%)
	Cyclotron, ^{89}Y(d,2n)^{89}Zr		EC (77%)
^{124}I	Cyclotron, ^{124}Te(p,n)^{124}I	4.18 d	β^+ (23%)
			EC (85%)

The selection of the PET radioisotope considers its physical and chemical properties. The decay half-life, for instance, must be long enough for chemical preparation process; synthesis, purification and analysis, and for biological process to allow the accumulation at

target organs as well as the clearance from blood pool of the radiopharmaceutical.[29] Another factor that should be examined is β^+ emission energy, which determines the distance that positrons travel before they annihilate,and influences the resolution of the PET scan.[30]

As the short half lived PET isotopes are limited to development of radiopharmaceuticals for rapid biological processes,[31] the long half-life isotopes have been attracting attention especially in the field of immuno-PET imaging. Antibody-based imaging needs radioisotopes that have an isotope half-life that matches the pharmacokinetic half-life of immunoglobulin.[32] In a group of long half-life PET isotopes, ^{124}I and ^{89}Zr are of the greatest interest. However, dehalogenation of ^{124}I functionalised molecules has been found *in vivo* resulting in accumulation of radioactivity in the thyroid and stomach.[33-36] Therefore, zirconium-89 has become a lead candidate for immuno-PET imaging.

1.1.4.1. Immuno-PET

Immuno-PET describes a discipline in which a relatively long-lived PET radionuclide is used to label monoclonal antibodies (mAbs). mAbs have been considered as suitable candidates for diagnosing and staging cancer, monitoring of targeted therapy, as well as dose planning for radioimmunotherapy.[37] There is the potential to obtain valuable target-specific information.[38] mAbs have high antigen specificity which gives the ability to bind selectively at the target site. Moreover, target-to-background activity ratios are improved as images are collected after multiple days of accumulation of radioactive compound in the target organ and the clearance of tracer that is not bound to the target from the blood pool.[39] A schematic of the conjugation of bifunctional chelating agents to monoclonal antibodies is shown in Figure 5.

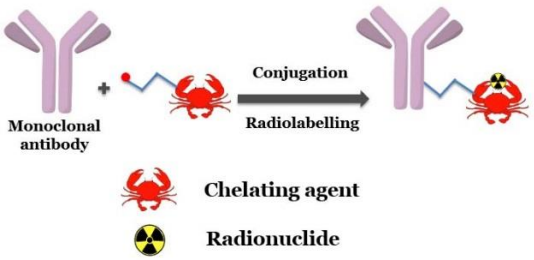

Figure 5 - Principles of conjugation of BFCs to mAbs.

There are many factors which need to be considered when designing an immuno-PET agent.[40]

1. Biological targeting molecule: Size of biomolecule influences the clearance rate; for instance, small antibody fragments can be removed from blood pool faster than large biomolecules.
2. Radionuclide: The physical half-life of radionuclides has to be compatible with the pharmacokinetic half-life of the mAb.
3. Other factors, such as stability of the radiopharmaceuticals. mAbs have slow pharmacokinetics and require several days to reach targeted organs; therefore, it is important that radiopharmaceutical is stable *in vivo* in order not to release the radiometal which may cause an increased background signal and radiation of non-targeted tissue.

Early development of immuno-imaging focused on SPECT and the development of theranostic isotope pairs.[41] For example, the ^{111}In-labelled anticarcinoembryonic antigen monoclonal antibody ZCE-025 was tested in patients with a history of adenocarcinoma,[42] and ^{99m}Tc labelled anti-DR5 antibody was used in breast tumour xenografts in nude mice.[44] Furthermore, antibody fragments have been of interest for theranostic approaches in oncology.[45] Theranostics involves the sequential use of two different radioisotopes, the antibody is initially labelled with an isotope for imaging (e.g. gamma emitting isotope for SPECT) which will be used to confirm localisation of the mAb at the disease site and then a treatment will be administered using the mAb labelled with a therapeutic isotope (α or β emitter). For example, ^{90}Y-J591 was used for prostate cancer, ^{153}Sm-DTPA-Cetuximab was used as a theranostic agent in epithermal growth factor receptor expressing tumours,[46] and ^{111}In and ^{177}Lu-labelled IMP288 were used as pretargeted radioimmunotherapy in an intraperitoneal nude mouse model of human colon cancer[43]. Despite the provision of high quality images via SPECT, PET has the advantage over SPECT in terms of sensitivity. Therefore, immuno-PET imaging is desired for more accurate quantification.

Immuno-PET imaging agents have been increasingly developed in recent years. For example, ^{124}I-labelled cMAb U36 was studied in nude mice bearing subcutaneously implanted human xenografts of the cell line HNX-OE.[47] The labelling yield was more than 70% and radiochemical purity was higher than 95%. A biodistribution study showed that tumour uptake increased from 12% at 24 hours to 16% at 72 hours after injection. PET studies showed visualisation of the cardiac blood pool, liver and nose area were visible. Compared with ^{131}I-labelled cMAb U36, ^{124}I-labelled cMAb U36 gave fully concordant tissue uptake values. Furthermore, ^{64}Cu-DOTA-HB22.7 was studied in mice bearing non-Hodgkin's lymphoma

xenografts.[48] The result showed that tumour uptake increased between 24 to 48 hours after injection and the amount of ^{64}Cu in blood decreased over time as expected. It was suggested that ^{64}Cu-DOTA-HB22.7 could be used as a therapeutic agent in the future.

The US Food and Drug Administration (FDA) has now approved more than 50 mAbs,[49] most of which are used for cancer therapy, such as rituximab, panitumumab, bevacizumab and trastuzumab. Additionally, the market for mAbs as therapeutic agents has been growing rapidly and new mAbs labelled and engineered mAb fragments labelled with various radionuclides have been researched by the pharmaceutical industry and academic institutes in order to provide efficient antibody-based PET imaging agents for optimised diagnosis and therapy.[50]

1.1.5. [^{89}Zr]Zr(IV)

[^{89}Zr]Zr(IV) is a radiometal produced via a cyclotron by the ^{89}Y(p,n)^{89}Zr or ^{89}Y(d,2n)^{89}Zr reaction. It decays with a half-life of 78.41 hours via positron emission and electron capture to ^{89m}Y which decays to ^{89}Y via gamma ray (909 keV) emission with a half-life of 15.7 seconds, see Figure 6. As [^{89}Zr]Zr(IV) has a relatively long half-life, it is suitable for antibody-based PET imaging (immuno-PET). [^{89}Zr]Zr(IV) has advantages over others PET isotopes which decay with comparable half-life such as ^{124}I. In terms of production, the ^{89}Y target does not need to be enriched and the energy required for [^{89}Zr]Zr(IV) production is lower.[51] Moreover, in terms of imaging, dehalogenation of ^{124}I-labelled antibodies *in vivo* causes radioactive uptake in non-targeted organs, an issue which is circumvented if kinetically inert [^{89}Zr]Zr(IV) complexes are formed.

In spite of advantageous decay characteristics of [^{89}Zr]Zr(IV), the 909 keV gamma ray, which is a highly penetrating photon, has approximately twice half-value layer for 511 keV photon. Therefore, [^{89}Zr]Zr(IV) needs more shielding for safe handling and transporting than positron decay isotopes such as ^{18}F.[52]

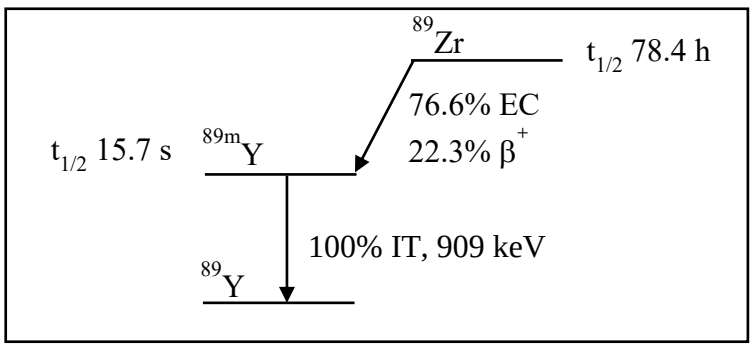

Figure 6 - Decay scheme of [^{89}Zr]Zr(IV).

Radiation dose is considered as [^{89}Zr]Zr(IV) is a relatively long half-life (78.4 hours) radionuclide and has a daughter isotope which also emits radiation. A study of safety and evaluation of human radiation dosimetry of [^{89}Zr]Zr(IV) has been reported by Laforest *et al.* in 2016.[105] They conducted their research by using [^{89}Zr]ZrDFO-trastuzumab (62 MBq dose) in twelve patients with HER2-positive breast cancer. PET/CT imaging were performed within 7 days post-injection to collect biodistribution data. Human dosimetry was calculated and it was found that the effect dose was 0.47 mSv/MBq, no adverse effects were observed, and liver, which is the dose-limiting organ, showed radiation dose of 1.63 mSv/MBq. Therefore, at 62 MBq injection, the estimated dose to liver is approximately 100 mSv which is lower than several FDA-approved radiopharmaceuticals such as ^{111}In-pentetreotide, the limit of which is 125 mSv to spleen for a dose of 222 MBq. This indicates that despite some challenges, if properly managed, then zirconium-89 can be used safely. However, dose will be limited if there are problems with transchelation.

1.2. Bifunctional chelators

Bifunctional chelators (BFCs) are molecules containing a metal chelator and a reactive functional group to form covalent bonds with groups such as amines, thiols or alcohols.[53] BFCs are usually composed of three parts; donor atoms, ligand framework and conjugation group. The donor atoms can be in groups such as hydroxamate, amino acid, diamine, aminethiol, *etc.* The ligand framework is the backbone of the chelator; for example, cyclen and cyclam are macrocyclic ligand frameworks. The conjugation group is usually an electrophile used to react with a nucleophile in the biomolecules used for targeting.

A new BFC needs to be validated to find out whether it is suitable for biological application.[54] The properties that are used to validate a novel BFC include:

1. Thermodynamic stability: BFC should have high thermodynamic stability of the metal complex which forms.
2. Transchelation study: BFC should have high kinetic inertness in order to compete with other metal ions to form a stable complex with radiometal.
3. Acid catalysed dissociation: Acid catalysed dissociation should show minimum dissociation of radiometal from complex under *in vivo* simulated conditions.
4. Serum stability: Stability in serum can be used to predict whether or not BFC is suitable for *in vivo* application.

There are other minor requirements for BFCs; for example, a BFC should generally have high hydrophilicity which helps to increase blood clearance, and the functional group should react easily with the intended biomolecule.

The labelling of BFCs with metal ions is well known and routinely used in medicine as diagnostic and therapeutic pharmaceuticals. For example, Gd^{3+} and Mn^{2+} are used as contrast agents in MRI, ^{99m}Tc and ^{68}Ga are used in SPECT and PET, and beta emitters such as ^{90}Y are used for treatment.

1.2.1. Acyclic and macrocyclic ligands

Acyclic ligands are ligands with a linear structure, also called open-chain-compounds. The chains can be either non-branched or branched. The structures of representative acyclic compounds are shown in Figure 7. The early BFCs were acyclic compounds such as HBED, DTPA, EDTA and their derivatives. However, DTPA and EDTA labelled with ^{67}Cu were found to be unstable in human serum.[55] It was reported that DTPA and EDTA are not suitable for complexation with lanthanide metal ions as they cannot completely wrap around the metal ion (insufficient donors and flexibility). Moreover, EDTA has higher affinity for bivalent metal ions such as Ca^{2+} and Zn^{2+} than for trivalent ones such as Gd^{3+}.[56]

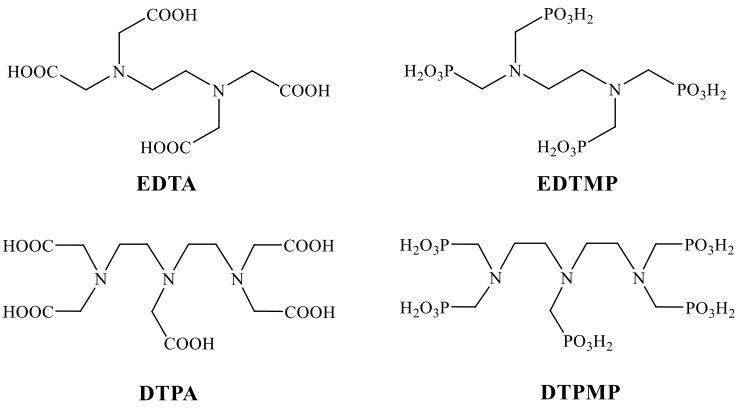

Figure 7 - Structures of sample acyclic compounds.

Macrocyclic ligands are polydentate ligands which contain donor atoms attached to a cyclic backbone. Usually, macrocyclic ligands consist of a minimum of seven atoms in the ring, with at least three donor atoms (such as DATA).[57] A metal ion normally forms a complex with donor atoms in the macrocyclic backbone and fits into the macrocyclic cavity.[58] In this case, the type of donor atom and size of macrocyclic ring are the major parameters influencing stability of the metal complex and its formation conditions. In nuclear medicine applications,

compounds labelled with radioactive metals should be stable *in vivo*; otherwise, free radiometal released from ligand would circulate in the blood pool or accumulate in non-target organs, which results in an increase in the background signal and potentially an increase in patient dose. The rate of dissociation of radiometal from the radiolabelled compound, known as kinetic inertness, plays a significant role for *in vivo* stability. It has been reported that macrocyclic ligands have much higher kinetic inertness of their metal complexes than acyclic ligands.[56,59] Therefore, macrocyclic ligands have become a major type of compounds used in medical imaging. The stability of metal complexes with macrocyclic ligands can be increased by rigidifying the chelate.[60] For example, an ethylene bridge between nitrogen atoms of cyclam either side- or cross-bridge can be used to increase rigidity.[61] This compound has shown favourable stability when labelled with copper-64 (as Cu^{2+}).Structures of common macrocyclic compounds are shown in Figure 8.

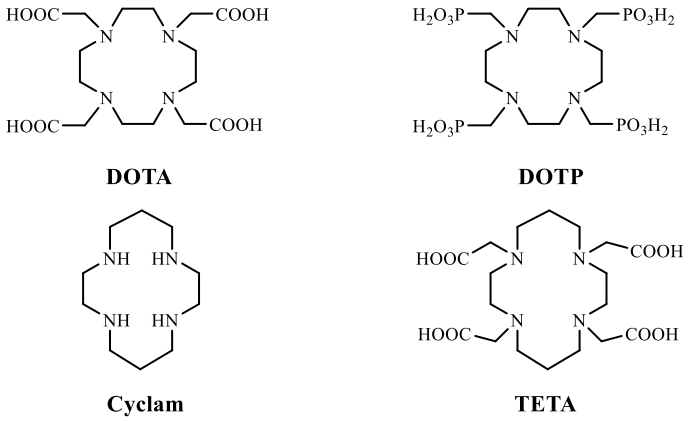

Figure 8 - Structures of sample macrocyclic compounds.

However, there is also an argument that macrocycles may exhibit slow complex formation as well as the desired slow decomplexation. The hypothesis that the work in this thesis is based on is the idea that macrocyclic scaffolds can be used as platforms. The donor atoms are part of the pendant arms and the metal ion will form a complex without involving the heteroatoms of the macrocycle itself. The macrocycle could solely be used to arrange the pendant arms in space.

1.3. Deferoxamine (DFO): an ideal chelator for zirconium(IV)?

Deferoxamine (DFO) is a naturally occurring hexadentate siderophore produced by *Streptomyces pilosus* in order to trap iron(III) from the environment for its growth. In medical

applications, DFO can be used as a chelating agent used for the management of excess iron from the body and used as a chelator in immuno-PET study as its three hydroxamate groups are suitable for metal chelation and the amine tail, which is used to conjugate to a biomolecule, such as an antibody.

In the past decade, the use of [^{89}Zr]Zr(IV) for PET imaging has been increasingly studied. The most commonly used methods to label mAbs with [^{89}Zr]Zr(IV) use DFO as a chelator, see Figure 9.[62] Examples of antibodies used as [^{89}Zr]Zr(IV) imaging agents are shown in Table 2.

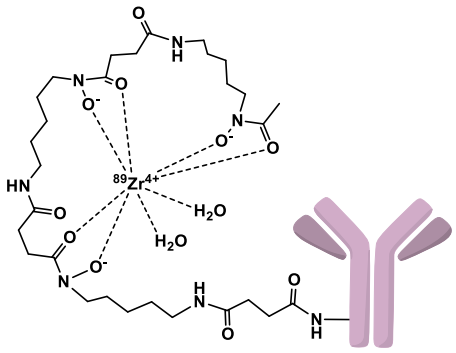

Figure 9 - [^{89}Zr]Zr(IV) labelled antibody using DFO as chelator.

Table 2 - [^{89}Zr]Zr(IV) labelled antibodies used for imaging in several cancers.[63, 64]

Antibodies used	Target cancer
bevacizumab	tumour angiogenic vessels
cetuximab	various cancers
fresolimumab	breast cancer
Zevalin	non-Hodgkin's lymphoma
panitumumab	head and neck tumours
Onartuzumab	glioblastoma
rituximab	malign lymphoma cells
trastuzumab	colorectal carcinoma
J591	prostate cancer

There are two common DFO-mAb coupling strategies; based on the lysine group of mAbs such as DFO-thioether-mAb, N-suc-DFO-mAb and DFO-Bz-NCS-mAb, or based on the thiol group of engineered ThiomAbs such as DFO-Ac-ThiomAb and DFO-Chx-Mal-ThiomAb, see Figure 10.[65] [^{89}Zr]ZrDFO linked through a thioether bond to the mAb was

studied in nude mice bearing OVCAR-3 xenografts and compared with antibodies labelled with ^{123}I and ^{99m}Tc. The tumour uptake of the [^{89}Zr]Zr(IV) compound was higher than that of ^{123}I and ^{99m}Tc. There was no free [^{89}Zr]Zr(IV) detected in the bone although there was some liver accumulation observed at 3 days after injection which requires further investigation.[66] For N-suc-DFO-mAb, [^{89}Zr]ZrDFO-N-suc-mAb was studied in nude mice bearing HNX-OE xenografts. A PET study showed that small tumours in the range of 19-154 mg could be visualised.[67,68] For DFO-Bz-NCS-mAb, [^{89}Zr]ZrDFO-Bz-NCS labelled panitumumab was studied in nude mice bearing human breast cancer tumours. The radiochemical yield was less than 10%. After purification by size exclusion chromatography, the complex showed more than 98% radiochemical purity and stability in human serum at 37ºC for 5 days. The biodistribution study showed high specific uptake but slower clearance thanexpected.[69] For ThiomAbs, Tinianow *et al.* synthesised a DFO-mAb conjugated to three thiol reactive reagents; Df-Bac, Df-Iac and Df-Chx-Mal. Each chelate was labelled with [^{89}Zr]Zr(IV) in a radiochemical yield of more than 75% and purity over 93% after purification by HPLC. The biological studies carried out appeared to show that the [^{89}Zr]ZrDFO-mAbs were stable in serum and specific in uptake experiments *in vivo* although it is now generally accepted that there are stability issues with [^{89}Zr]ZrDFO, which are discussed in section 1.3.1.[70]

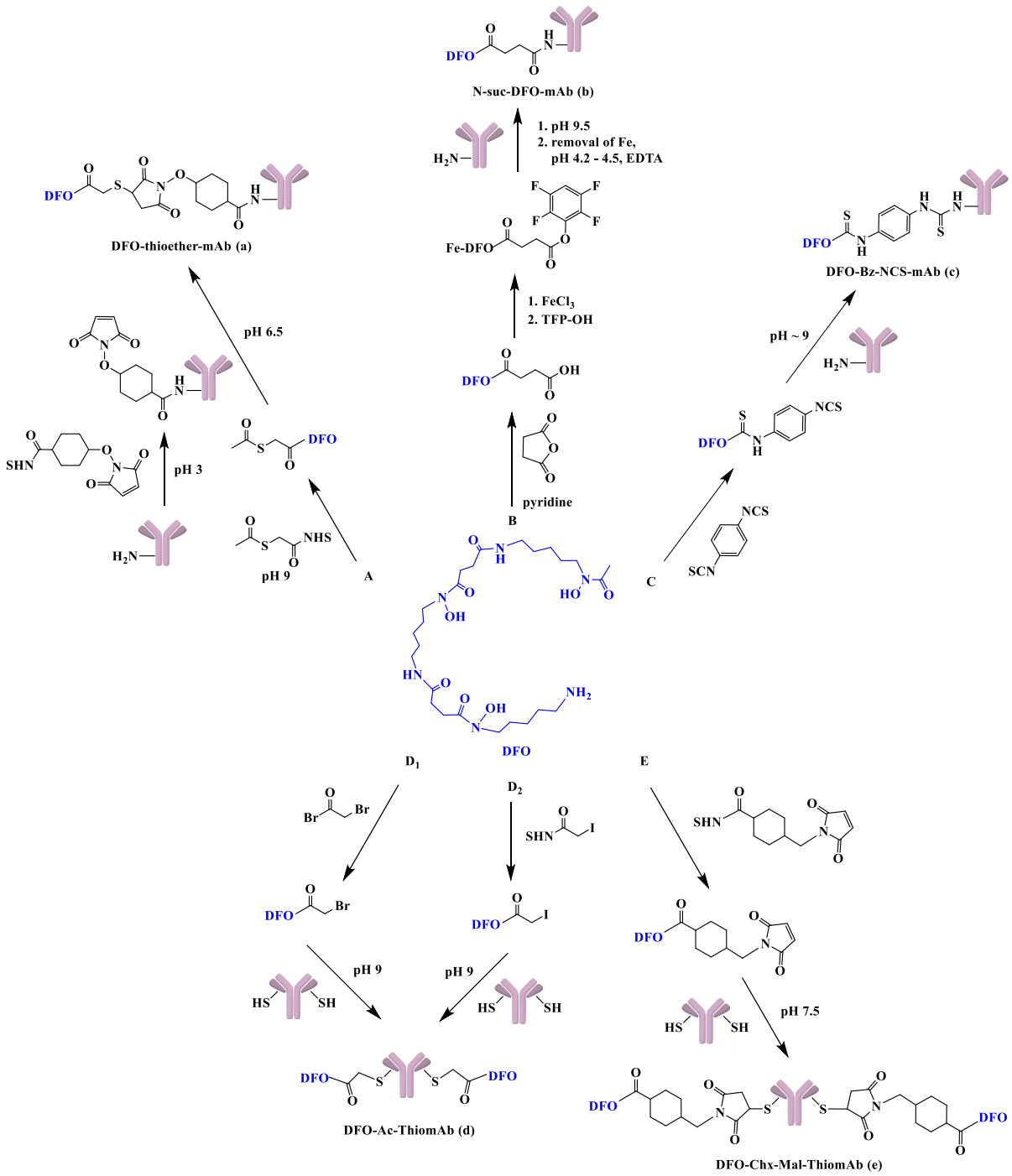

Figure 10 - Summary of the different DFO coupling strategies reported by Vugts *et al.* in 2011.[65]

In addition, [^{89}Zr]Zr(IV) has been used to label nanoparticles. Baur *et al.*[71] have developed a radiolabelling procedure for mesoporous silica nanoparticles (MSNs) with [^{89}Zr]Zr(IV). Karmani *et al.*[72] have compared the biodistribution of [^{89}Zr]ZrDf–Bz–NCS–cetuximab before and after the coupling reaction to gold nanoparticles in mice. Miller *et al.*[73] synthesised MSNs functionalised with APTMS in order to introduce anchoring groups for DFO,

then amino groups on MSNs were linked to DFO-NCS, see Scheme 1. The conjugated DFO-MSNs were labelled with [^{89}Zr]zirconium(IV) chloride to form [^{89}Zr]ZrDFO-MSNs which was used to study mice with implanted prostate carcinoma tumours. The radiosynthesis study showed DFO-MSNs were capable of complexing large amounts of [^{89}Zr]Zr(IV) and no purification step was needed to remove free [^{89}Zr]Zr(IV) due to the high DFO content on the surface of the MSNs. Biodistribution experiments showed [^{89}Zr]ZrDFO-MSNs accumulate in heart, lung, liver and spleen, which might be because the [^{89}Zr]ZrDFO-MSNs had not been optimised to maximise tumour uptake. Perez-Medina *et al*. studied [^{89}Zr]Zr(IV) radiolabelled nanoliposomal doxorubicin in a breast cancer mouse model to determine its effectiveness in drug delivery and found accumulation in the tumour. This indicates the potential for further development as a targeted therapeutic agent.[74]

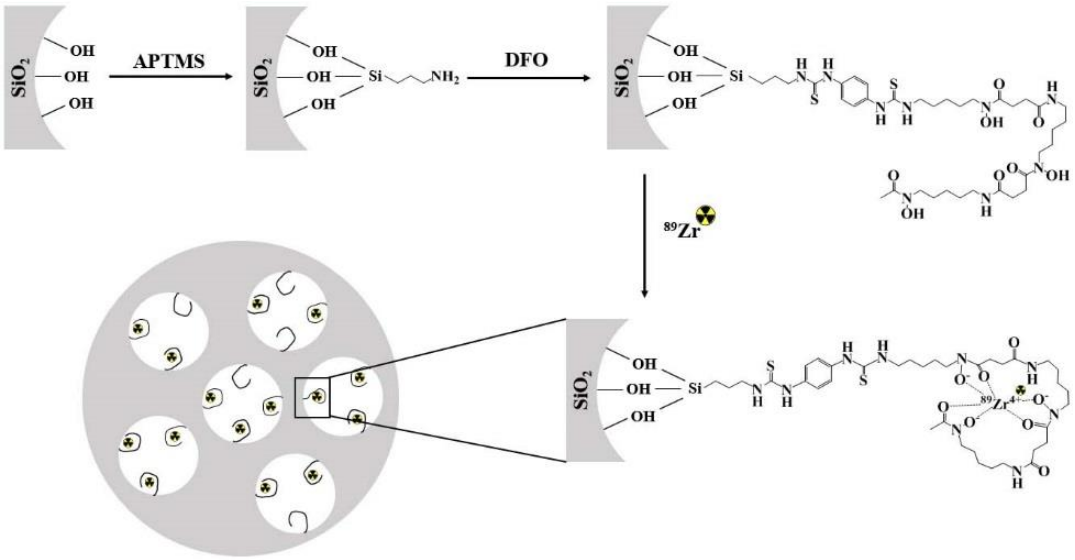

Scheme 1 - MSNs coupled with DFO-NCS and labelled with [^{89}Zr]Zr(IV) reported by Miller *et al.*[73]

1.3.1. Limitations of DFO

New chelators for [^{89}Zr]Zr(IV) have recently been developed in order to improve the stability of [^{89}Zr]Zr(IV) complexes. The release of [^{89}Zr]Zr(IV) from DFO is unfavourable as the Zr^{4+} ion is known to be osteophilic and [^{89}Zr]Zr(IV) is a relatively long half-life isotope. The accumulation of radioisotope in bone results in increased radiation dose to bones and tissues, and also image quality issues. According to Holland, 2% demetalation of [^{89}Zr]ZrDFO-J591 used for immuno-PET imaging of prostate cancer was found *in vitro* after incubation in either saline or bovine serum albumin at 37^{o}C for 7 days.[75] [^{89}Zr]ZrDFO-panitumumab

incubated in human serum at 37ºC for 5 days revealed a decrease of 4% intact tracer.[69] Moreover, it has been reported that bone uptake of [^{89}Zr]Zr(IV) was observed in animal studies, which suggests that [^{89}Zr]Zr(IV) is released from DFO *in vivo*.[76,77] It was clear that the bone uptake occurred from [^{89}Zr]Zr(IV) released from ligand after administration, as the [^{89}Zr]ZrDFO-mAb conjugate had been purified and radioimmunoconjugates have the ability to bind specific sites. In aqueous solution, Zr^{4+} is relatively large and highly-charged preferring to form octadentate complexes with anionic oxygen donors. This was confirmed for hydroxamic acids by Guerard *et al.* in 2013.[78] They studied two hydroxamic acids; acetohydroxamic acid (AHA) and N-methyl acetohydroxamic acid (Me-AHA), see Figure 11. Single crystal x-ray diffraction showed Zr(IV) formation of an octadentate complex with four ligand molecules. Moreover, in 2014, Holland and Vasdev investigated the mechanism of the reaction of Zr-oxalate and Me-AHA by density functional theory (DFT). The reaction was stimulated under both acidic and basic conditions in order to understand the coordination requirements for Zr(IV) complex formation. They reported the pathway of oxalate dissociation and hydroxamate addition reactions. This study showed that the reaction under acidic conditions is not feasible. Under basic conditions, the hydroxamate was deprotonated and so the replacement of oxalate to hydroxamate occurred in the following order: $[Zr(C_2O_4)_4]^{4-} \rightarrow [Zr(C_2O_4)_3]^{2-} \rightarrow [Zr(C_2O_4)_3(MeAHA)]^{3-} \rightarrow [Zr(C_2O_4)_2(MeAHA)]^{-} \rightarrow [Zr(C_2O_4)_2(MeAHA)_2]^{2-} \rightarrow [Zr(C_2O_4)(MeAHA)_2] \rightarrow [Zr(C_2O_4)(MeAHA)_3]^{-} \rightarrow [Zr(MeAHA)_3]^{+} \rightarrow Zr(MeAHA)_4$.[79] The DFO offers only hexadentate coordination via three groups of hydroxamate and then two molecules of water complete the coordination sphere.[80] The incomplete coordination of [^{89}Zr]ZrDFO was thought to be the main reason for the instability of the labelled compound. It is believed that an octadentate ligand should offer much better stability compared to DFO when forming a complex with Zr(IV).

(A) (B)

Figure 11 - Chemical structures of (A) AHA and (B) Me-AHA.

1.4. Development of novel chelators for [^{89}Zr]Zr(IV)

The development of chelators which could provide higher stability than DFO is an area of recent interest. There have been six main types of functional group incorporated in these chelators; hydroxamates, hydroxypyridinones, terephthalamides, catecholates, carboxylates and phosphonates. For many of the novel chelators, radiolabelling with [^{89}Zr]Zr(IV) and *in vitro* and *in vivo* studies are reported.

1.4.1. Hydroxamate group

In 2014, Guérard *et al.* developed macrocyclic tetrahydroxamic acid chelators for complexation with Zr(IV), see Figure 12.[81] Varying numbers of methylene groups from five to seven for the linker groups were compared. It was found that the C7 derivative demonstrated excellent complex formation properties. Complex formation with [^{89}Zr]Zr(IV) occurred in a 99% radiochemical yield after incubation at 50^{o}C for 30 minutes or at room temperature for 120 minutes. Stability studies showed 99% of [^{89}Zr]ZrC7 chelator complex remained intact after 7 days in phosphate buffer pH 6.5 and showed higher stability in 50 mM EDTA solution (pH 7) at 37^{o}C over 7 days (>90% intact) than [^{89}Zr]ZrDFO (~50% intact).

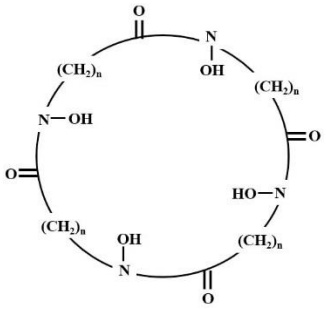

Figure 12 - Schematic structure of tetrahydroxamic acid chelators C5, C6 and C7, each chelators link by a chain of five, six and seven methylene groups respectively reported by Guérard *et al.*[81]

An extended DFO was designed by Patra *et al.* in 2014.[82] It was synthesised by adding a hydroxamate group to a DFO molecule to give a new chelator called DFO*. The complex formation with the Zr(IV) stable isotope showed that it formed a 1:1 metal-to-ligand complex. Radiolabelling of DFO* and conjugated DFO* with the monoclonal antibody trastuzumab were performed and compared with DFO by Vugts *et al.* in 2017, see Figure 13.[83] It was found that [^{89}Zr]ZrDFO*-trastuzumab was more stable in saline and had higher tumour uptake than [^{89}Zr]ZrDFO, as well as significantly lower bone uptake.

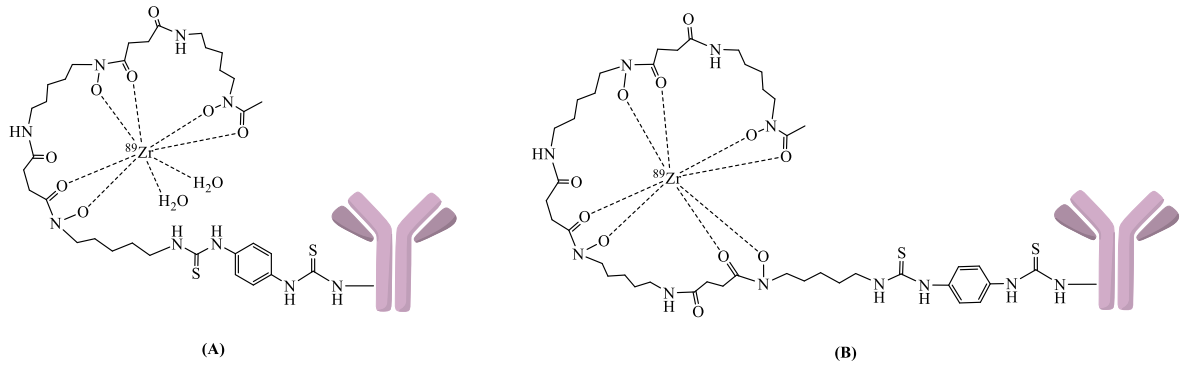

Figure 13 - Structure of (A) [^{89}Zr]ZrDFO-trastuzumab and (B) [^{89}Zr]ZrDFO*-trastuzumab reported by Vugts *et al*. in 2017.[83]

In 2015, fusarinine C (FSC), which had previously been studied for complex formation with ^{68}Ga, was labelled with [^{89}Zr]Zr(IV). FSC has complexing properties similar to DFO; therefore, it was considered to be an alternative chelator worthy of further investigation.[84] FSC and its derivative, TAFC, see Figure 14, can be labelled with [^{89}Zr]Zr(IV) at room temperature in greater than 95% RCY after 90 minutes. *In vitro* stability studies showed no transchelation of TAFC in EDTA at pH 7 but minor transchelation in EDTA at pH 6 after 7 days, which was still an improvement on [^{89}Zr]ZrDFO, which was observed to have 60% transchelation in EDTA at pH 7 after 7 days and more than 90% in EDTA at pH 6 after 3 days. In terms of *in vivo* studies, the conjugation of FSC to an RGD-peptide show rapid pharmacokinetic distribution and blood clearance as well as low bone uptake. FSC emerged as a promising chelator for Zr following these results. Although it has only six binding sites from three hydroxamate groups, FSC could form a stable complex with [^{89}Zr]Zr(IV) as the cyclic nature of the construct improves the stability via the macrocyclic effect.[56]

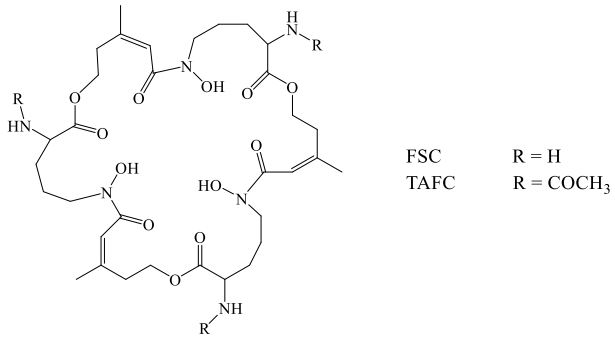

Figure 14 - Chemical structure of fusarinine C and its derivative.

Rudd *et al.* synthesised a DFO squaramide ester chelator, see Figure 15. It was modified from DFO by adding squaramide linker to the DFO molecule and then bifunctional version was produced and conjugated to trastuzumab.[85] The results showed improved radiolabelling yield, higher stability and reduced bone uptake compared with [^{89}Zr]ZrDFO-trastuzumab.

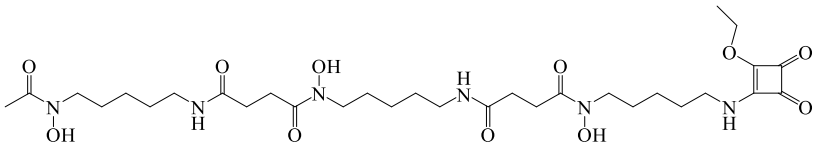

Figure 15 - Chemical structure of DFO squaramide ester.

Rousseau *et al.* designed and synthesised new tetrahydroxamate chelators, see Figure 16.[86] The ligands contained four hydroxamate groups on a 2,2'-iminodiacetamide chain and included an isothiocyanate group for coupling to mAbs. The ligands were conjugated to trastuzumab and radiolabelled with [^{89}Zr]Zr(IV) in >90% radiolabelling yields and >99% yields after purification using a PD-10 column. However, *in vitro* stability showed that the labelled compounds were less stable in mouse plasma when compared with [^{89}Zr]ZrDFO-trastuzumab. PET imaging studies also showed higher bone uptake. The researchers believed that the instability of the complexes was because of steric constraints. They suggested that extending the length of the linker between the hydroxamate and amide groups or extending the iminodiacetamide chain could reduce steric constraints and improve complex stability.

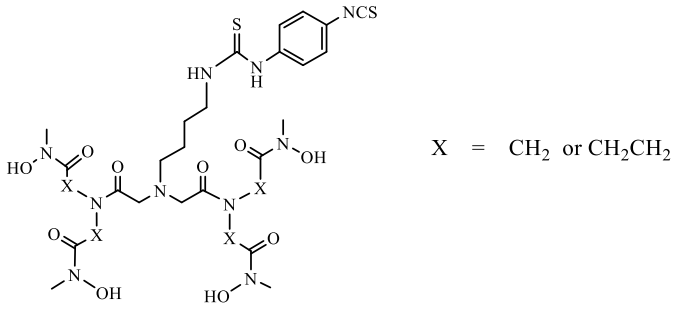

Figure 16 - Tetrahydroxamate chelators.

Macrocycle based hydroxamate pendant arm chelators were also studied. Cyclen and cyclam were *N*-functionalised with three or four hydroxamate groups of various lengths, see Figure 17.[87] The bifunctional chelator was conjugated with trastuzumab and labelled with [^{89}Zr]Zr(IV). However high bone uptake was observed.

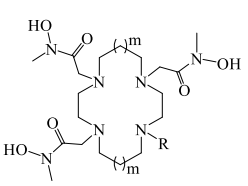

m = 0 or 1,
R = H or $CH_2CONOHCH_3$

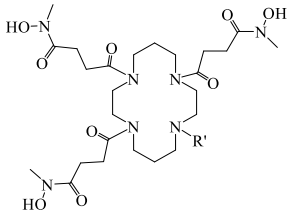

R' = H or $CH_2CONHCH_2COOH$

Figure 17 - Macrocyclic based hydroxamate chelators.

1.4.2. Hydroxypyridinone group

Deri *et al.* studied an octadentate ligand (HOPO) as a novel chelator for [^{89}Zr]Zr(IV) PET imaging, see Figure 18.[88] HOPO derivatives were originally designed for plutonium(IV) complex formation.[89, 90] As Pu(IV) and Zr(IV) have similar ionic radii; 85 and 86 pm respectively [91], HOPO was an interesting candidate to investigate for Zr(IV) complex formation. The researchers investigated the synthesis, characterisation, radiolabelling, *in vitro* stability and biodistribution for these compounds. Radiolabelling could be performed at room temperature at pH 7. The complex was not very soluble in water; however, there was enough compound in solution for analysis. A serum stability study showed that the [^{89}Zr]ZrHOPO was stable over 7 days at 37ºC in human serum. EDTA challenge showed HOPO had the ability to withstand transchelation as it remained intact by more than 99% in a 100-fold excess of EDTA at pH 5-8 over 7 days. Metal cation competition, which is used to evaluate if other metal cations could compete with Zr(IV) for chelator binding, showed HOPO released about 17% of the [^{89}Zr]Zr(IV) after incubation in $FeCl_3$ for 7 days compared with DFO which released more than 50% of the [^{89}Zr]Zr(IV). A biodistribution study showed no radioactivity observed in bone and rapid clearance, although the clearance was slower than DFO. The x-ray crystal structure was reported by the same research group by reacting HOPO with an excess (1.5 equiv) of non-radioactive $ZrCl_4$. It was confirmed that the Zr^{4+} ion formed a complex with eight oxygen donor atoms from the HOPO hydroxypyridinone moieties.[92]

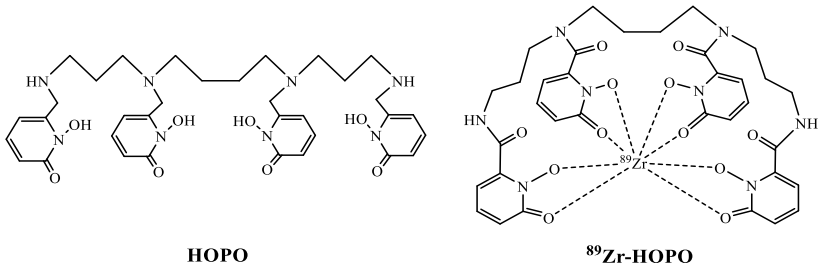

Figure 18 - Chemical structures of HOPO and [^{89}Zr]ZrHOPO.

Bismacrocyclic ligand 2,3-HOPO and its bifunctional version were radiolabelled with [^{89}Zr]Zr(IV) and evaluated for *in vitro* and *in vivo* stability, see Figure 19.[93] The radiolabelling was achieved in quantitative yield in 15 minutes incubation at room temperature. The labelled compound was stable in 50 mM DTPA at pH 7; however, decomplexation occurred in human serum. [^{89}Zr]Zr2,3-HOPO-trastuzumab was studied in mice bearing HER2 positive ovarian carcinoma. PET imaging showed high tumour uptake but with some bone and liver uptake showing no advantage when compared with [^{89}Zr]ZrDFO-trastuzumab.

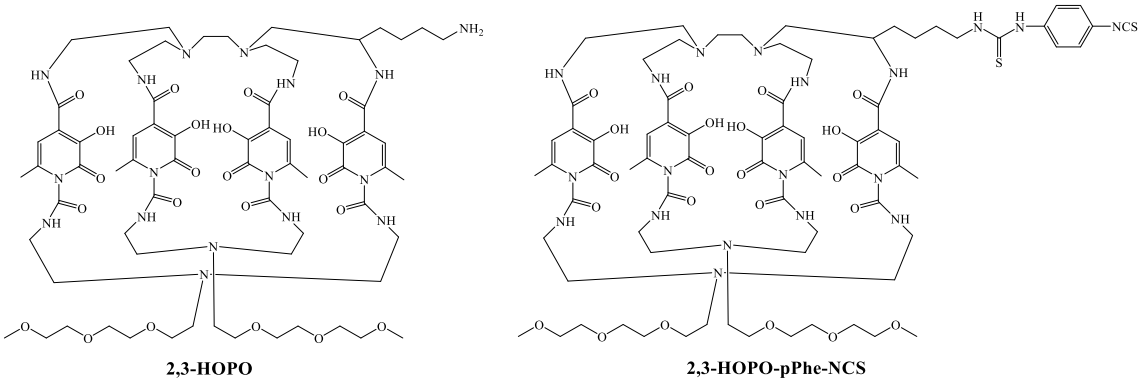

Figure 19 - Chemical structures of 2,3-HOPO and its bifunctional version.

Tripodal tris(hydroxypyridinone), CP259, and its maleimide derivative, YM103, were synthesised and evaluated for [^{89}Zr]Zr(IV) radiolabelling and subsequently compared with DFO and DFO conjugated maleimide group, see Figure 20.[94] Although CP259 can only provide six oxygen donors, the same as DFO, it was tested to see whether the 1,6-dimethyl-3-hydroxy-pyridin-4-one groups could effectively coordinate Zr before modification to produce a compound with four hydroxypyridinone groups. Radiolabelling of CP259 was performed at ambient temperature at pH 6 - 7 and the labelled derivative obtained in a >90% radiochemical yield at a concentration of ligand >100 μM, whereas DFO could be labelled in a 1 μM concentration. The conjugate of YM103 with trastuzumab was compared with the DFO

equivalent via an *in vivo* study. This indicated that [^{89}Zr]Zr(IV) was released from YM103-trastuzumab and accumulated at bones and joints 25.88 ± 0.58% ID g^{-1} at 7 days after injection. In contrast, [^{89}Zr]ZrDFO-trastuzumab found < 8% ID g^{-1}.

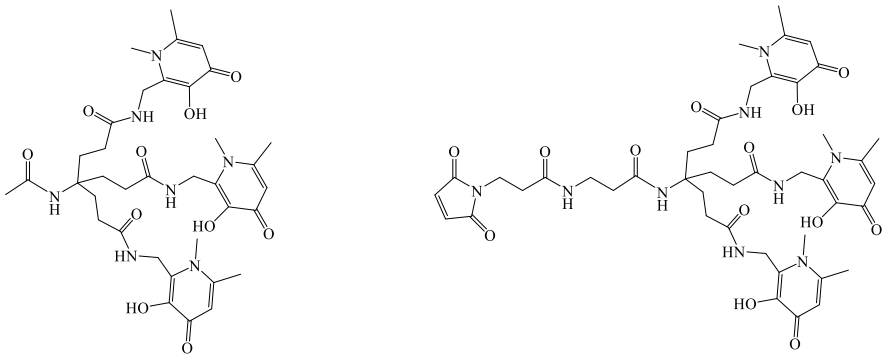

Figure 20 - Chemical structures of tripodal tris(hydroxypyridinone) ligands.

In 2017, Buchwalder and co-workers developed a tetrapodal hydroxypyridinone ligand, THPN, see Figure 21.[95] The octadentate chelator could be labelled with [^{89}Zr]Zr(IV) at room temperature in a >95% radiochemical yield in 10 minutes with 1 μM chelator concentration. EDTA challenge showed that [^{89}Zr]ZrTHPN was more stable than [^{89}Zr]ZrDFO in 100-fold excess of EDTA at pH 5 - 8 for 7 days. [^{89}Zr]ZrTHPN also resisted in 100-fold excess of DFO for 73 hours, while [^{89}Zr]ZrDFO was found to show transchelation in 1:1 THPN-to-DFO mol ratio within 30 minutes. A biodistribution study of [^{89}Zr]ZrTHPN showed rapid clearance via the kidneys in 24 hours with no bone uptake (as would be expected for the non-conjugated complex). Further studies are required to show stability on the longer timescale for antibodies to bind and clear *in vivo*.

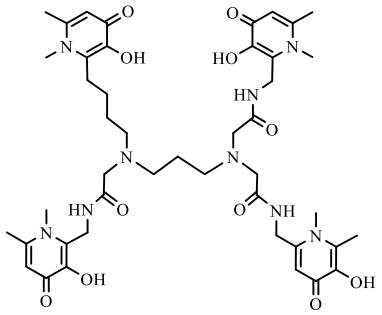

Figure 21 - Chemical structure of tetrapodal 3-hydroxy-4-pyridinone, THPN.

1.4.3. Terephthalimide group

Pandya *et al.* developed the bismacrocyclic terephthalimide derivative ligands as octadentate chelators, see Figure 22.[96] Terephthalimide (TAM) derivatives were originally designed for plutonium(IV), in a similar way to the hydroxypyridinone chelators.[91] TAM has four catechol type donors to provide eight coordination sites for Zr and the primary amine was used to conjugate to a biomolecule. Radiolabelling of both ligands **L1** and **L2** could be performed at ambient temperature within 15 minutes. *In vitro* stability tests showed both labelled compounds were stable in human serum for 7 days and they were more stable under DTPA challenge than [^{89}Zr]ZrDFO. Biodistribution of [^{89}Zr]Zr**L1** demonstrated faster clearance than [^{89}Zr]Zr**L2** and bone uptake was not significantly different from [^{89}Zr]ZrDFO. Although [^{89}Zr]Zr**L1** had higher uptake in the liver and kidney, but it was believed that the antibody conjugation could improve these properties and so it was the preferred candidate for further studies.

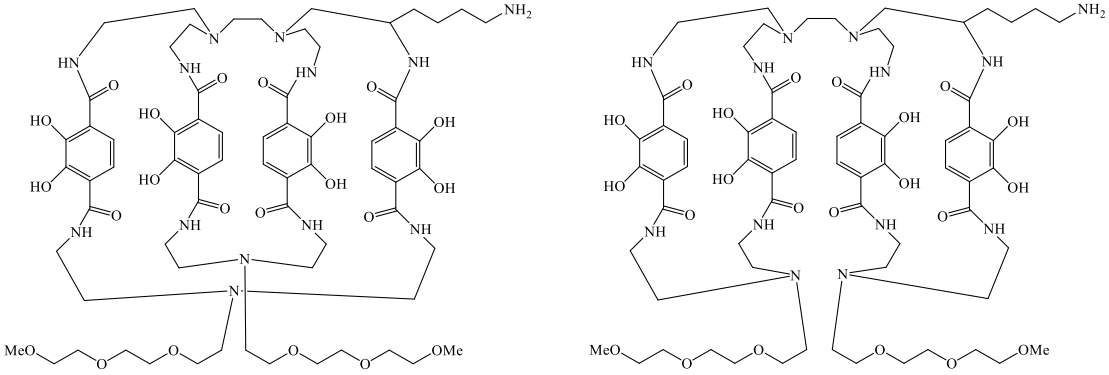

L1 **L2**

Figure 22 - Chemical structures of di-macrocyclic terephthalamide **L1** and **L2**.

1.4.4. Catecholate group

Deri and co-workers selected a catecholate-based ligand 3,4,3-LICAM (LICAM) to investigate radiolabelling with [^{89}Zr]Zr(IV), see Figure 23. However, after varying temperature, pH and reaction time, the maximum radiolabelling efficiency was only 30%. They believed that the issue was due to pK_a of catechol group (13.0) which require a higher pH for radiolabelling to be efffective.[97]

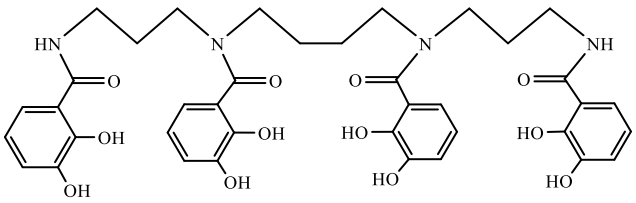

Figure 23 - Chemical structure of LICAM.

1.4.5. Carboxylate and phosphonate group

Price and co-workers reported the acyclic chelators containing carboxylate and phosphonate groups, H_4octapa and H_6phospha, see Figure 24. However, both chelators were unsuitable for [^{89}Zr]Zr(IV) as <12% radiolabelling yields were observed. [98, 99]

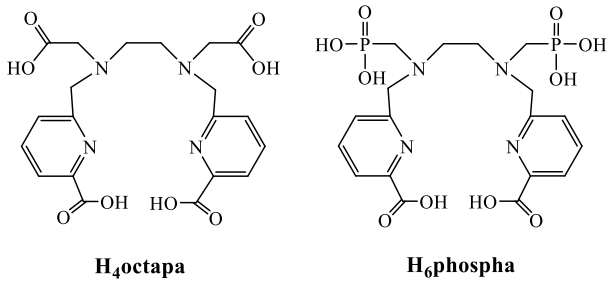

Figure 24 - Chemical structures of H_4octapa and H_6phospha.

1.5. Research aims

This research work is based around the synthesis of azamacrocyclic based compounds as [^{89}Zr]Zr(IV) chelators.

To summarise the argument for further investigation of novel zirconium-89 chelators. As it has ideal properties for immuno-PET, [^{89}Zr]Zr(IV) has increasingly been studied in the field of antibody-based PET imaging. Most of the [^{89}Zr]Zr(IV) labelled mAbs investigated up to this point in time use DFO as a chelator to form hexadentate complexes through three hydroxamate groups and additionally incorporate two water molecules in the coordination sphere. However, as Zr(IV) is a 4+ ion in aqueous solution and prefers to form eight coordinate complexes, providing eight binding sites for zirconium should increase the complex stability in comparison to DFO.

The development of chelators using azamacrocycles as a base to arrange various types of coordinating groups for chelation is of interest. It is an extension of the siderophore type approach where cyclic molecules are used to arrange the pendant arms in space to orientate them for binding to the metal ion and combines this approach with the wide array of

functionalisation strategies for tetraazamacrocycles as the four nitrogen positions. Some of these new macrocyclic chelators were designed to exploit the macrocyclic ring as scaffold and then *N*-functionalised with various types of functional groups to provide pendant arms for binding Zr(IV), see Figure 25. The macrocyclic structures mimic natural siderophore enterobactin; the macrocyclic backbone of the siderophore is appended with three catecholate moieties as metal binding units to form a stable complex with Fe(III). A series of known and novel cyclen and cyclam based chelators were synthesised and radiolabelled with [^{89}Zr]Zr(IV) to investigate the complex stability. Designs for both "in cavity" binding (see Chapter 2), where it is expected that the azamacrocycle nitrogens will be coordinated and "out of cavity" binding (see Chapter 3) where it is expected that only the pendant arms will coordinate, have been investigated.

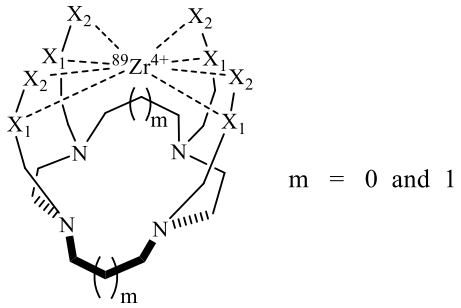

Figure 25 - Macrocycle-based chelators designed for [^{89}Zr]Zr(IV) complex.

Novel chelators combining azamacrocycles with DFO were also prepared (see Chapter 4). DOTA, DOTAGA and NOTA were attached to the DFO molecule, see Figure 26. These chelators were synthesised to investigate the stability of complexation with [^{89}Zr]Zr(IV), when both "in cavity" binding with the macrocycle or "out of cavity" binding with DFO are possible. These chelators all have more than eight donor atoms and so could have different coordination modes for zirconium-89 which may be driven by kinetics or thermodynamic factors.

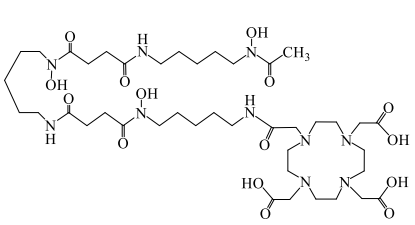

DOTA-DFO

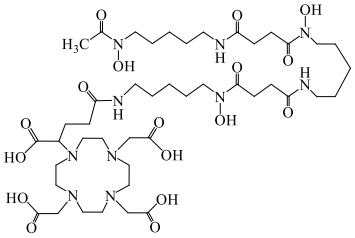

DOTAGA-DFO

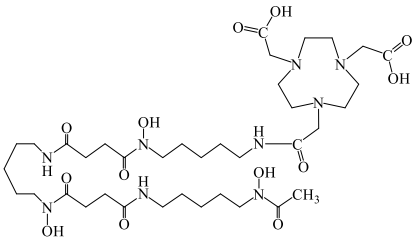

NOTA-DFO

Figure 26 - Macrocyclic-based DFO.

Chapter 2

Synthesis and [^{89}Zr]Zr(IV) radiolabelling of cyclen-based chelators

2. Synthesis and [^{89}Zr]Zr(IV) radiolabelling of cyclen-based chelators

2.1. Introduction

Macrocyclic chelators can be defined as large cyclic molecules composed of nine or more atoms, some of which are donor atoms to form coordinate bonds with metal centres. The application of macrocycles as metal ion chelators began in the early 1960s. The macrocyclisation of a long chain linear molecule causes a change of molecular shape, increases structural organization and influences conformation. It was reported that the preorganisation of macrocyclic compounds increases binding affinity and selectivity.[100] In the biomedical field, macrocyclic complexes with metal ions have been of interest as biologically active compounds such as enzyme mimics, anti-HIV compounds and medical imaging agents. There are four main types of donor atoms in macrocycles; aza (N), oxa (O), phospha (P) and sulfa (S), resulting in the difference of ring size, flexibility, conjugation and specificity of metal ions. This study focused on azamacrocycles which have been widely investigated and precursors are commercially available.[100]

Functionalisation of azamacrocycles has been studied in order to combine the rigid structure of the cyclic ring and the flexibility of pendant arms, see Figure 27. Triazamacrocycles, for example, have been exploited by the *N*-functionalisation of TACN (1,4,7-triazacyclononane) to give derivative **L3** for technetium(IV) complexation and could be used to form a BFC.[101] Triphosphinic acid NOTA derivative **L4** was prepared for complexation with gallium(III) and it was found that phosphinic arms allowed formation of the complex more efficiently than carboxylic acid arms.[102] Mono and bis[12]aneN3 compounds (**L5**, **L6** and **L7**), which have different linkers between two [12]aneN3 groups and different N-methylation on two backbones, were synthesised and catalytic activities compared for their metal complexes. The results showed that the linker plays a crucial role in catalytic effects.[103] *N*-Functionalisation of cyclam with three hydroxamic acid groups has also been investigated; TETMAHA, was synthesised and its complexation with copper(II), aluminium(III) and iron(III) were characterised. It was found that TETMAHA formed stable complex with these three metal ions.[104]

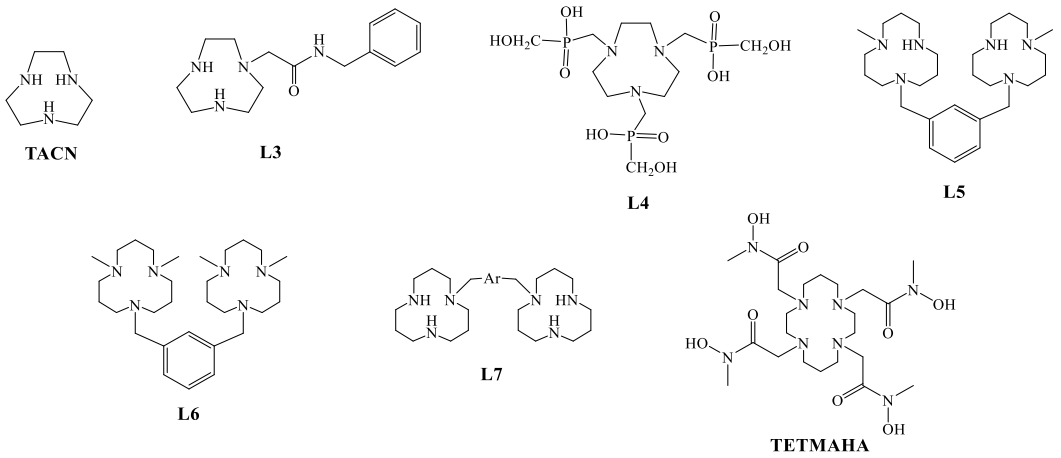

Figure 27 - Examples of *N*-functionalisation of azamacrocycles.

As discussed in the introduction, tetraaza macrocycles are also used as components of radiopharmaceuticals. Functionalised cyclen and cyclam as well as other tetraazamacrocycles and polyazamacrocycles have been used to expand the applications in biological and medical fields, see Figure 28. For example, compound **L8** was investigated for its copper(II) complexation properties and the compound **L9** was designed for complex formation with lanthanide(III) ions. Cyclam based ligands such as **L10** and **L11** were also investigated the complexation with nickel(II) and iron(III). The complex of **L12** with zinc(II) was synthesised and anti-HIV properties studied.

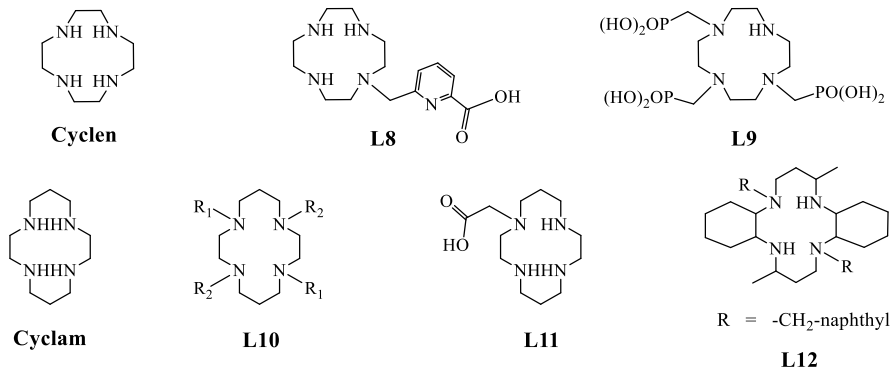

Figure 28 - Examples of N-functionalisation of tetraazamacrocycles and polyazamacrocycle.

To recap from the introduction, [^{89}Zr]Zr(IV) labelled mAbs have used deferoxamine (DFO) as a chelate to form six bonds to the metal centre through three hydroxamate groups and two water molecules; however, the stability of the complex *in vivo* is not sufficient for most applications. The stability of the complex results in the release of osteophilic Zr^{4+}, and

the unwanted uptake in bones reduces image quality and introduces the risk of a high radiation dose.

Therefore the development of both novel conjugation moiety and novel chelators has been the focus of recent research. Examples of hexadentate and octadentate ligands developed for zirconium(IV) in the last few years are shown in Figure 29. It has been found that the cyclic Fusarinine C and its derivatives having three hydroxamate moieties similar to DFO can be labelled with [^{89}Zr]zirconium(IV) oxalate under mild conditions with high labelling yield and high stability *in vitro* and *in vivo*.[84] However, as discussed in chapter 1, octadentate chelators for zirconium(IV) should be more stable than hexadentate ones. A linear ligand HOPO has been reported to have crystal structure of Zr-HOPO complex by eight oxygen atoms from four hydroxypyridinone groups.[92] The octadentate chelator DFO* has been developed by attaching a DFO molecule to a protected hydroxamic acid building block so that it can provide eight binding sites for Zr complexation.[82] DFO* was conjugated to trastuzamab and showed superior *in vitro* and *in vivo* stability.[83] THPN was designed to contain four groups of 3,4-HOPO as binding sites and [^{89}Zr]Zr(IV) labelling was performed at room temperature.[95]

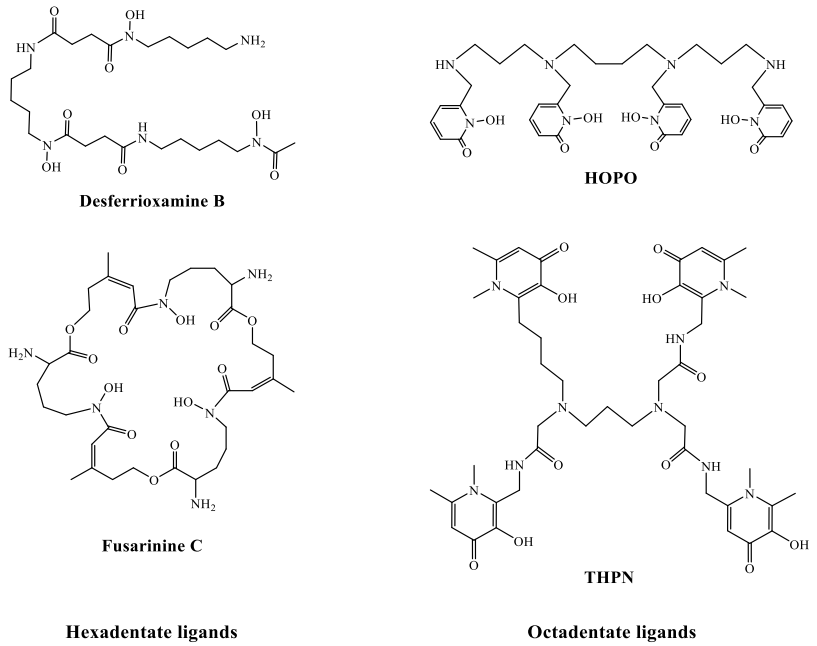

Figure 29 - Examples of hexadentate and octadentate ligands developed for zirconium(IV).

In terms of macrocycles, there have been studies of Zr-macrocyclic complexes for catalysis; for example, cyclam-based Zr complexes with heteroallenes, but these are not generally applicable to aqueous systems.[106,107] While, in molecular imaging, during the course

of the work carried out for this research project, the well-known tetraazamacrocyclic compounds; DOTA, DOTP and DOTAM, have been investigated for complexation with zirconium(IV).[108] The structures showed that Zr(IV) forms octadentate coordination, where the metal ion binds in the cavity to both macrocyclic and pendant arm donor atoms, with four nitrogen atoms of backbone and four donor atoms of pendant arms coordinated to the metal centre, see Figure 30. Radiolabelling was successfully achieved by using [^{89}Zr]zirconium(IV) chloride at 95^{o}C for 45 minutes. EDTA challenge, metal ion competition, and *in vitro* serum study showed superior stability for all labelled compounds when compared to DFO. Biodistribution study revealed that [^{89}Zr]ZrDOTA had less bone uptake than [^{89}Zr]ZrDFO. However, for [^{89}Zr]ZrDOTP and [^{89}Zr]ZrDOTAM, high uptake in liver, kidney and bone was observed.

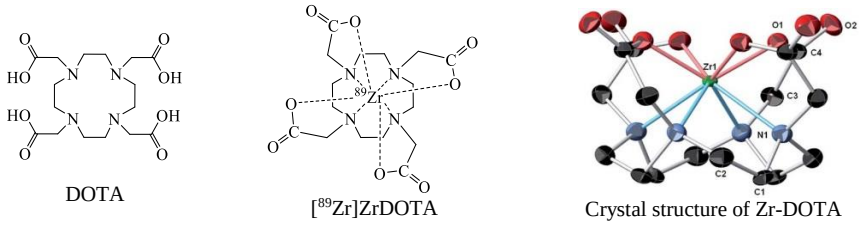

Figure 30 - Structure of DOTA and its Zr(IV) complex reproduce from Wadas *et al.* in Chemical Science, 2017.[108]

It is known that the rigid structure can offer more kinetically inert metal complexes than flexible chelators and so this could be investigated in the future. Additionally, functionalisation can be performed on macrocyclic ring and/or pendant arms with various functional groups. The development of chelators using the macrocycle cyclen to arrange coordinating groups for chelation is of interest.

2.2. Synthesis of macrocyclic compounds

Further investigation of macrocyclic complexes to form [^{89}Zr]Zr(IV) labelled antibodies is of interest in immuno-PET imaging.[109] Zr^{4+} ion is a large highly charge cation; it therefore, prefers to form complex with high coordination number and anionic oxygen atom.[52] Several chelators containing hydroxamate moieties have been previously investigated. During the course of the research work for this thesis, tetraazamacrocycle-based hydroxamate ligands, which were developed by using macrocycles as a scaffold with three or four hydroxamate pendant arms for binding Zr(IV), were reported.[87] This study showed out of cavity binding

complexes. The use of three hydroxamate arms offers hexadentate coordination like DFO and it was shown that the complexes were less stable than Zr-DFO. Four short hydroxamate groups would be unlikely to form octadentate coordination due to steric constraints. The extension of pendant arm length was one of the strategies used to improve the flexibility, and this maps onto the strategy in this work that is reported in chapter 3. Although the modified compounds with the longer linker hydroxamate arm on cyclam showed decomplexation *in vivo*, this research indicates the possibility to develop macrocyclic chelators for binding Zr(IV) solely to the macrocycle pendant arms, which is the same strategy that is investigated in this work (see chapter 3).

For the initial studies in this work, the ligands prepared for [^{89}Zr]Zr(IV) labelling were short arm cyclen chelators. The backbone was *N*-functionalised with various types of functional groups. The known compounds; cyclen-based picolinic acid, cyclen-based phosphinic acid DOTPI, and cyclen-based phosphonic acid DOTP were selected for investigation in zirconium-89 complex formation, see Figure 31. The three known chelators were synthesised and then radiolabelling studies performed with two zirconium-89 salts (chloride and oxalate).

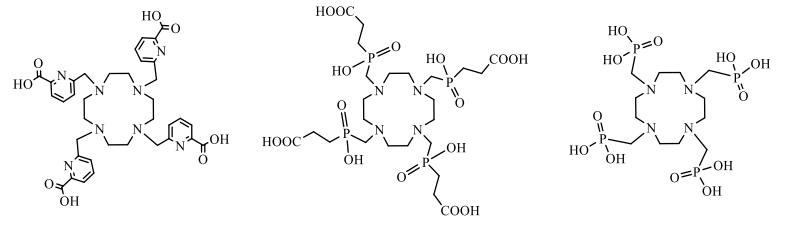

Figure 31 - Short arm cyclen chelators studied in this work.

Cyclen-based picolinic acid has four picolinic acid groups, which contain nitrogen and oxygen donor atoms for Zr to form out-of-cavity complex. The use of the picolinic functional group for complex formation with ^{111}In, ^{90}Y, ^{177}Lu and [^{89}Zr]Zr(IV) has previously been reported. The linear compound H_4octapa has two carboxylic acid and two picolinic acid groups and H_6phospa has two phosphoric acid and two picolinic acid groups. H_4octapa was labelled with ^{111}In and compared to DTPA and DOTA. The results showed that H_4octapa had slightly better stability than DTPA and DOTA.[98] The bifunctional chelator *p*-SCN-Bn-H_4octapa was labelled with ^{90}Y to obtain >95 % radiochemical yield and had comparable *in vivo* performance to *p*-SCN-Bn-CHX-A"-DTPA.[110] H_6phospa was labelled with ^{111}In and ^{177}Lu. However H_4octapa and H_6phsopa were not suitable for [^{89}Zr]Zr(IV) complex formation. Although

H_4octapa and H_6phospa did not show good [^{89}Zr]Zr(IV) radiolabelling efficacy, picolinic acid function group on macrocyclic backbone is worth studying further.

Cyclen-based phosphinic acid DOTPI includes carboxylic acid groups at the end of the phosphinate pendant arms. The linear phosphinate pendant arm could potentially form octadentate complexes with Zr either using the azamacrocycle nitrogens or in an "out of cavity" binding mode. The Gd(III) complex of this compound was reported that it formed "out of cavity" binding with four phosphinate oxygen atoms, two carbonyl oxygen atoms from carboxylate groups and two water molecules as an intermediate, it then rearranged to form "in cavity" complex.[111] DOTPI has previously been radiolabeled with ^{177}Lu and ^{64}Cu and the results showed that the complexes were stable under DTPA and EDTA challenges.[99]

During this work another competing group also investigated the cyclen-based phosphonic acid chelator DOTP for complexation with Zr(IV). [^{89}Zr]Zr(IV) radiolabelling condition with 100% radiochemical yield by using [^{89}Zr]zirconium(IV) chloride.[108]

2.2.1. Synthesis of 1,4,7,10-tetraazacyclododecane-1,4,7,10-tetra(methylenephosphonic acid) (DOTP)

As already discussed, azamacrocyclic compounds are reported to have greater thermodynamic stability and kinetic inertness than linear ligands.[112] There were a number of macrocycles studied for the complexation with lanthanide cations (Ln^{3+}). One of them is DOTP, which is an acronym of 1,4,7,10-tetraazacyclododecane-1,4,7,10-tetra(methylenephosphonic acid). The cyclen has four methylene phosphonate pendant arms attached. The lanthanide ions are thought to be positioned above the macrocyclic ring but coordinated by the four atoms of nitrogen.[113] This complex showed the higher stability constant and stereochemical rigidity than the standard lanthanide tetraacetic acid equivalent complex, $Ln(DOTA)^-$.[114] DOTP is an appropriate complex formation with the hard cation, Zr^{4+}, which generally prefers anionic oxygen donor atoms.[52]

The synthesis of DOTP can be performed by two methods; a one-pot synthesis and via a protective group strategy.[115-118]

For the one-pot synthesis, the procedure has been reported by different synthetic routes. The ratio of starting materials, reaction time and concentrations were varied. In this work, the synthesis procedure was following a modified literature method based on the report by Sherry, *et al.* in 1992 which indicated that the reaction was complete in 60 minutes and the product obtained in a relatively high yield (78 - 82%).[115] Formaldehyde was added drop-wise into a mixture of cyclen, phosphorus acid and hydrochloric acid while refluxing. The reaction time

was varied from 4 to 48 hours, then the reaction mixture was cooled to room temperature and evaporated. The residue was redissolved in acetone (100 mL) and stirred at 0ºC for 3 hours. The precipitate was filtered and dried *in vacuo* for 8 hours to yield an off-white solid, see Scheme 2.

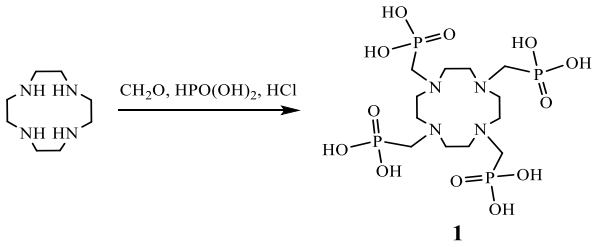

1

Scheme 2 - Synthesis of DOTP **1**.

N-functionalisation of six nitrogen atoms on hexaaza macrocycle was reported by Griffin J., *et al.* in 1999, and the reaction could be completed in 4 hours.[119] However, in this work, it was found that the reaction was not complete in 4 hours. ^{31}P NMR showed several peaks from 4.53 to 9.40, which were considered to be impurities from the phosphoric acid. Although, the product was purified by precipitation, the ^{31}P NMR still showed peaks for impurities.

To improve the reaction, after addition of formaldehyde, the mixture was refluxed for 24 hours. Nevertheless, ^{31}P NMR still showed peaks of unreacted phosphoric acid at 4.92 to 8.94, see Figure 32A. Therefore, the reaction time was extended to 48 hours.

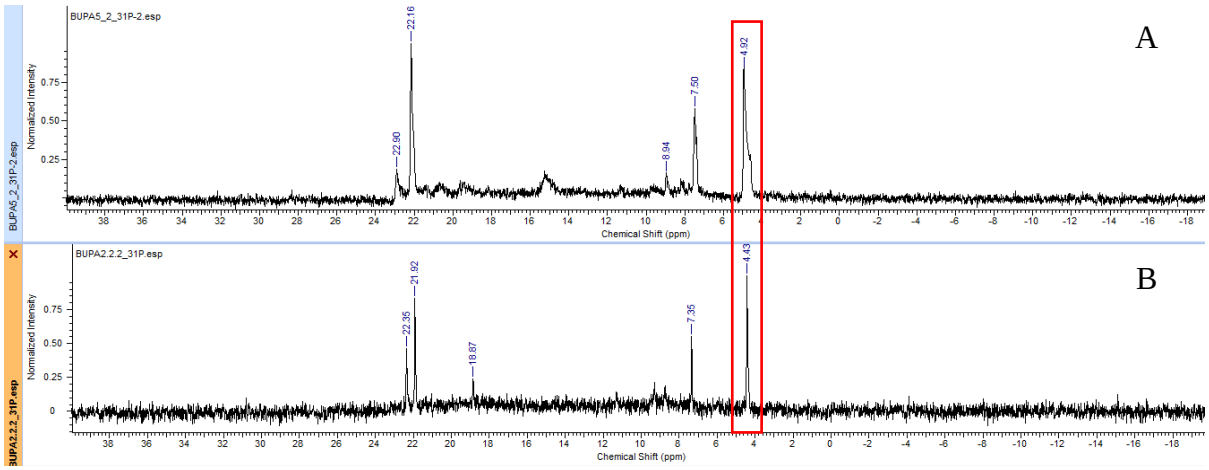

Figure 32 - ^{31}P-NMR of DOTP (**1**) after reflux for (A) 24 and (B) 48 hours.

After 48 hours, the yield for this reaction was only 29%. ^{31}P NMR showed singlet peaks at δ 21.92 and 22.35 for multiple macrocycle products, and other impurities were still present at 4.43 and 7.35, see Figure 32B. The ^{1}H NMR showed broad peaks for the macrocycle CH_2 signal. ESI-MS(+) detected the $[M+H]^+$ of the product as well as partially reacted three arms and two arms compounds.

It is very difficult to purify the obtained product by silica gel column chromatography as its high polarity prevents the product from eluting. Therefore, to improve the purity, DOTP was synthesised by an alternate multi-step method.

The alternative method was synthesis of octaethyl ((1,4,7,10-tetraazacyclododecane-1,4,7,10-tetrayl)tetrakis(methylene))tetrakis(phosphonate) to be a starting material for synthesis of DOTP.

The synthesis of octaethyl ((1,4,7,10-tetraazacyclododecane-1,4,7,10-tetrayl)tetrakis (methylene))tetrakis(phosphonate) followed the literature procedure[118], see Scheme 3. It was synthesised from cyclen by reaction with paraformaldehyde and excess triethylphosphite at 40°C for 3 days, then the crude product was purified by silica gel column chromatography using a gradient elution method.[120] Triethyl phosphite was eluted with $(C_2H_5)_2O$: MeOH (70:30) and the product **2** was eluted with $(C_2H_5)_2O$: MeOH : NH_4OH (65:30:5).

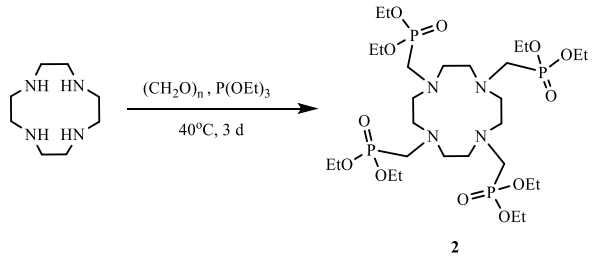

2

Scheme 3 - Synthesis of octaethyl((1,4,7,10-tetraazacyclododecane-1,4,7,10-tetrayl)tetrakis(methylene))tetrakis(phosphonate) (**2**).

The product was obtained in various yields ranging from 25 to 53% which was significantly lower than the literature reports (>90% yield). This may have been due to the alternative purification process used. A Dowex 50 column ion exchange chromatography was used to purify the tetraphosphonate chelate in the published method, whereas silica gel column was used in this work as it was used for almost all chelators synthesised in this study. The conditions for silica gel column chromatography emulated the purification used in the purification of the DOTA derivative, 1-(1-octyl-methyl-phosphonate)-4,7,10-tris(methylene phosphonate)-1,4,7,10-tetraazacyclododecane.

^{31}P, ^{1}H and ^{13}C NMR showed the isolated compound to be relatively pure. According to ^{31}P NMR, the purity of the product was about 92%. ESI-MS(+) detected the $[M+H]^+$ of the product.

Octaethyl ((1,4,7,10-tetraazacyclododecane-1,4,7,10-tetrayl)tetrakis(methylene)) tetrakis(phosphonate) **2** was hydrolysed by heating under reflux in 6 M HCl for 4 days, see Scheme 4.[61] The product **1** showed 92% purity, which was characterised by ^{31}P NMR in a yield of 98%.

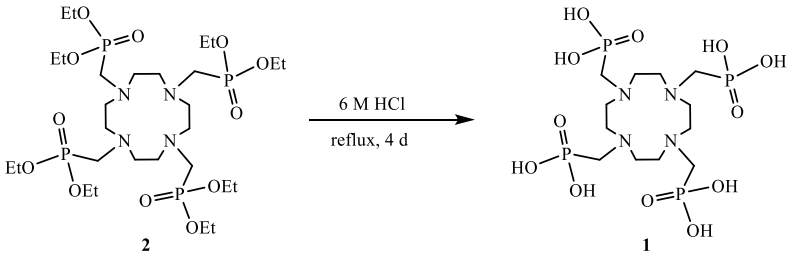

Scheme 4 - Synthesis of **1** from **2**.

NMR analysis showed that the DOTP synthesised by an the multi-step method had much better purity and the average product yield was higher than DOTP from the initial method attempted; therefore, DOTP from the multi-step method was used in the [^{89}Zr]Zr(IV) radiolabelling study.

2.2.2. Synthesis of 1,4,7,10-tetraazacyclododecane-1,4,7,10-tetra[methyl(2-carboxyethyl) phosphinic acid] (DOTPI)

DOTPI, a cyclen based phosphinic acid, was a macrocycle-based phosphinate derivative developed by Notni and co-worker from 1,4,7-triazacyclononane-1,4,7-tris[methyl(2-carboxyethyl)phosphinic acid] (TRAP-Pr), see Figure 33.[111]

TRAP-Pr is *N*-substitution of triazacyclononane with (2-carboxyethyl)phosphinic acid arms. It was used as ^{68}Ga and ^{64}Cu tracer to improve pH range of radiolabelling condition. Due to the lower pK_a of phosphinic acid (<1) compared to carboxylic acid (~4), it was found that TRAP-Pr could be radiolabelled at a much lower pH than NOTA and DOTA.[121-125] For Ga(III) complexation of TRAP derivatives it was reported that, in acidic conditions (even at pH 0) Ga(III) formed the "in cavity" complex, but formed the "out of cavity" complex under neutral conditions.[102] As the complexation occurs at pH as low as 0, it allows ^{68}Ga radiolabelling in the presence of 0.1 M HCl.[126] Furthermore, the advantage of phosphinic acid functional group

is that the three carboxylic acid moieties can be functionalised and used as conjugation sites without protection of the phosphinic acid moieties during *N*-functionalisation of TACN so that the synthesis can be performed using a one-pot method.[121, 127]

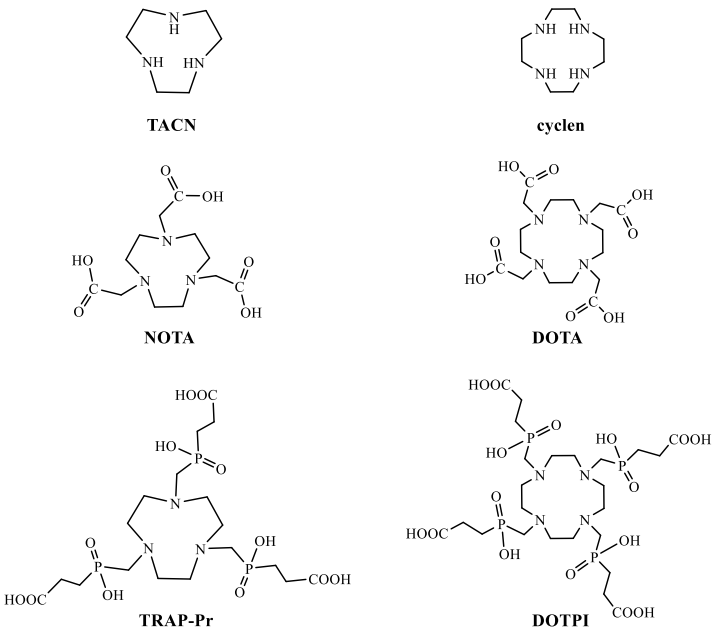

Figure 33 - Structures of TACN and cyclen-based carboxlic and phosphinic acids.

For cyclen-based tetraphosphinic acid chelator DOTPI, it was first synthesised by using cyclen (1 equiv.) reacted with (2-carboxyethyl)phosphinic acid (15 equiv.) and paraformaldehyde (36 equiv.) in 6 M HCl at 70ºC for 46 hours, then purified by ion exchange chromatography and crystallised by isopropanol to give a 21% yield of the product.[111] The complexation with Gd(III) was performed and X-ray structure showed that it formed out-of-cage complex with 1:1 metal-to-ligand ratio in acidic condition.

To synthesise DOTPI in this work, the pendant arm; (2-carboxyethyl)phosphinic acid, was prepared and the cyclen was then *N*-functionalised with this derivative.

2.2.2.1. Synthesis of (2-carboxyethyl)phosphinic acid

(2-Carboxyethyl)phosphinic acid was synthesised to be a pendant arm for a macrocyclic chelator; 1,4,7,10-tetraazacyclododecane-1,4,7,10-tetra[methyl(2-carboxyethyl)phosphinic acid] (**5**).

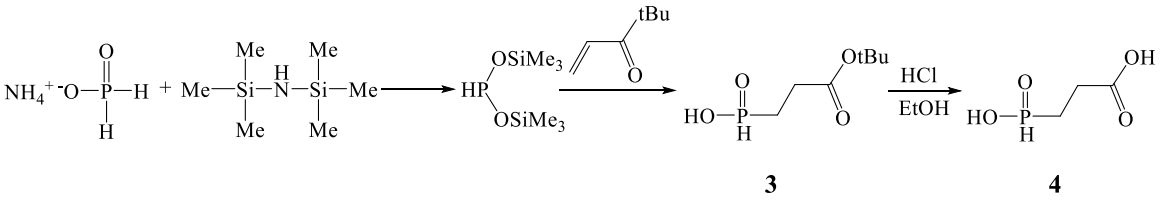

Scheme 5 - Synthesis of (2-carboxyethyl)phosphinic acid (**4**).

The synthesis of (2-carboxyethyl)phosphinic acid followed the literature procedure, see Scheme 5.[121] The first step of the reaction was performed under an N_2 atmosphere as the intermediate $HP(OSiMe3)_3$ is pyrophoric. According to the literature, this step was expected to be complete in about 6 hours; however, it could be considered to be finished when ammonia gas production ceased. The yield (96%) was as expected as it was reported that 95% yield had been obtained in the literature preparation. The purity of the product was analysed by ^{31}P NMR and shown to be 96%, which is similar to the literature report.

2.2.2.2. Reaction of (2-carboxyethyl)phosphinic acid with cyclen to form 1,4,7,10-tetraazacyclododecane-1,4,7,10-tetra[methyl(2-carboxyethyl) phosphinic acid] (DOTPI)

1,4,7,10-Tetraazacyclododecane-1,4,7,10-tetra[methyl(2-carboxyethyl)phosphinic acid] **5** was developed to test for the first time as a [^{89}Zr]Zr(IV) chelator. The synthesis of **5** was initially attempted following a modified literature procedure, see Scheme 6.[111]

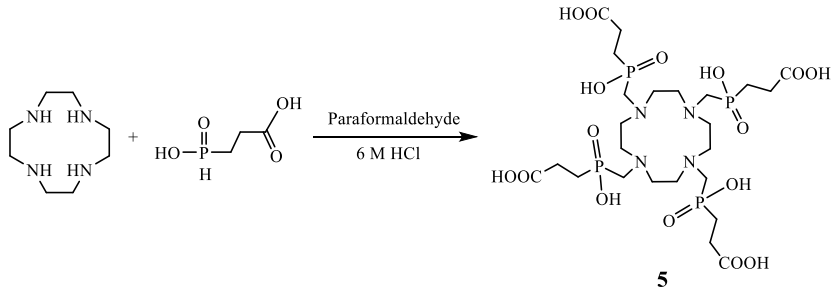

Scheme 6 - Synthesis of DOTPI **5**.

(2-Carboxyethyl)phosphinic acid, in a twelve-fold excess, and cyclen were dissolved in 6 M HCl (10 mL) and the reaction mixture was heated to reflux. Paraformaldehyde (23 equiv.) was then added in 6 portions over 24 hours with stirring. ^{31}P NMR was used to monitor the reaction at 24, 48 and 72 hours. It was found that the peak for the starting material; (2-carboxyethyl)phosphinic acid **4**, at 36.69 ppm decreased over 72 hours, while the peaks at

51.65 and 56.21 which were assigned to the product and the by-products from *N*-methylation increased, see Figure 34. The product peak was detected in MS at 771.3.

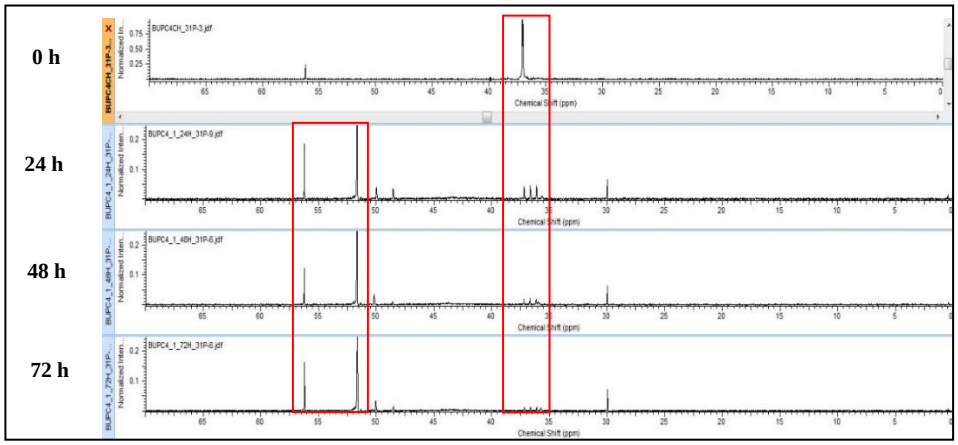

Figure 34 - Reaction monitoring of synthesis of DOTPI (**5**) by ^{31}P NMR.

An attempt was made to purify the crude product by dialysis; however, this was not successful. The purification method by ion-exchange chromatography was performed by using DOWEX Marathon C H^+-form, column size 10 x 1 cm, eluted with water 1 mL for each fraction, and the fractions analysed by MS. The fractions where the product was detected were collected. ^{1}H NMR showed that the product still was not pure with a mixture of the product and excess (2-carboxyethyl)phosphinic acid, see Figure 35. Crystallisation was attempted by concentrating the fractions containing product to a volume of ~ 5mL, and adding methanol (50 mL) and isopropanol (25 mL) but no crystal was observed after 3 days.

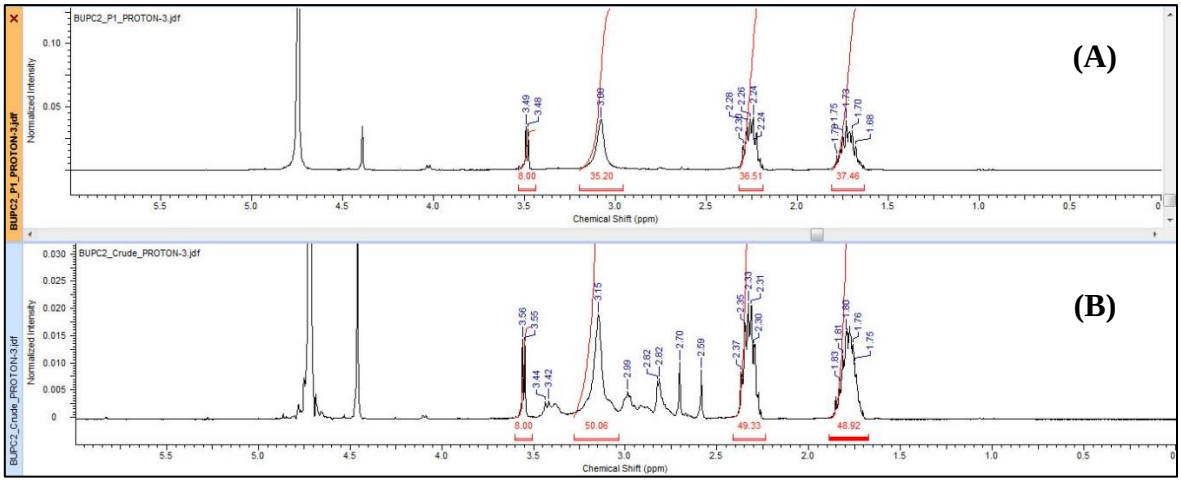

Figure 35 - ^{1}H NMR of DOTPI (**5**) (A) after purification by ion exchange resin, (B) reaction mixture.

Despite the compound not being pure, a preliminary radiolabelling study was still carried out, see section 2.3.6.4. This was used to assess whether further research effort should be put into isolation of the pure compound as indication of radiolabelling potential.

2.2.3. Synthesis of 6,6',6'',6'''-((1,4,7,10-tetraazacyclododecane-1,4,7,10-tetrayl)tetrakis (methylene))tetrapicolinic acid (9)

Picolinic acid is an isomer of nicotinic acid, see Figure 36.[128]

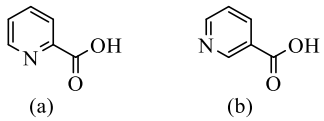

Figure 36 - Chemical structures of (a) picolinic acid and (b) nicotinic acid.

Picolinic acid and its derivatives have been widely studied for complexation with transition metal such as the complexation of Cu(II) with acyclic compounds; 3,6-dichloropicilinic acid and 3,4,5-trichloropicolinic acid [129], and complexation of ^{111}In with Bn-H_3nonapa, *p*-NO2-Bn-H_3nonapa and Bn-H_3trenpa.[130] It was also reported the application for MRI as contrast agent of macrocyclic compounds based picolinic acid Mn^{2+},[131] see Figure 37.

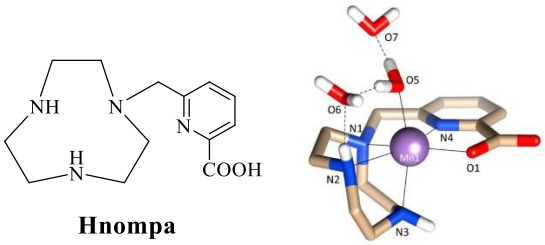

Figure 37 - An example of Mn complex studied for MRI.[131]

The complex formation of picolinic acid with Zr was reported by Muller and co-workers in 2011.[132] The crystal structure showed that Zr is coordinated with four picolinate anions with Zr-O distances of 2.120 (2) Å and Zr-N distances of 2.393 (2) Å, and N-Zr-O bond angle of 67.79 (7)^o, see Figure 38.

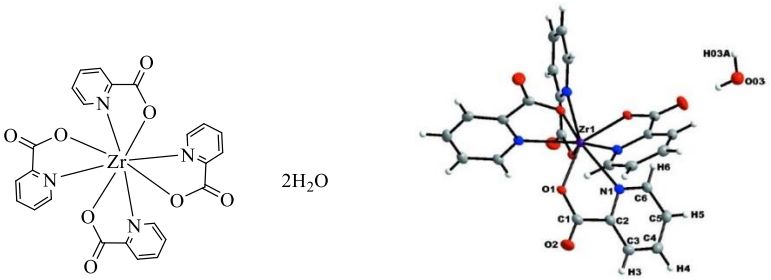

Figure 38 - Structure of Zr-picolinate.[132]

The potential for binding Zr is of interest in the development of macrocyclic compound functionalised with picolinic acid arms for Zr complexation; therefore, cyclen with picolinic acid pendant arms was synthesised in order to provide eight binding sites for zirconium.

2.2.3.1. Synthesis of 6-chloromethylpyridine-2-carboxylic acid methyl ester

6-Chloromethylpyridine-2-carboxylic acid methyl ester was synthesised to be used as a pendant arm for attachment to cyclen. The synthesis was performed following the literature procedure published by Rodrıguez-Blas *et al*. in 2008 as this reaction is completed in a few hours, see Scheme 7.[133] Pellet-Rostaing *et al.* used an alternate synthesis route which was run overnight and gave the product in an 82% yield.[134]

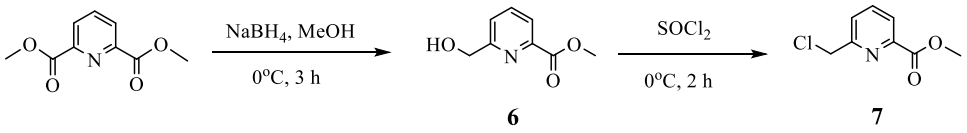

Scheme 7 - Synthesis of 6-chloromethylpyridine-2-carboxylic acid methyl ester (**7**).

The synthesis of **7** was performed in two reaction steps. The first reaction is the reduction of one of the two methoxy groups of dimethylpyridine-2,6-dicarboxylate methyl ester, carried out in methanol. Three equivalents of sodium borohydride were added in small portions within 30 minutes then the reaction was maintained at 0°C for 3 hours, followed by extraction with chloroform. The product was obtained in a moderate yield (53%). A larger excess sodium borohydride accelerated the reaction; however, it could reduce both ester groups. To produce the compound **7**, thionyl chloride was added drop-wise to compound **6** while it was stirred at 0°C under N_2 atmosphere for 2 hours, it was then extracted with toluene and precipitated in diethyl ether to give the product in a 78% yield similar to Rodrıguez-Blas's method.[133]

2.2.3.2. Synthesis of 6,6',6'',6'''-((1,4,7,10-tetraazacyclododecane-1,4,7,10-tetrayl)tetrakis (methylene))tetrapicolinic acid (9)

The synthesis of 6,6',6",6'"-((1,4,7,10-tetraazacyclododecane-1,4,7,10-tetrayl)tetrakis (methylene))tetrapicolinic acid (**9**) was developed from the protocol reported by Pellet-Rostaing *et al.* in 2015.[134] In this literature report, cyclen was reacted with 6-chloromethylpyridine-2-carboxylic acid methyl ester in acetonitrile at 80ºC for 12 hours, purified by extraction with dichloromethane to give 82% yield of compound **8**. The intermediate product was hydrolysed in 6 M HCl to gain the final product in a 93% yield.

In this work, the synthesis of the compound **8** was initially attempted with 6-chloromethylpyridine-2-carboxylic acid methyl ester (4 equiv.) using basic conditions at 50ºC, see Scheme 8.

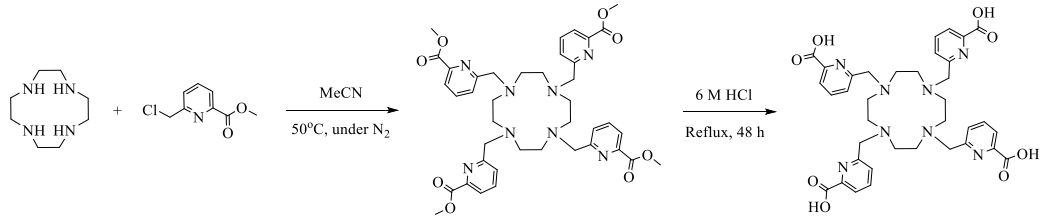

8 **9**

Scheme 8 - Synthesis of 6,6',6",6'"-((1,4,7,10-tetraazacyclododecane-1,4,7,10-tetrayl)tetrakis(methylene))tetrapicolinic acid (**9**).

However, partially reacted products were found even if the reaction was performed for 2 days, see Figure 39. The number of equivalents of 6-chloromethylpyridine-2-carboxylic acid methyl ester used was then increased to five equivalents to form more of the desired product **8**.

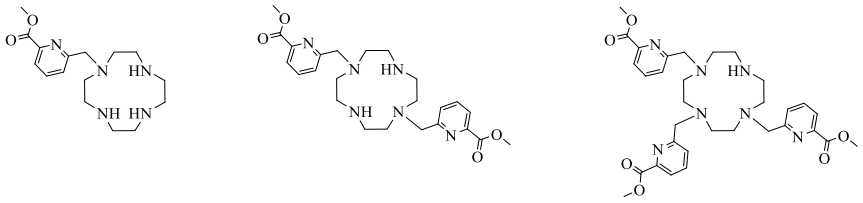

Figure 39 - By products from the reaction of synthesis of **8**.

The crude product was purified by silica gel column chromatography. The first elution with hexane:ethyl acetate (1:3) removed the excess 6-chloromethylpyridine-2-carboxylic acid methyl ester, while the second elution with chloroform:methanol (8:2) flushed off the product **8** (47% yield). The yield could possibly be further improved if the amount of 6-

chloromethylpyridine-2-carboxylic acid methyl ester and temperature of the reaction were increased. The purified ester **8** was hydrolysed by reflux in 6 M HCl for 48 hours to obtain **9** (93% yield).

HPLC analysis was used to show that **9** was pure using an ACE5 C18 column, 250 x 4.6 mm, flow rate 1 mL/min, gradient of A (methanol) and B (0.2 M ammonium formate pH 3), t = 0 min, 5% A; t = 25 min, 50% A; t = 26 min, 5% A; t = 30 min, 5% A., see Figure 40.

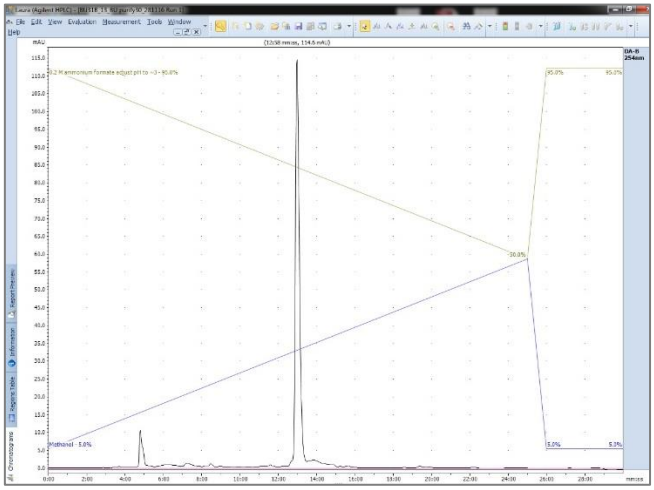

Figure 40 - HPLC chromatogram of **9**.

2.3. Radiolabelling with zirconium-89

Complex formation of compounds **1**, **5** and **9** was attempted with the stable Zr isotope to give a "cold standard" compound; however, there were problems with the formation of insoluble species. Therefore the compounds were moved on to radiolabelling studies where it is easier to analyse low concentration amounts due to high sensitivity detection of the radioactive species.

2.3.1. [^{89}Zr]zirconium(IV) oxalate for radiolabelling

[^{89}Zr]Zr(IV) in 1.0 M oxalic acid was supplied by Perkin Elmer. Zirconium forms a stable complex with oxalic acid at low pH. The simulation of the mechanism of the reaction from Zr-oxalate; $[Zr(C_2O_4)_4]^{4-}$, to Zr-hydroxamate; $Zr(MeAHA)_4$, was investigated by density functional theory method for both acidic and basic condition.[79] It was found that under acidic conditions, it is very difficult to dissociate oxalate and coordinate hydroxamate. For this reason, [^{89}Zr]Zr(IV) has to be neutralised with 1 M Cs_2CO_3 to reach pH 7 before radiolabelling.

2.3.2. Characterisation methods to analyse [^{89}Zr]Zr(IV) complexes

DFO and three chelators; **1**, **5** and **9**, were labelled with [^{89}Zr]Zr(IV). In order to analyse [^{89}Zr]Zr(IV) complex, radio-HPLC was attempted by using the reverse phase Jupiter Phenomenex 5 µm C-18 300A 150x4.6 mm. eluting with gradient of A (acetonitrile with 0.1% TFA) and B (distilled water with 0.1% TFA), t = 0 min, 2% A; t = 15 min 36 sec, 52% A; t = 17 min, 2% A; t = 18 min, 2% A. [^{89}Zr]ZrDFO was eluted at 6:21 min. However, free [^{89}Zr]Zr(IV) could not be eluted out of the column. It needed to be washed out by injecting a DFO solution several times. Therefore, with this column, the radio-HPLC cannot be used and radio-ITLC was used to analyse [^{89}Zr]Zr(IV) radiolabelling for all compounds in this research. It is important to know how much unreacted zirconium-89 is present to determine the reaction yields and optimise the conditions.

This was done by radio-ITLC equipped with a NaI detector at a scan speed of 0.1 mm/sec. It was shown that the slower speed could improve the signal of chromatogram, see Figure 41. Data was recorded using Lablogic Laura (version 4.1.7.70) software.

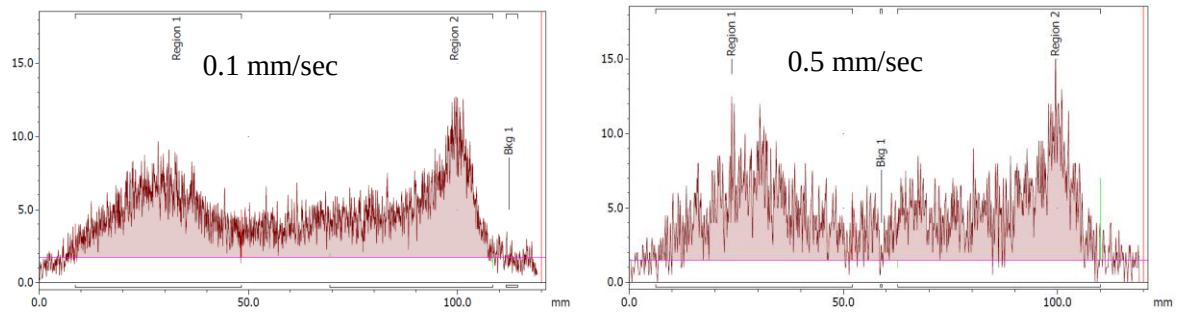

Figure 41 - Comparison of radio-ITLC chromatograms of [^{89}Zr]ZrDFO at concentration of DFO 0.1 µM using slow and fast scan speeds.

The analysis of [^{89}Zr]Zr(IV) complexes is performed on a basis of [^{89}Zr]Zr(IV) complex remains at the baseline whilst the unreacted [^{89}Zr]Zr(IV) salt moves with the mobile phase to the solvent front. There are various types of mobile phase reported for use with [^{89}Zr]Zr(IV) such as DTPA 50 mM pH 7[135], citric acid/ trisodium citrate[136], and EDTA 0.1 M pH 5[108] or 10 mM pH 6 [137]. However, Guerard has claimed that using ITLC-SG strips and 10 mM EDTA solution pH 6 as mobile phase was found to be the best way to distinguish "free" [^{89}Zr]Zr(IV) ions from the formed [^{89}Zr]Zr(IV) complex.[137] The comparison of radio-ITLC conditions for [^{89}Zr]ZrDFO was tried by using ITLC-SG with citric acid/ trisodium citrate, EDTA 0.1 M pH 5, and 10 mM pH 6. The results are shown in Table 3.

It was found that all three eluents could complex the "free" [^{89}Zr]Zr(IV) ions and move them to the solvent front. Nevertheless citric acid/ trisodium citrate was not an appropriate mobile phase as [^{89}Zr]ZrDFO did not remain at origin but had an R_f of ~0.45. While EDTA 0.1 M pH 5 and 10 mM pH 6 showed similar results but the tail observed was a disadvantage of using EDTA 0.1 M pH 5. Therefore, the selected ITLC conditions for radiolabelling reactions used ITLC-SG with EDTA 10 mM at pH 6.

Table 3 - Comparison of radio-ITLC chromatograms of free [^{89}Zr]Zr(IV) and [^{89}Zr]ZrDFO using different eluents

Mobile phase	Free [^{89}Zr]Zr(IV)	[^{89}Zr]ZrDFO
citric trisodium citrate	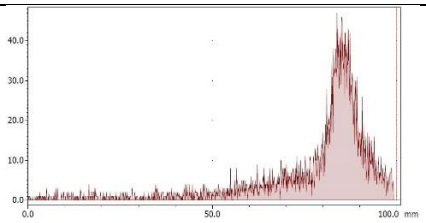	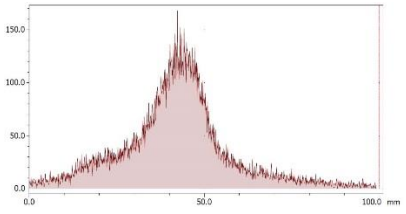
EDTA 0.1 M pH 5	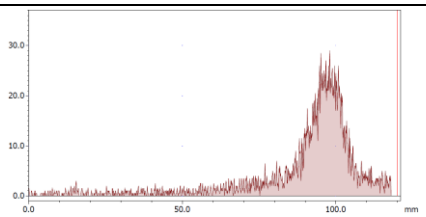	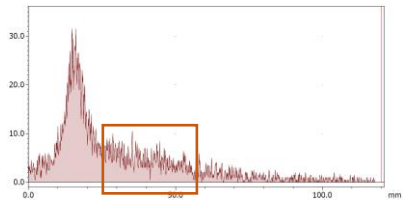
EDTA 10 mM pH 6	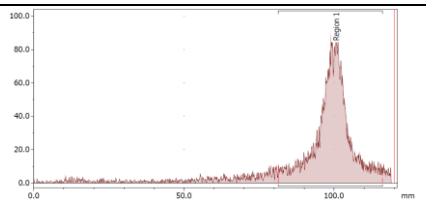	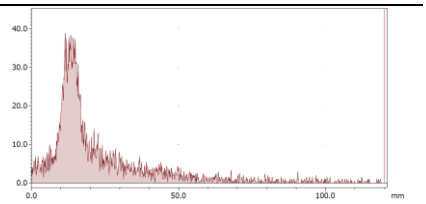

2.3.3. [^{89}Zr]zirconium(IV) oxalate radiolabelling of DFO

A solution of 1 mg/ml DFO (20 nmol) was labelled with neutralised [^{89}Zr]Zr(IV) (3 MBq) in water, total volume 100 µL, see Scheme 9. The reaction was carried out at room temperature for 30 minutes. Radio-TLC showed 100% labelling yield.

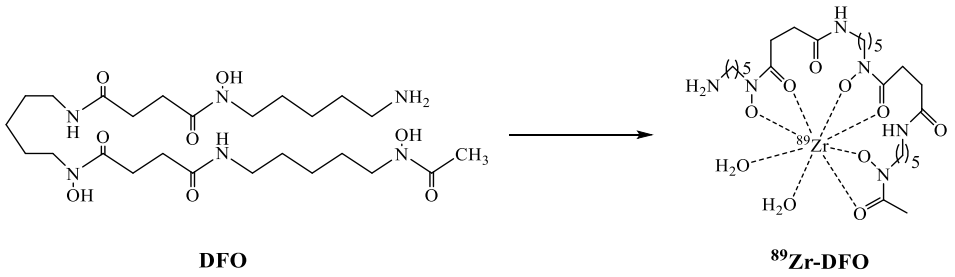

Scheme 9 - [^{89}Zr]Zr(IV) radiolabelling of DFO to form [^{89}Zr]ZrDFO.

Moreover, DFO was also labelled under various concentrations. The solutions of DFO were labelled with 0.5 MBq of [^{89}Zr]Zr(IV) and incubated at room temperature for 30 minutes (n = 3). The concentration curve indicated that the labelling yield reached 100% at the concentration of 0.56 µM (log [M] = -0.25), see Figure 42. The specific activity achieved was 8.8 GBq/mmol (237 mCi/mmol).

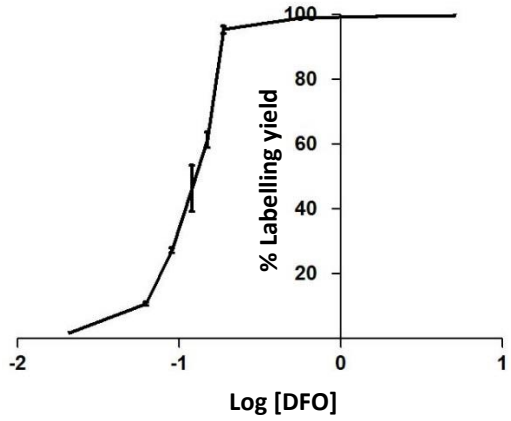

Figure 42 - Concentration curve of [^{89}Zr]ZrDFO using [^{89}Zr]zirconium(IV) oxalate for labelling.

2.3.4. [^{89}Zr]zirconium(IV) oxalate radiolabelling of macrocycles

In a preliminary study, all of the macrocyclic compounds were labelled under the same conditions, which was 0.2 mM of the compounds, 3 MBq of [^{89}Zr]Zr(IV) in 1 M ammonium acetate buffer pH 7, incubated at 95^{o}C for 2 hours. The results showed low labelling yields, see

Figure 43. Although the differences in the results were not significant in all cases due to the large error bars, the compound **9** was selected for further study.

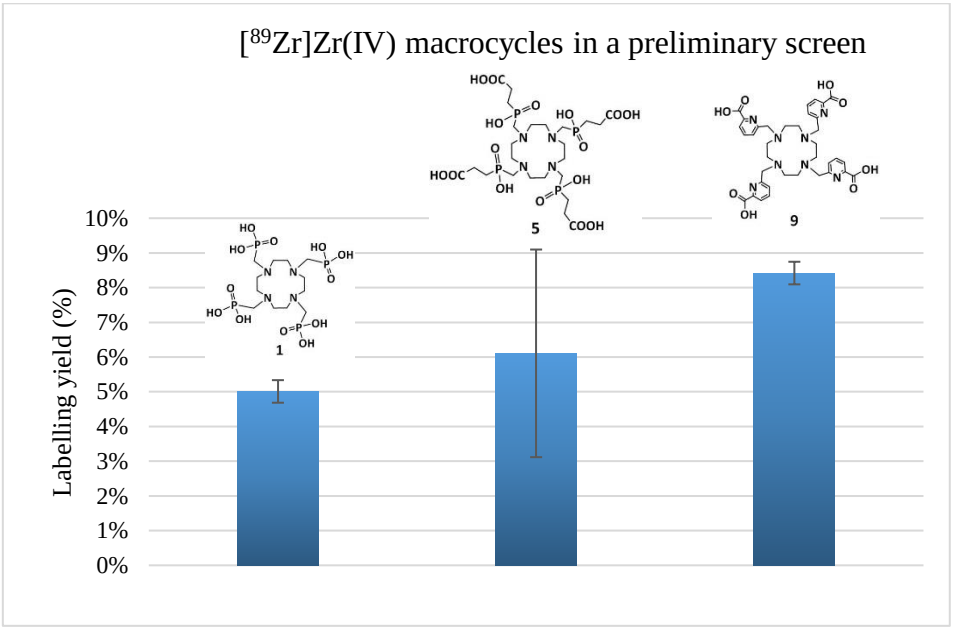

Figure 43 - Labelling yield in preliminary screen of [^{89}Zr]Zr(IV) macrocyclic compounds.

2.3.5. Optimisation of [^{89}Zr]Zr(IV) radiolabelling of cyclen based picolinic acid derivative (9)

The labelling conditions were optimised by using different pH solutions with 1 M and 0.2 M acetate buffer, water, and 0.1 M HCl.

To investigate the effect of buffer, the reaction in water and 0.2 M ammonium acetate buffer at pH 7 were compared. The yield of the reaction in buffer was much higher than in water. While the reactions in same buffer (0.2 M acetate buffer) but at different pH (7 and 4) were compared and found that the labelling was optimal in acetate buffer at pH 4. As the lower pH seems to be better, radiolabelling under acidic conditions was attempted by using 0.1 M HCl. However, the labelling yield was not improved, see Table 4. Therefore, it was concluded that the compound **9**, under the optimal conditions, can be labelled with [^{89}Zr]zirconium(IV) oxalate in 0.2 M acetate buffer pH 4 at 95^{o}C for 2 hours to give a 40% yield.

Table 4 - [^{89}Zr]Zr(IV) cyclen based picolinic acid yield at various conditions.

Solvent	pH	Labelling yield (%)
1 M acetate buffer	7	8
water	7	< 5
0.2 M acetate buffer	7	< 5
0.2 M acetate buffer	4	40
0.1 M HCl	2	7

In a report, carried out concurrently with this research work, that was published in 2017, the complexation of zirconium and tetraazamacrocycles; DOTA, DOTP and DOTAM, was demonstrated to be more effective using a zirconium-89 chloride precursor. Therefore it was decided to attempt labelling of the three macrocycles synthesised in this research with the [^{89}Zr]zirconium(IV) chloride precursor.

2.3.6. Radiolabelling with [^{89}Zr]zirconium(IV) chloride

Zirconium-89 chloride is of interest as a labelling precursor as the toxicity of oxalic acid is problematic. Oxalic acid can result in decalcification of blood and, ultimately, kidney failure.[138] The production of [^{89}Zr]zirconium(IV) chloride was investigated in 2009 by using Sep-pak Light QMA strong anion exchange cartridge, eluted with 1 M HCl and reconstituted in either water, 0.9% saline or 0.1 M HCl. Radionuclidic and radiochemical purity were not less than 99.99%.[139] [^{89}Zr]zirconium(IV) chloride was neutralised by Na_2CO_3 and labelled with DFO at room temperature to give a 100% radiochemical yield within 15 minutes. PET imaging was studied in mice that were injected with either [^{89}Zr]ZrDFO or [^{89}Zr]zirconium(IV) chloride. Images demonstrated that [^{89}Zr]ZrDFO localised in bladder and excreted rapidly through the kidneys while [^{89}Zr]zirconium(IV) chloride localised in the liver and remained there for more than 8 hours after administration. It was believed that [^{89}Zr]zirconium(IV) chloride forms insoluble species. The researchers suggested that the best way to radiolabel with [^{89}Zr]zirconium(IV) chloride is to use acetate buffer at pH 4.5-6.0. This relates to the study reported by Abou in 2011 which indicates that zirconium forms complexes with hydroxides and water molecules to give a colloidal form.[140]

As [^{89}Zr]zirconium(IV) chloride was found to be hydrolysed and then remains at the baseline of the TLC plate, it needs to be ensured that the conditions used for radiolabelling do not cause [^{89}Zr]Zr(IV) colloid formation.

2.3.6.1. Preparation of [^{89}Zr]zirconium(IV) chloride

[^{89}Zr]zirconium(IV) chloride was prepared following Wadas's method reported in 2017 [108] by using Sep-pak Light accell plus QMA strong anion exchange cartridge (300 Å, 37-55 µm) pre-washed with 6 mL MeCN, 0.9% NaCl 10 mL, and water 10 mL. A solution of [^{89}Zr]zirconium(IV) oxalate in 1.0 M oxalic acid was loaded on to the Sep-pak cartridge then washed with water (> 50 mL) to remove oxalic acid and eluted [^{89}Zr]Zr(IV) with 1.0 M HCl (0.4 - 0.5 mL) to obtain the product with a 60-90 % recovery.

2.3.6.2. Control reactions to determine colloidal species formation

Control reactions were performed in water pH 4-7, 0.2 M acetate buffer at pH 4-7, and 0.5-1 M HEPES adjusted to pH 7, with [^{89}Zr]zirconium(IV) chloride (0.5 MBq) at 95^{o}C for 2 hours, see Table 5.

Table 5 - Control reactions with [^{89}Zr]zirconium(IV) chloride in different solvent systems.

	pH 4	pH 5	pH 6	pH 7
Water	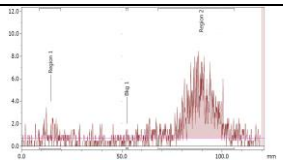	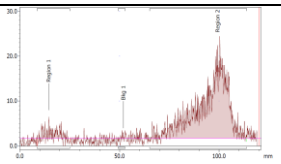	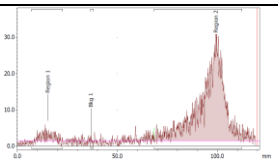	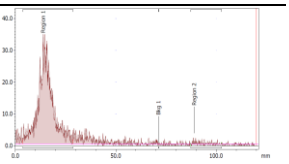
0.2 M acetate buffer	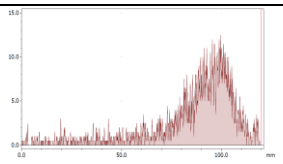	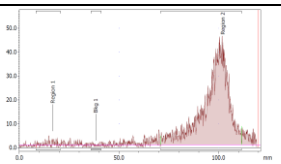	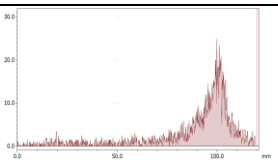	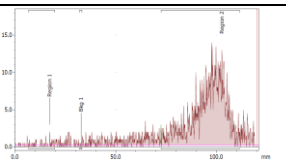
0.5 M HEPES	-	-	-	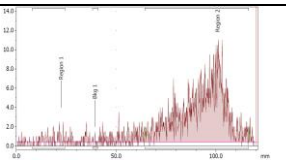
1 M HEPES	-	-	-	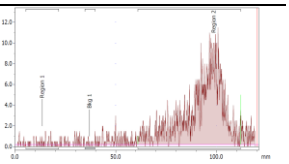

Therefore [^{89}Zr]zirconium(IV) chloride labelling should not be performed in water at pH above 6 to avoid colloidal species formation.

2.3.6.3. [^{89}Zr]zirconium(IV) chloride radiolabelling of DFO

[^{89}Zr]zirconium(IV) chloride (0.5 MBq) was labelled with DFO in water at pH 6 at a chelator concentration of 0.06 to 5.07 µM at room temperature for 30 minutes. The concentration curve showed that the labelling yield increased with the increasing concentration of DFO and reached 100% when the concentration was 5 µM (log [M] = 0.71), see Figure 44.

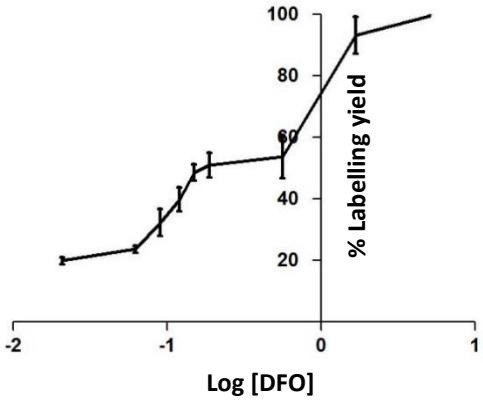

Figure 44 - Concentration curve of [^{89}Zr]ZrDFO using [^{89}Zr]zirconium(IV) chloride for labelling.

2.3.6.4. [^{89}Zr]zirconium(IV) chloride radiolabelling of macrocycles

According Pandya *et al.* 2017, macrocyclic compound DOTP (10 µg) was labelled with [^{89}Zr]zirconium(IV) chloride 40 MBq in water at pH 7-7.5 in total volume 110 µL at 95^{o}C for 45 minutes. An attempt was made to label **1** using similar conditions. The solution of 1 mg/mL of the compound (10 µL) was labelled with [^{89}Zr]zirconium(IV) chloride (0.5 MBq) due to the limited amount of activity available for the reactions, this is sufficient for radio-ITLC measurements. The reaction was performed in water adjusted to pH 6 as described previously, in a total volume of 110 µL. After incubation at 95^{o}C for 1 hour, the labelling yield was only 7.5 ± 2.0%, see Figure 45. It seems pH of the reaction is the major factor and further study of the labelling conditions is required to improve the yield.

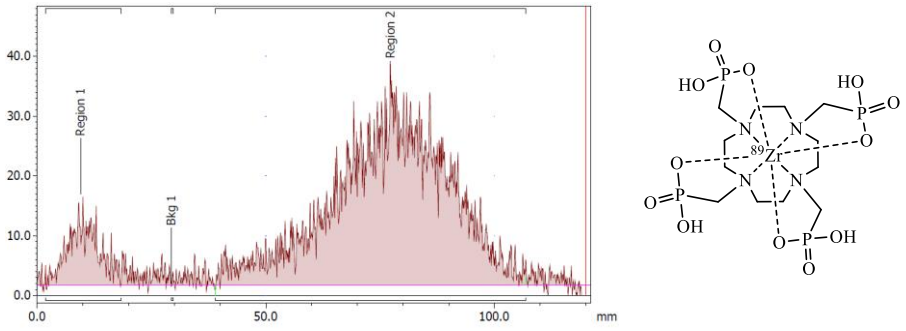

Figure 45 - Radio-ITLC of [^{89}Zr]Zr**1**.

Labelling of **5** was attempted with [^{89}Zr]zirconium(IV) chloride with the same conditions as used for **1** but this was not successful, with no product isolated. It has been reported previously that the complex of DOTPI with Gd was found both “in cavity” and “out of cavity” binding, see Figure 46.

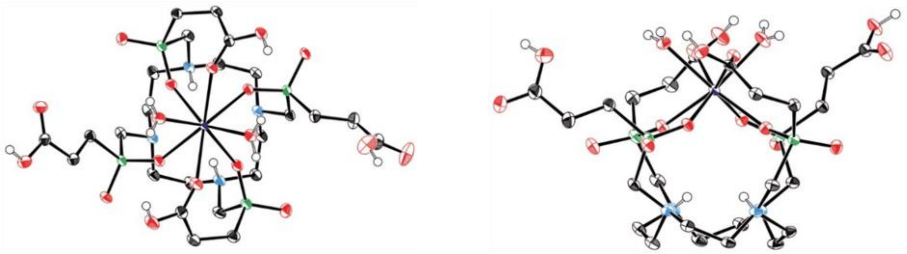

Gd-DOTPI in-cavity **Gd-DOTPI out-of-cavity**

Figure 46 - The structures of Gd-DOTPI.[111]

It is a possibility that DOTPI could complex with Zr(IV) by the four N atoms of cyclen and four O atoms of the arms, similar to DOTP. “Out of cavity” binding with eight oxygen donor atoms of phosphinic moieties is also possible, see Figure 47.

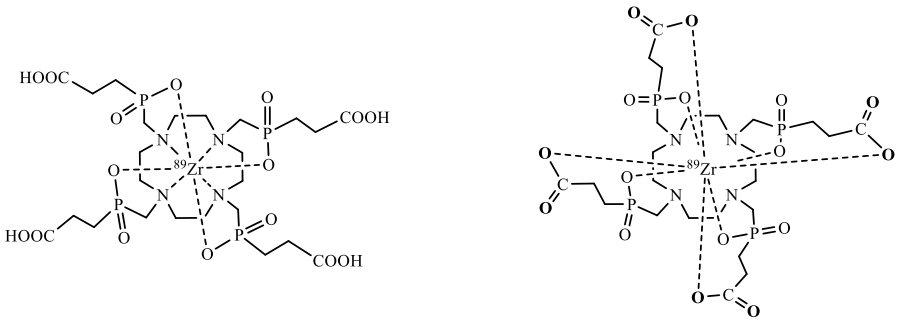

"in cavity" binding **"out of cavity" binding**

Figure 47 - The predicted structures of [^{89}Zr]Zr**5**.

In a similar way as considered for **5**, **9** might form complexes with Zr in both “in cavity” and “out of cavity” forms, see Figure 48.

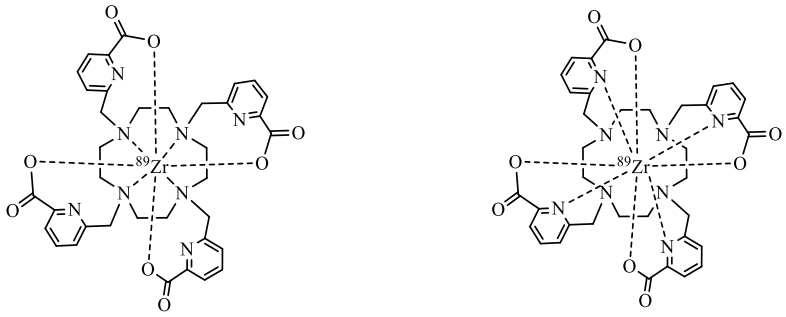

"in cavity" binding **"out of cavity" binding**

Figure 48 - The predicted structures of [^{89}Zr]Zr**9**.

An attempt was also made to label **9** with [^{89}Zr]zirconium(IV) chloride. The reaction was performed in water, 0.5 M HEPES and acetate buffer. The solution of 1 mg/mL of **9** (10 µL) was reacted with [^{89}Zr]zirconium(IV) chloride (0.5 MBq) adjusted to the required pH in a total volume of 110 µL and incubated at 95ºC for 2 hours. The results are shown in Table 6.

Table 6 - Radiolabelling yields of 9.

Solvent	pH of the reaction	% Labelling yield
Water	6	22.3 ± 3.1
0.2 M acetate buffer	4	25.6 ± 1.1
0.2 M acetate buffer	5	22.4 ± 0.5
0.2 M acetate buffer	6	49.3 ± 3.4
0.2 M acetate buffer	7	42.8 ± 4.9
0.5 M HEPES	7	0

The labelling of the three macrocyclic chelators **1**, **5** and **9** using zirconium-89 chloride can be compared under the same reaction conditions (water at pH 6), showing that the best labelling yield was achieved for **9** (7.5%, 0% and 22.3% respectively). This is similar to the labelling results with [^{89}Zr]zirconium(IV) oxalate where the yield observed with **9** was the highest. The reaction conditions were studied for **9** in order to optimise buffer and pH of the labelling conditions. This showed that the reaction in 0.2 M acetate buffer at pH 6 gave the best labelling yield.

It is possible that Zr forms complex with these chelators in different ways. As picolinic acid arms themselves can offer eight donor atoms, Zr could form octadentate coordination out of cyclen ring with these pendant arms, although this may be sterically strained. While, for DOTP, Zr has to bind four nitrogen atoms in cavity and four oxygen atoms of the pendant arms if the chelator is to bind as an octadentate chelator. For DOTPI, phosphinic acid arms also provide eight potential binding sites; however, the purity of the compound was a concern and this factor may have resulted in the radiolabelling failure. The development for second generation chelators focussed on out-of-cavity binding and the use of the picolinic acid functional group.

2.4. Conclusion

Three known cyclen-based macrocyclic chelators were synthesised that, at the time of carrying out the work, had not been investigated for zirconium-89 labelling. *N*-Functionalisation was performed by reacting with phosphoric acid, phosphinic acid and picolinic acid. [^{89}Zr]Zr(IV) radiolabelling was attempted with both oxalate and chloride precursors. For labelling with [^{89}Zr]zirconium(IV) oxalate, the preliminary study showed that the cyclen-based picolinic acid compound **9** gave the highest labelling yield. When radiolabelling with [^{89}Zr]zirconium(IV) chloride the formation of insoluble species needed to be considered, as this gives a radio-ITLC peak at the same place as the formed [^{89}Zr]Zr(IV) complex. Test reactions in water, 0.2 M ammonium acetate buffer and 0.5-1 M HEPES at various pH were carried out and it was found that the labelling reaction in water should not be performed at pH above 6. Issues with [^{89}Zr]Zr(IV) colloid formation were not encountered in acetate buffer and HEPES buffer.

In the course of this work, Wadas *et al.* published a study labelling DOTP **1** using zirconium-89 chloride. They reported that the labelling of [^{89}Zr]zirconium(IV) chloride with DOTP in water at pH 7-7.5 reached 100% yield. In contrast to this work, it was found that the formation of colloidal species occurred at pH 7, hence **1** was labelled at pH 6 which gave a yield of only 7.5%. Labelling of the cyclen-based phosphinic acid compound **5** was not successful but this may have been due to impurities present. As was observed when labelling with [^{89}Zr]zirconium(IV) oxalate, the cyclen based picolinic acid compound showed a better yield than the other macrocycles when labelled with [^{89}Zr]zirconium(IV) chloride. The picolinic acid functional group was selected for development of the next generation chelators with extended arms. The longer picolinic arm length could be explored on both cyclen and cyclam platform as this would offer some further flexibility to allow the pendant arms to adopt an ideal geometry for octadentate complex formation with zirconium(IV) which would improve the stability of the complex.

Chapter 3

The effect of pendant arm alkyl chain length and macrocycle ring size on zirconium-89 complex formation

3. The effect of pendant arm alkyl chain length and macrocycle ring size on zirconium-89 complex formation

3.1. Introduction

Siderophores are low molecular weight compounds, which are produced by bacteria and fungi that can bind effectively to iron(III). They are generally made up from three bidentate hydroxamates, catecholates or α-hydroxy-carboxylates units that have been combined to form a hexadentate chelator. Examples of natural siderophores for each type of coordination unit are shown in Figure 49.[141] Iron is an essential transition metal for physiological function in humans, however, excess iron results in the uncontrolled formation of free radicals and reactive oxygen species (ROS).[142] The use of siderophores as iron-chelating therapeutic drugs has been reported due to their optimal binding characteristics for iron(III).[143]

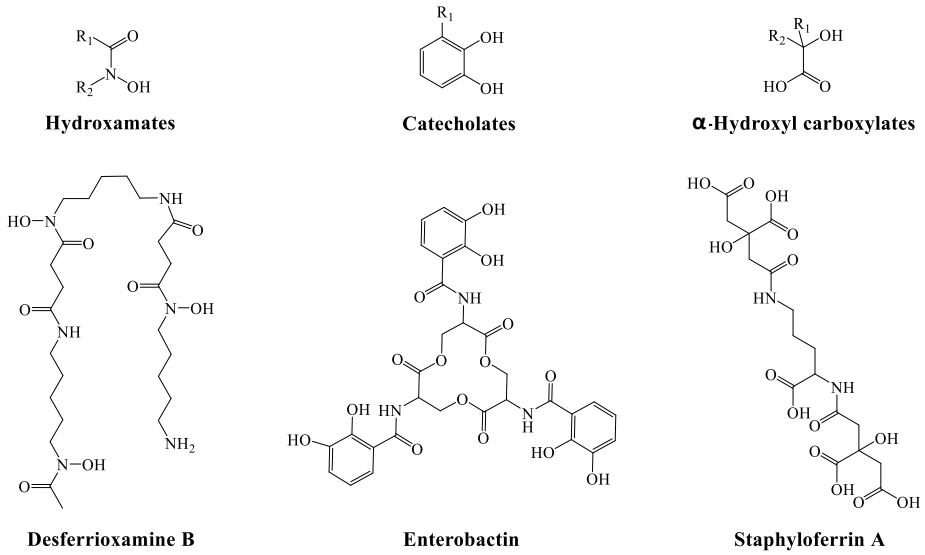

Figure 49 - Ferric-coordination units and examples of siderophores.[144]

The natural siderophore named enterobactin, also known as enterochelin, is a cyclic polyester consisting of 2,3-dihydroxy-*N*-benzoylserine.[145] It is produced by members of Enterobacteria family such as *Escherichia coli*.[146] Enterobactin forms a highly stable hexadentate complex with Fe(III) with a stability constant of *ca.* 10^{49}, see Figure 50.[147, 148] The molecular design of this chelator is of high interest to coordination chemists as it uses a cyclic backbone to arrange three arms in space so that they can fold up around the metal centre. However the role of the macrocycle is not to coordinate the metal centre into the ring structure but rather to arrange the arms and rigidify the structure to increase stability and allow for rapid

kinetics of complex formation. The three catecholate moieties fold up around the metal centre to provide an ideal octahedral coordination environment for iron(III).[148]

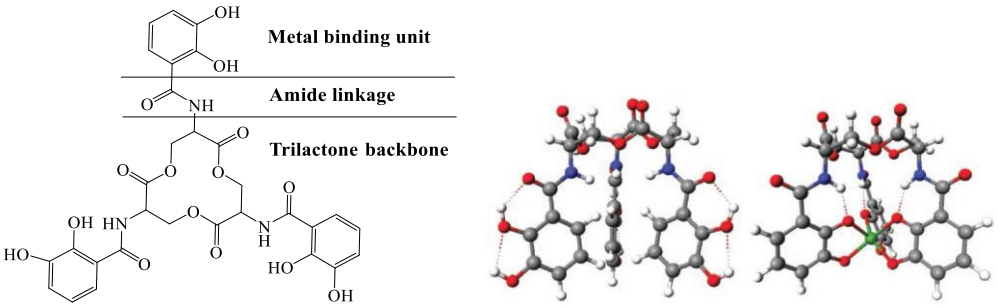

Figure 50 - Structure of enterobactin and representations of its Fe(III) complex reproduced from Raymond *et al*., 2003.[148]

A number of macrocycle-based siderophore analogues, some of which form similar "out of cavity complexes" where the metal does not directly coordinate to the macrocycle itself, have been investigated, synthesised and characterised. For example, in 1995, Esteves and co-workers synthesised a macrocyclic trishydroxamate ligand containing triamine macrocycle as backbone with three hydroxamic acid groups as pendant arms, DOTRMAHA.[149] Fe(III) complexation was studied and the molecular modelling indicated that the Fe(III) ion binds to the six oxygen atoms from the pendant arms. A few years later, Gaspar and co-workers synthesised the cyclam-based trishydroxamate; TETMAHA.[104] The complexation with Fe(III) showed that TETMAHA formed complex with 1:1 metal to-ligand ratio with oxygen atoms of hydroxamate moieties. The Al(III) complexation showed similar coordination behaviour but the Cu(II) complex was different. The copper ion binds in the cavity of the macrocycle to give a five coordinate species with the four nitrogen atoms of the macrocycle and a molecule of water bound and the three hydroxamate groups protonated. The structures of DOTRMAHA and TETMAHA are shown in Figure 51.

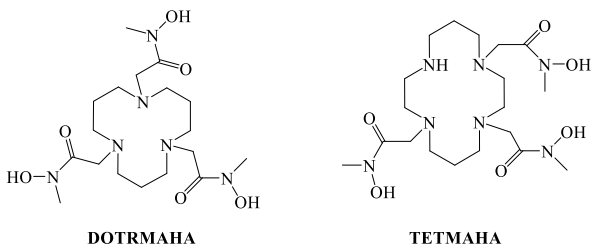

Figure 51 - Structures of DOTRMAHA and TETMAHA.

In terms of [^{89}Zr]Zr(IV) radiolabelling, as described in chapter 2, Wadas and co-workers published Zr(IV) complexation of tetraazamacrocyclic chelators; DOTA, DOTP and DOTAM, see Figure 52. Zr-DOTA crystal showed that it formed in cavity complexes. However, this requires labelling conditions with a high temperature (90-95^{o}C)[108]; and it is known that macrocyclic compounds although having high thermodynamic stabilities can also have slow formation kinetics.[150] The molecular design concept of using macrocycle as platform and pendant arms as metal binding sites to form out of cavity complex has been considered in order to allow complex formation at mild temperature. This was a key concept that formed one of the planned aspects of this research work in the initial project plan.

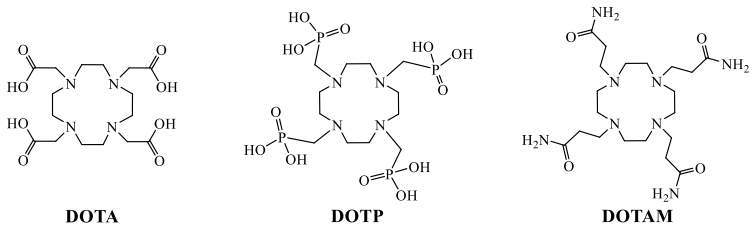

Figure 52 - Structures of tetraazamacrocyclic chelators reported radiolabelling with [^{89}Zr]Zr(IV) by Wadas *et al*., 2017.[108]

During the course of this work two other groups had also come up with similar ideas and were investigating the synthesis of azamacrocyclic precursors for labelling in an "out of cavity" coordination with zirconium-89. One group was in Harvard University in the USA and the other at the University of Burgundy in France. Some of their results have now been published but personal communication indicated some of the further and ongoing work in these groups.[87] Caravan, Boros and co-workers investigated cyclen and cyclam as scaffolds for *N*-functionalisation to attach either three or four groups with hydroxamate donors, see Figure 53. Initially, the ligands **L13**, **L14** and **L15** were synthesised. The zirconium-89 labelling reaction (**L13** and **L15**) was carried out at room temperature to give quantitative yields after 5 minutes and stability was tested by incubation in incubated in 1000-fold excess EDTA and with rat plasma at 37^{o}C. The results showed that **L15** was more stable than **L13** in both experiments. [^{89}Zr]Zr**L15** remained 88% intact in EDTA and almost 40% in blood plasma at 24 hours while 78% and less than 5% of [^{89}Zr]Zr**L13** were found. Density functional theory (DFT) was used to investigate the structure of the complexes. It revealed that both **L13** and **L15** may not form eight coordinate species but more likely formed seven coordinate species.

It was shown that steric constraints from cyclen and cyclam backbone and the short length of hydroxamate arm prevented binding with eight donor atoms.

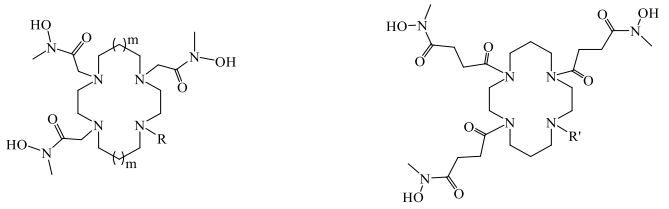

L13; m = 0, R = $CH_2CONOHCH_3$
L14; m = 1, R = H
L15; m = 1, R = $CH_2CONOHCH_3$

L16; R' = H
L17; R' = $CH_2CONHCH_2COOH$

Figure 53 - Aza-macrocycle tethered polyhydroxamates **L13**, **L14**, **L15**, **L16** and **L17**.[87]

The effect of the number of hydroxamate arms was studied using the cyclam scaffold. The ligand **L14** containing three hydroxamate groups, which provide six donor atoms, was compared with cyclam-based four hydroxamate arm ligand **L15**. Surprisingly, [^{89}Zr]Zr**L14** was more stable in EDTA solution than [^{89}Zr]Zr**L15**. Nevertheless the stability of [^{89}Zr]ZrDFO was much better with 90% intact after 144 hours. Therefore, a cyclam derivative with three longer hydroxamate arms **L16** was designed to increase the flexibility of the chelator in complex formation. DFT calculations indicated that the longer arms could reduce ligand strain and enhance the stability of the complex. Although **L16** offers only six binding sites like DFO, the calculations predicted that the extension of arm length could provide similar hexadentate coordination geometry, see Figure 54, and it is likely that water molecules would complete the coordination sphere.

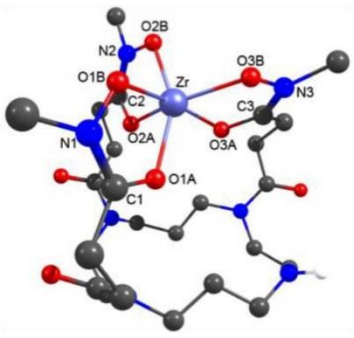

Figure 54 - DFT calculation of Zr-**L16** structure reproduced from Caravan *et al.*, 2016.[87]

L16 was labelled with [^{89}Zr]Zr(IV) and the complex properties were compared with [^{89}Zr]ZrDFO. The complex stability of [^{89}Zr]ZrDFO in EDTA was comparable to [^{89}Zr]Zr**L16**

but the DFO was much less stable in blood serum. However, the biodistribution data showed that [^{89}Zr]Zr**L16** had slightly higher accumulated activity in bones but this may have been due to alternate processing of the chelator and as conjugates may have different properties further investigation was of interest.

The researchers also synthesised the bifunctional ligand **L17** which was an **L16** analogue that could be conjugated to trastuzumab to compare with [^{89}Zr]ZrDFO-trastuzumab. However, again the *in vivo* study showed significantly higher bone uptake and radioactivity accumulation in normal tissues was similar to [^{89}Zr]Zr**L16**. It was concluded that **L17** was not suitable for [^{89}Zr]Zr(IV) chelation application in PET imaging. Pre-organisation of three modified hydroxamate arms on cyclam platform allowed the labelling reaction at room temperature but did not form a sufficiently stable complex in vivo with Zr. Although these macrocycle-based ligands were not suitable for Zr(IV) coordination further development of out of cavity metal binding is clearly warranted.

Denat and co-workers at the University of Burgundy reported the preparation of eight octadentate macrocyclic-based chelators and labelled them with [^{89}Zr]Zr(IV).[151] Cyclen, cyclam, TACN and 13(ane)N4 were used as platforms and functionalised with picolinic acid and hydroxyquinoline. The results showed promising radiolabelling data, especially for the cyclam-based chelators.

In the work carried out for this thesis, the original aim was the same as that independently arrived at by the Caravan/Boros and Denat groups; to develop tetraazamacrocycle derivatives with pendant arms for octadentate "out of cavity" chelation with zirconium-89. The aim was to combine rapid kinetic of binding with high stability. The encouraging results from the pendant picolinic acid arm chelator reported in the previous chapter revealed that **9** could bind [^{89}Zr]Zr(IV). The picolinic acid pendant arms offer eight donor atoms for Zr(IV) to form octadentate coordination in an "out of cavity" complex. However, the picolinic acid arms **9** are short. As reported by Caravan *et al.*, steric constraint from macrocycle backbone resulting in their related complexes being likely to form with a heptadentate chelated metal ion complex. Therefore novel compound were synthesised by extending the length of picolinic acid pendant arms alkyl chains to connect to the cyclen backbone in order to increase the flexibility and allow an eight coordinate complex octadentate complex to form with [^{89}Zr]Zr(IV). The longer alkyl chain arms were also investigated using the cyclam tetrazamacrocycle backbone in order to investigate the effects of steric constraint dependent on the macrocycle ring size, see Figure 55.

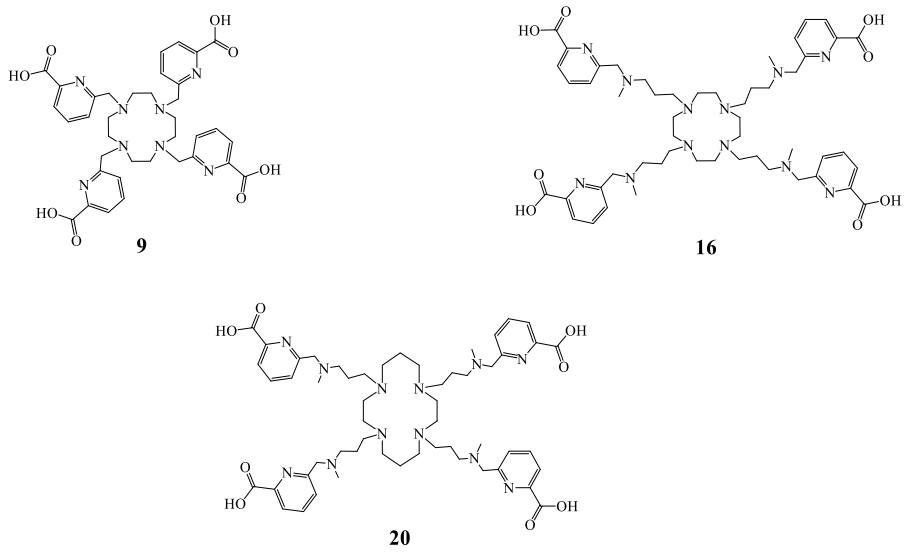

Figure 55 - Azamacrocycle chelators as synthetic targets to investigate the effects of increased chain length on pendant arm coordination to zirconium-89.

3.2. Preparation of the arm linker

The arm linker, benzyl (3-bromopropyl)(methyl)carbamate **12**, was synthesised to vary the length between the coordinating group and macrocycle backbone. The alkylation was performed on the four nitrogen atoms of both cyclen and cyclam rings before functionalisation with picolinic acid. This arm linker was used to increase the length of picolinic acid donor arms so that it would increase flexibility of bonding between donor atoms and Zr^{4+} ion.

It was reported by Verma and co-workers in 2012 that **12** could be synthesised from 3-(methylamino)propan-1-ol (10 mmol) reacted with benzyl chloroformate (13 mmol) in 50 mL of a mixture of dioxane and water (1:1). The reaction needed to be maintained at pH 10 using 3.5 M potassium hydroxide solution. After 1 hour, the reaction mixture was extracted with diethyl ether and purified by silica gel column eluted with ethyl acetate : hexane (4:6) to obtain **10** (80% yield). Then the hydroxide group of **10** was converted to bromide using the Appel reaction with triphenylphosphine (2 equiv.) and tetrabromomethane (2 equiv.) in dichloromethane. The reaction was carried out at room temperature for 1 hour and the crude product was purified by silica gel column eluted with ethyl acetate : hexane (1.5:8.5) to give **12** (80% yield), see Scheme 10.[152]

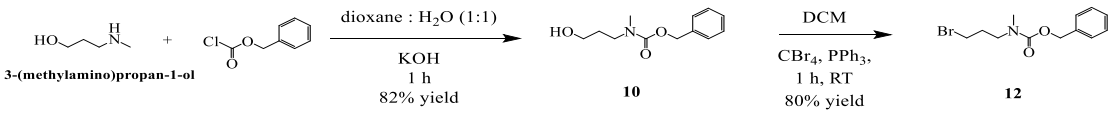

Scheme 10 - Synthesis of benzyl (3-bromopropyl)(methyl)carbamate **12** reported by Verma *et al*. in 2012.[152]

It has been reported that **10** could be prepared by a different method. Kumar and co-workers published the protection of amines and amino acids with benzyl chloroformate using β-cyclodextrin as catalyst. Different amines and amino acids were studied. The reactions were performed in either water or 0.1 M carbonate buffer pH 8 and purified by silica gel column chromatography. **10** was synthesised in a 89% yield.[153]

In this work, the synthesis **12** was completed using this alternate synthetic route. It started with the protection of the amine in 3-(methylamino)propan-1-ol with benzyl chloroformate to produce **10** without purification at this stage. Then tosylation with *p*-toluenesulfonyl chloride was performed in the second step to change hydroxyl group into a more reactive leaving group and generate **11**, then the reaction with lithium bromide was carried out in the final step, see Scheme 11.

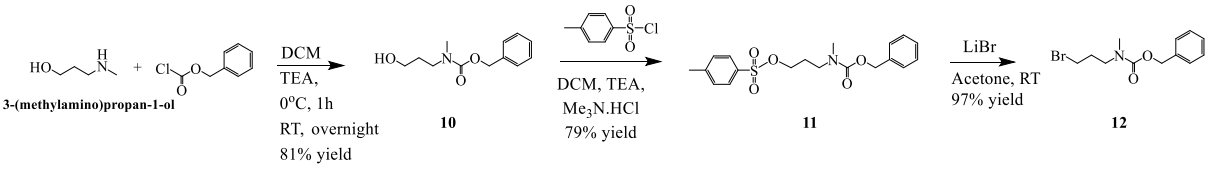

Scheme 11 - Synthesis of benzyl (3-bromopropyl)(methyl)carbamate **12** in this work.

The amine protection in the first step was to avoid the undesired side reaction in the second step with *p*-toluenesulfonyl group. The *p*-toluenesulfonyl group can also be used as an amine protecting group; for example, in the synthesis of *p*-toluenesulfonyl-L-isoleucine.[154] Protection of the amino group avoids production of 3-((*N*,4-dimethylphenyl)sulfonamido) propyl 4-methylbenzenesulfonate as a by-product, see Figure 56.

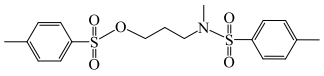

Figure 56 - Structure of 3-((*N*,4-dimethylphenyl)sulfonamido)propyl 4-methylbenzenesulfonate.

Benzyl carbamate protecting groups (Cbz) were chosen for use in this study as they are frequently utilised tools for the protection of oxygen and nitrogen functional groups.[155] It has been used in peptide synthesis because of the ease of removal by hydrogenolysis.[156] The protection of the amine group by conversion of amino acid to *N*-carbobenzoxy derivative is known as the Bergmann-Zervas carbobenzoxy peptide synthesis method[157] which was published in 1932.[158] The amine protection reaction in the first step was performed by reacting with benzyl chloroformate (1 equiv.) in DCM anhydrous overnight then the crude product was extracted and the solution was evaporated to give the product as a yellow oil (81% yield).

Tosylate is also used as a leaving group for substitution reaction.[159] Tosylate is widely used in organic synthesis as it is easy to produce by *p*-toluenesulfonyl chloride or *p*-toluenesulfonic acid in various reaction conditions.[160-162] It is a better leaving group than hydroxyl; therefore, in the second step, *p*-toluenesulfonyl chloride was used to convert alcohol to tosyl group. The reaction was performed in dichloromethane anhydrous in the presence of base. Small portions of *p*-toluenesulfonyl chloride were added over 30 minutes while the reaction mixture was stirred at 0^{o}C. Then the reaction was kept at 0^{o}C for 2.5 hours and warmed to room temperature for an hour. The extraction was performed in dichloromethane and the purification was carried out using silica gel column chromatography, eluting with ethyl acetate and hexane (1:3) to remove impurities followed by ethyl acetate and hexane (1:1) to elute the product (79% yield).

The last step was conversion of the tosylate to bromide. The reaction conditions were modified from the reaction reported by Perry and co-workers in 2003.[163] They converted the tosyl group to iodide by using potassium iodide in acetone at 56^{o}C for 4 hours to give the product (89% yield). In this research, the reaction was performed by using lithium bromide in acetone. The reaction was kept at room temperature for 24 hours and then extracted into ethyl acetate to give the compound **12** in a 97% yield.

3.3. Synthesis of macrocycles derivatised with picolonic acid

3.3.1. Synthesis of 6,6',6'',6'''-((((1,4,7,10-tetraazacyclododecane-1,4,7,10-tetrayl)tetrakis (propane-3,1-diyl))tetrakis(methylazanediyl))tetrakis(methylene))tetrapicolinic acid (16)

There were four steps used in the synthesis of **16**, shown in Scheme 12. *N*-Functionalisation of cyclen was performed to prepare the intermediates **13** and **14**.

The secondary amine groups on the four pendant arms were used to attach **7** to convert them to picolinate groups and the hydrolysis was carried out in the final reaction step.

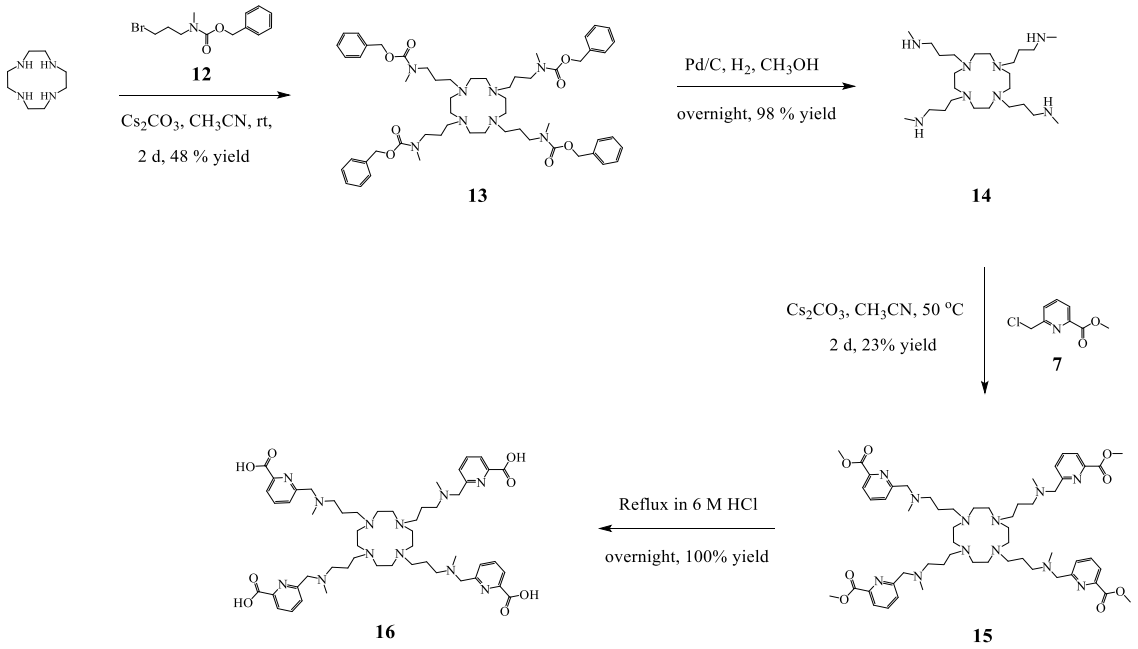

Scheme 12 - Synthesis route of 6,6',6",6"'-((((1,4,7,10-tetraazacyclododecane-1,4,7,10-tetrayl)tetrakis(propane-3,1-diyl))tetrakis(methylazanediyl)) tetrakis(methylene))tetrapicolinic acid (**16**).

Unlike **L16**, see Figure 53, for which the long hydroxamate arm was synthesised and then attached to the macrocycle, attempts to prepare the long picolinic acid pendant arm were not successful. First of all, bromopropylamine was reacted with **7** in acetonitrile in an attempt to prepare **26** methyl 6-(((3-bromopropyl)amino)methyl)picolinate, see Scheme 13. The reaction was monitored by MS; however, no sign of product was observed and MS showed only starting materials after 24 hours. It was possible that this reaction was not occurring as bromopropylamine needs to be kept under acidic conditions to prevent self-reaction hence the nitrogen atom is remaining protonated unreactive despite the addition of base.

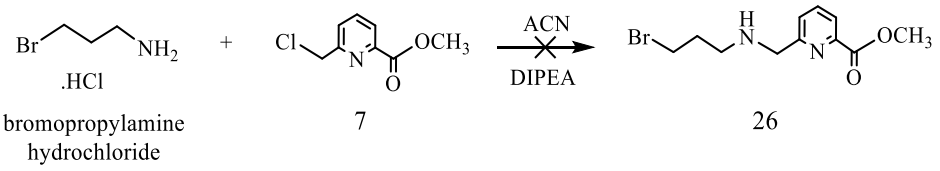

Scheme 13 - Attempted synthesis of compound **26**.

1,4-Dibromobutane was also reacted with **6** in an attempt to the produce **27**, see Scheme 14.

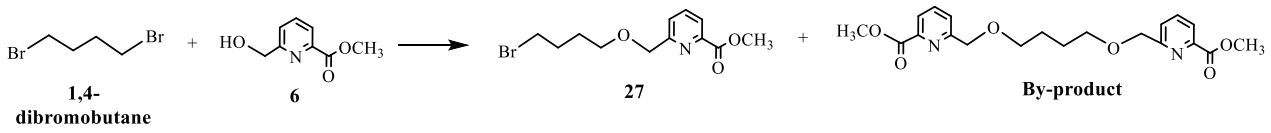

Scheme 14 - Attempted synthesis of compound **27**.

The reaction conditions were modified from the synthesis of bromoacetate derivatives as precursors for radiofluorination that were reported by Degrado and co-workers in 2012.[164] In the reported work, the formation of methyl 18-bromo-4-thiaoctadecanoate and methyl 18-bromo-6-thiaoctadecanoate were performed by coupling 1,14-dibromotetradecane with methyl 3-mercaptopropionate and 1,12-dibromododecane with methyl 6-mercaptopentanoate respectively, using sodium hydride in THF anhydrous, see Scheme 15.

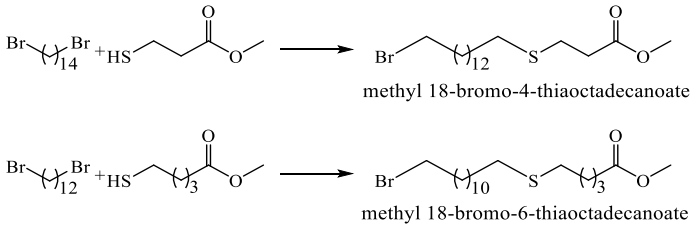

Scheme 15 - Synthesis of methyl-18-bromo-4-thiaoctadecanoate and methyl 18-bromo-6-thiaoctadecanoate reported by Degrado *et al*. in 2012.[164]

For synthesis of the **27**, the starting material dibromoalkane was reacted with methyl 6-(hydroxymethyl)picolinate **6**. However, both Br atoms of 1,4-dibromobutane were reactive and this generated the unwanted by-product which was detected by MS and the desired product **27** was not isolated.

The other strategy was the two-step preparation. The alkylation of the secondary amine of the aminoalcohol with **7** was carried out in anhydrous acetonitrile under basic conditions. Then tosylation of the intermediate compound methyl 6-(((3-hydroxypropyl)(methyl)amino) methyl)picolinate **28** was attempted as the tosylate is a better leaving group than OH, see Scheme 16.

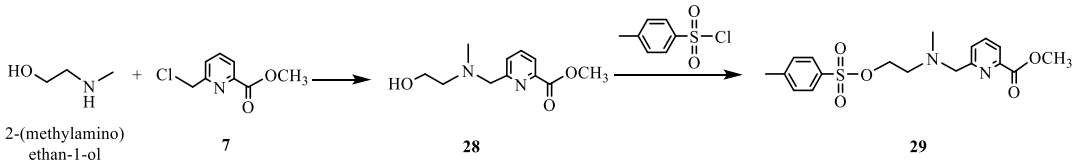

Scheme 16 - Synthesis of the compound **28** and **29**.

The first step was successfully carried out by reacting 2-(methylamino)ethan-1-ol (31.6 mmol), **7** (20.7 mmol) and K_2CO_3 (10.4 mmol) in anhydrous acetonitrile (100 mL) at 70°C overnight. The purification was carried out by silica gel column chromatography (5 x 20 cm) eluting with dichloromethane:methanol (9:1). The excess 2-(methylamino)ethan-1-ol remained on the column and unreacted **7** was eluted (R_f ~ 0.86), while **28** was eluted later (R_f ~ 0.21) (8.7 mmol, 42% yield). The second step was to add the tosylate group using *p*-toluene sulfonyl chloride. Tosylate precursors have been used for the synthesis of cross-bridged cyclam derivatives[165] such as PCB-TE2A and PCB-TE1A1P macrobicycles, see Figure 57.

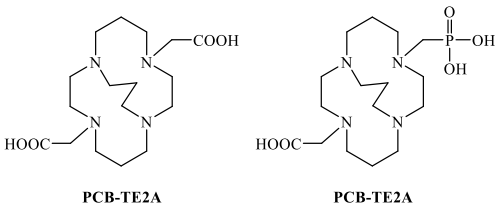

Figure 57 - Structures of PCB-TE2A and PCB-TE1A1P macrobicycles.

Moreover, in 1998, Guilard and co-workers described the synthesis of a cyclam-based macrobicyclic ligand by using cyclam and a ditosylate compound refluxed in acetonitrile for 15 hours followed by purification by alumina column to give the product in a 30-37% yield.[166] This method offered another way to prepare polyazamacrocycles to provide suitable cavity size for complexation with metal ions, see Scheme 17A. Additionally the use of tosylate for synthesis of a macrotricyclic compound was reported by Søtofte and co-workers in 1995, see Scheme 17B.[167,168]

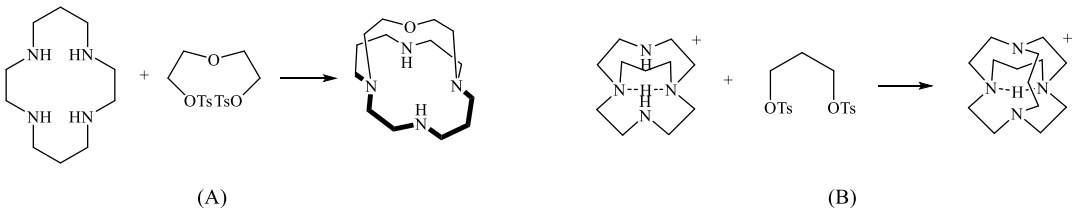

Scheme 17 - Examples of using tosylates in macrocycles.[167,168]

In this research work, the tosylate leaving group was added on to the picolinate arm precursor in the second step by using in DCM as solvent at 0°C for an hour and **29** was isolated as a yellow oil in a 50% yield. This picolinate arm precursor **29** was then reacted with cyclen and cyclam at reflux in anhydrous acetonitrile under an Ar atmosphere using Cs_2CO_3 as base. Although a two-fold excess of the picolinate arm precursor was used per nitrogen position and the reaction mixture was stirred for two days, only the one-arm by-product was detected in the mass spectrometry analysis.

Therefore **16** was synthesised by an alternative method consisting of four steps as shown in Scheme 12.

Firstly, the alkylation of cyclen with the arm precursor **12** (5 equiv.) was performed in anhydrous acetonitrile at room temperature for two days and purified by silica gel column chromatography to give the intermediate compound **13** in a 48% yield. A slight excess of the pendant arm precursor **12** was used to increase the yield of the compound **13**, and so it was better to carry out the reaction under mild conditions as the five-arm by-product (quaternised) could be generated at higher temperatures (observed by MS).

Secondly, the hydrogenation of the compound **13** was carried using methanol as solvent with 10% Pd/C in a Parr shaker overnight. After filtration and evaporation, the intermediate product **14** was isolated as a light yellow oil (98% yield).

Thirdly, the picolinate compound **7** was attached to **14** by using similar conditions as the alkylation in the first step. The purification was performed using alumina column instead eluted with dichloromethane:methanol:triethylamine (99:1:0.1) to remove excess **7** and then with dichloromethane:methanol:triethylamine (97:1:0.1) to elute the product **15** as a yellow oil (23% yield).

Finally, the hydrolysis step was performed in 6 M hydrochloric acid. The reaction was heated to reflux overnight and then evaporated to give the final product **16** as a brown solid in quantitative yield.

3.3.2. Synthesis of 6,6',6'',6'''-((((1,4,8,11-tetraazacyclotetradecane-1,4,8,11-tetrayl) tetrakis(propane-3,1-diyl))tetrakis(methylazanediyl))tetrakis(methylene))tetrapicolinic acid (20)

The equivalent cyclam was also synthesised to compare the effect of larger macrocyclic ring with the cyclen derivative **16**. The cyclam-based "long arm" picolinic acid compound **20** was synthesised using a similar synthetic route to the one used to produce **16**, see Scheme 18.

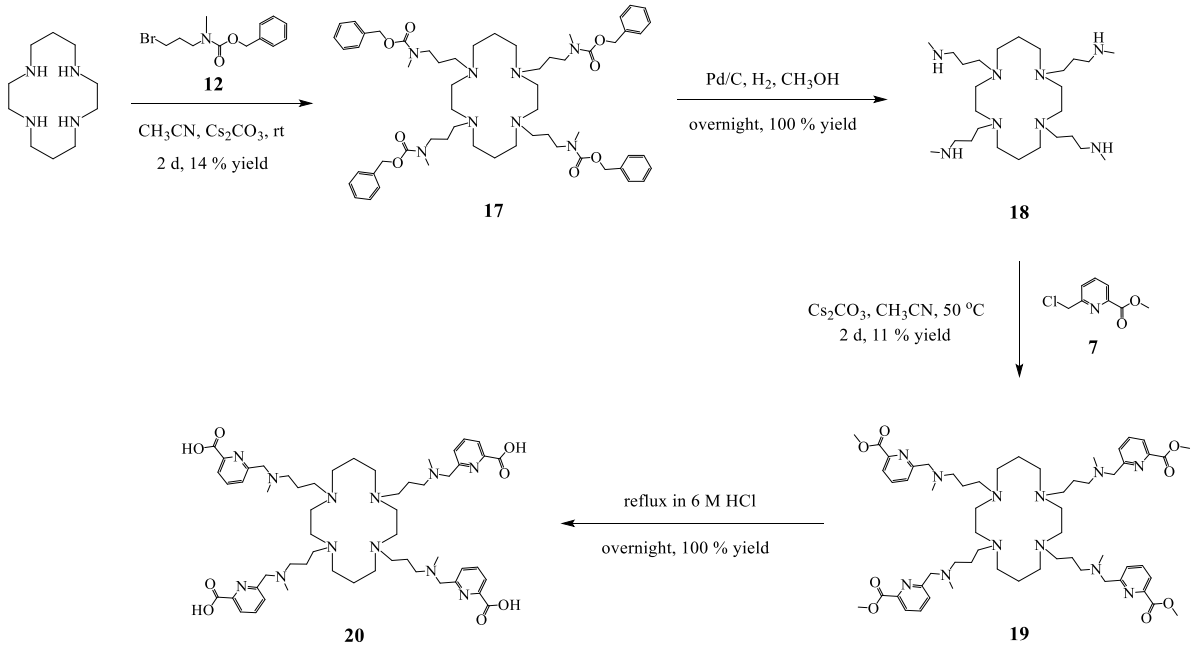

Scheme 18 - Synthesis route of 6,6',6",6"'-((((1,4,8,11-tetraazacyclotetradecane-1,4,8,11-tetrayl)tetrakis(propane-3,1-diyl))tetrakis(methylazanediyl)) tetrakis(methylene))tetrapicolinic acid (**20**).

The synthesis of **20** started with the alkylation of cyclam and the arm precursor **12** (5 equiv.). The reaction was performed in anhydrous acetonitrile at room temperature for two days and then purified by silica gel column to give the intermediate compound **17** as a yellow oil in a 14% yield. An attempt was made to improve the yield by increasing the temperature; however, as with the cyclen compound, the five-arm quaternised by-product was observed and so only 6% of the desired product was obtained after purification. **17** was hydrogenated using 10% Pd/C in methanol with Parr shaker overnight to give a quantitative yield of the intermediate **18**. Then the alkylation of the compound **18** with **7** was performed in acetonitrile and the product purified by chromatography on alumina to give the intermediate **19** as a yellow oil in an 11% yield. Finally, the target compound **20** was obtained after hydrolysis in 6 M hydrochloric acid overnight as a brown solid in a quantitative yield.

3.4. [^{89}Zr]Zr(IV) radiolabelling of "long arm" picolinate azamacrocycle derivatives

3.4.1. [^{89}Zr]Zr(IV) radiolabelling of 6,6',6'',6'''-((((1,4,7,10-tetraazacyclododecane-1,4,7,10-tetrayl)tetrakis(propane-3,1-diyl))tetrakis(methylazanediyl))tetrakis (methylene)) tetrapicolinic acid (16)

Attempts to radiolabel **16** with [^{89}Zr]Zr(IV) were made by using similar labelling conditions to those used for **9**. A solution of the compound **16** in 0.2 M ammonium acetate buffer at pH 6.0 was labelled with [^{89}Zr]zirconium(IV) chloride (0.5 MBq) in a total volume of 110 µL. The reaction mixture was incubated at 95^{o}C for 2 hours (n = 3). Labelling yield was analysed by ITLC-SG run in 10 mM EDTA at pH 6.

It was predicted that the Zr ion would coordinate with the picolinic acid arms through nitrogen and oxygen atoms rather than the azamacrocycle nitrogens. The lanthanide(III) complexes of "short-arm" cyclen-based picolinic acid chelators were studied, see Figure 58. It was found that both H_2DODPA and H_2MeDODPA formed complexes with Eu(III), Gd(III) and Tb(III) with four nitrogen atoms of the macrocycle, two nitrogen and two oxygen atoms of picolinic acid arms; the *N*-methyl groups of H_2MeDODPA increasing the steric bulk and distorted the coordination sphere.[169] The complexation of another cyclen-based picolinic acid compound H_2BP12C4 with lanthanide(III) ions was also studied and showed that metal ions was bound to eight donor atoms of the chelator including the macrocyclic ring oxygen and nitrogen donors.[133]

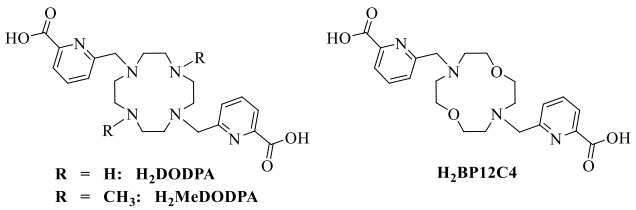

Figure 58 - "Short-arm" cyclen-based picolinic acid chelators studied in lanthanide(III) complexes.

Acyclic dipicolinic acid derivatives were synthesised and complexes formed with various metals including Gd(III), Ga(III) and La(III), see Figure 59. For MRI applications, for example, H_4DPABA; which is a dipicolinic acid chelator which also contains carboxylates functionalised was studied with Gd(III) by Mazzanti and co-workers.[170] While Rodríguez-Blas and co-workers reported the preparation of H_4BPEDA[171] which was then studied for Gd(III) complex formation by Merbach and co-workers.[172] In PET imaging, Orvig and co-workers published the synthesis and ^{68}Ga radiolabelling of H_2DEDPA. It was believed that H_2DEDPA

could be developed as bifunctional chelator for Ga(III) as the labelling reaction was completed quickly at room temperature and the complex stability was higher than that of DOTA with gallium(III).[173]

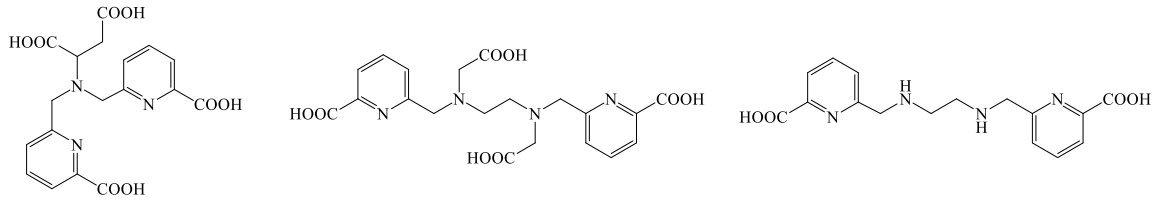

Figure 59 - Structures of acyclic dipicolinic acid derivatives.

Functionalised dipicolinic acid amine-derived compounds were synthesised and complexes formed with Ga(III) and La(III), see Figure 60.[174] The structures showed 1:1 metal-to-ligand ratio for all three compounds with both metal ions; however, there was also a 1:2 metal-to-ligand ratio compound found for La(III) complex of H_2DPA. For H_2DPAA, a stoichiometric 1:2 ratio of metal and ligand was found when complexed with Gd(III).[175] $[Gd(DPAA)(DPAAH)]^{2-}$ was the major species at pH 2-5 while the amount of $[Gd(DPAA)_2]^{3-}$ formed increased with increasing pH and became the major species at pH values above 5.

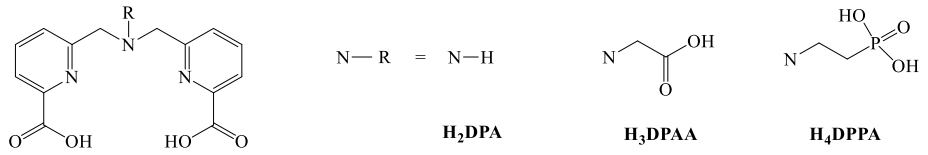

Figure 60 - Structures of functionalised dipicolinic acid amine-derived compounds.

The predicted structure of [^{89}Zr]Zr**16** was Zr(IV) forming an eight coordinate species with the eight donor atoms from the four picolinic acid pendant arms, see Figure 61A. It was also noted that there would be a possibility of 1:2 metal-to-ligand ratio complex formation as the concentrations for radiolabelling mean the chelator will always be in a large excess, see Figure 61B.

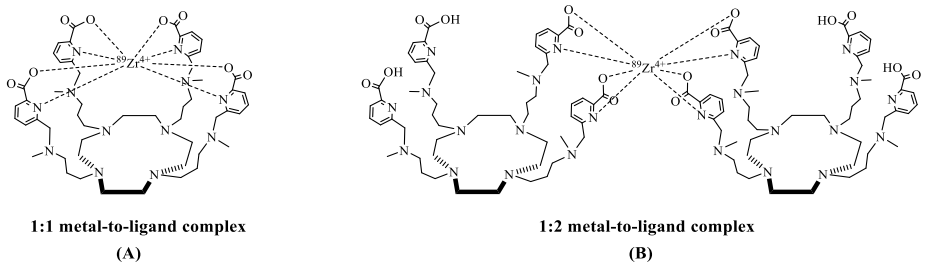

Figure 61 - Predicted [^{89}Zr]Zr**16** complex structures.

Chelator concentration is one of the reaction parameters used to maximise radiolabelling yields.[176-178] A series of chelator concentrations was investigated to determine the optimal conditions for radiolabeling of this compound.

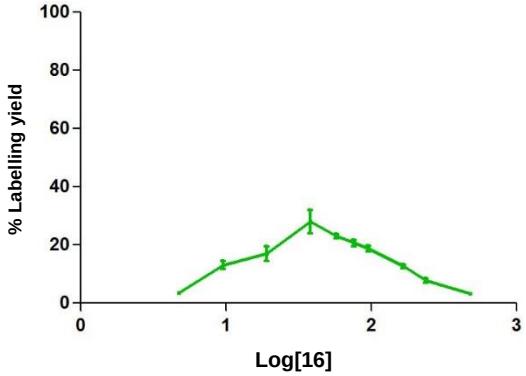

Figure 62 - Concentration curve of [^{89}Zr]Zr**16**.

The concentration curve of [^{89}Zr]Zr**16** was unexpected. Theoretically, labelling yield should increase with increasing chelator concentration and concentration curve should be S-shaped. The lowest chelator concentration of 4.76 µM (log[M] = 0.68) gave a 3.5% labelling yield. Increasing the concentration improved the labelling yields up to the maximum yield of 28.0% with a chelator concentration of 38.2 µM (log[M] = 1.58). However, above this point, the labelling yields decreased down to 3.3% at the highest concentration tested of 478 µM (log[M] = 2.68) as shown in Figure 62. This unexpected behaviour could be attributed to other complexes forming (i.e. two chelators to one metal centre) that are less stable under the conditions of analysis and fall apart on the TLC plate in the presence of the competing EDTA chelator in the eluent. Guerard and co-workers, have previously observed transchelation with weak ligands during ITLC elution using strong competitor chelators such as EDTA in the eluent.[137]

As discussed, some octadentate picolinic acid chelators (and many other chelators) can form complexes with both 1:1 and 1:2 metal-to-ligand structures. The increase in chelator concentration would enhance the tendency to form 1:2 species.

Caravan and co-workers conducted labelling experiments of **L13**, **L14**, **L15** and **L16**, see Figure 53, with [^{89}Zr]Zr(IV), however variations in concentration of the chelator were not studied. Codd and co-workers reported the energy calculations of octadentate Zr(IV) macrocyclic complexes formed 1:1 Zr(IV) tetrameric macrocycle and 1:2 Zr(IV) dimeric macrocycle, see Figure 63.[179] However, this is different as it was the comparison between Zr complexation of one large octadentate macrocycle providing eight binding sites and Zr complexation of two small tetradentate macrocycles each of them providing four binding sites. The calculations showed that 1:2 Zr(IV) dimeric macrocycle gave slightly lower energy than 1:1 Zr(IV) tetrameric macrocycle as the dimeric one did not have the ring strain of the larger chelator.

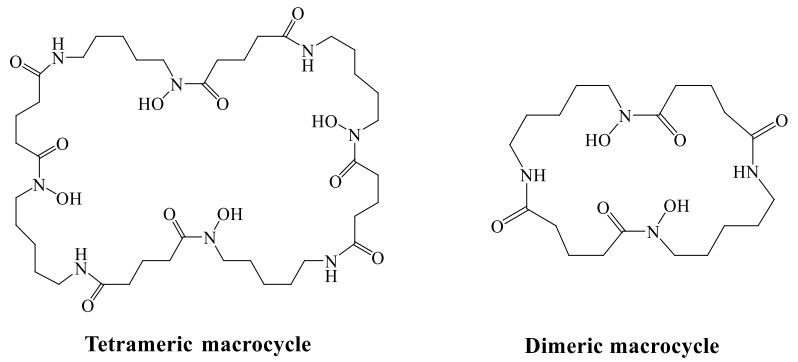

Figure 63 - Structures of tetrameric macrocycle and dimeric macrocycle studied by Codd *et al*.[179]

3.4.2. [^{89}Zr]Zr(IV) radiolabelling of 6,6',6'',6'''-((((1,4,8,11-tetraazacyclotetradecane-1,4,8,11-tetrayl)tetrakis(propane-3,1-diyl))tetrakis(methylazanediyl))tetrakis (methylene)) tetrapicolinic acid (20)

The radiolabelling of **20** was performed with similar labelling conditions as used to label **9** and **16**. A solution of the compound **20** in 0.2 M ammonium acetate buffer at pH 6.0 was labelled with [^{89}Zr]zirconium(IV) chloride (0.5 MBq) in total volume 110 µL, this was then incubated at 95ºC for 2 hours (n = 3). The labelling yield was analysed by ITLC-SG run in 10 mM EDTA at pH 6. As for the cyclen derivative, it was expected that the [^{89}Zr]Zr(IV) binds through nitrogen and oxygen donors of the picolinic acid arms rather than the

azamacrocycle nitrogen donors. As was postulated for [^{89}Zr]Zr**16**, complex formation could potentially be either in 1:1 or 1:2 metal-to-chelator ratio forms, see Figure 64.

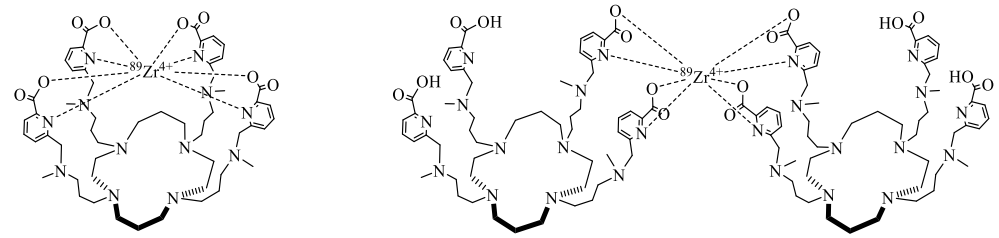

1:1 metal-to-ligand complex
(A)

1:2 metal-to-ligand complex
(B)

Figure 64 - Predicted [^{89}Zr]Zr**20** complex structures.

A series of ligand concentrations was explored, as in the previous study. The results showed that concentration curve of [^{89}Zr]Zr**20** was similar to [^{89}Zr]Zr**16**, see Figure 65. However labelling yield only increased from 5.3 % to 14.9% at the ligand concentration from 4.64 µM (log[M] = 0.67) to 55.7 µM (log[M] = 1.75) and then dropped at higher concentrations to a 2.5% yield at 464 µM (log[M] = 2.67).

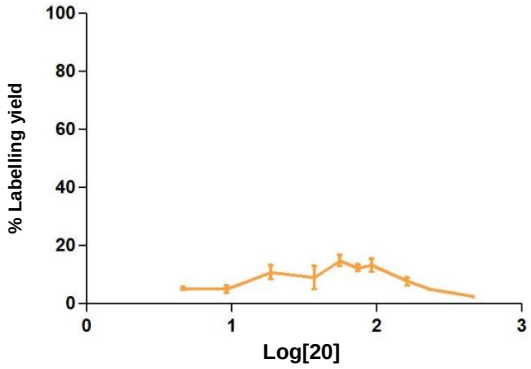

Figure 65 - Concentration curve of [^{89}Zr]Zr**20**.

There is some consistency in the behaviour of the two chelators in the radiolabelling reaction. It appears that there is binding competition for zirconium-89 from the EDTA present in the eluent used for the ITLC analysis which is influencing the observed results. Both studies indicate that the chelators are unlikely to have high enough stability for use asas imaging agents *in vivo.*

3.4.3. Comparison of radiolabelling yields of the [^{89}Zr]Zr(IV) labelled macrocyclic-based picolinic acid compounds

[^{89}Zr]Zr(IV) radiolabelling of the compounds **9**, **16** and **20** at a series of different concentrations were compared. The results showed that concentration curves of all three labelled compounds showed a similar trend, see Figure 66.

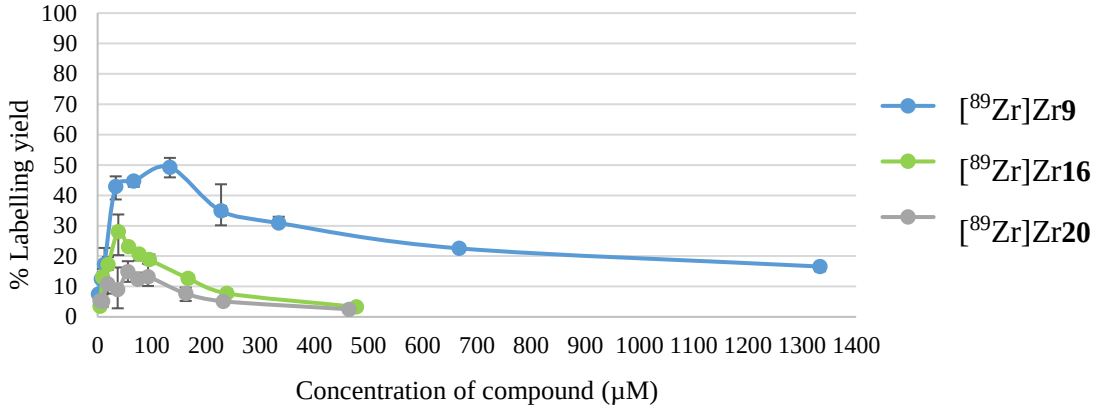

Figure 66 - Comparison of [^{89}Zr]Zr(IV) labelled macrocyclic-based picolinic acid compounds.

In vitro stability was not studied as the labelled compounds had very low labelling yields and the purification was not worth attempting as the scoping labelling experiments were performed with low activities (0.5 MBq). Only chelator concentration variation was studied and concentration curves revealed that labelling yields of [^{89}Zr]Zr**9** performed better than the others; even though the compound **9**, which was cyclen-based short pendant arms, will have the highest steric constraint from macrocyclic scaffold and is more likely to have a coordination sphere involving the azamacrocycle nitrogen atoms. For [^{89}Zr]Zr**9**, [^{89}Zr]Zr(IV) might form octadentate coordination by four oxygen donor atoms from the arms and four nitrogen atom from the azamacrocylic ring, as is observed for Zr(IV) complex formation with DOTA, while [^{89}Zr]Zr**16** and [^{89}Zr]Zr**20** may form complexes through eight binding sites of four picolinic acid groups (potentially from multiple chelators).

3.5. Conclusion

Three azamacrocyclic-based picolinic acid compounds were synthesised and radiolabelled with [^{89}Zr]zirconium(IV) chloride. The labelling of all compounds was performed under the same conditions (0.2 M acetate buffer at pH 6 at 95^{o}C for 2 hours). Labelling conditions only gave yields in the range 15 to 49% yield.

Concentration curves of labelled compounds were compared by conducting the labelling reactions of a series of different ligand concentrations. The three compounds showed similar trends with labelling yields improved with the initial increase in chelator concentrations and then the yield dropped at higher concentrations. It was possible that the compounds can form complexes with 1:1 and 1:2 ligand-to-metal ratios. The higher concentration is, the more 1:2 complex could form and this may not be stable under the analysis conditions.

In terms of the comparison of pendant arm length, the cyclen-based "short" arm picolinic acid compound **9** gave better labelling yields at all concentration points compared with cyclen-based "long" arm picolinic acid compound **16**. Although it has been reported that the extension of arm length increases the flexibility of the donor arms and minimises the steric constraint of the macrocyclic backbone, either the chelators may not be forming the predicted complexes or the selected length for the "long" picolinic chain might not be suitable for Zr complexation. The crystal structure of Zr-DOTA published by Wadas *et al*.[108], showed that Zr^{4+} ion formed an "in cavity" eight coordinate species with four macrocycle nitrogen atoms and four acetate oxygen pendant arms atoms binding to the metal centre. The [^{89}Zr]Zr**9** complex could be an "in-cavity" species, although this is likely to be strained.

The comparison of macrocyclic scaffolds between cyclen and cyclam was carried out with the "long" picolinic acid pendant arms with **16** and **20** but there did not seem to be a significant difference. Molecular modelling studies need to be combined with structural characterisation of Zr(IV) stable isotope complexes in future work to determine the structures, and predict the effect of macrocyclic rings and arm lengths to select the next generation of compounds that should be synthesised and radiolabelled.

Chapter 4

Synthesis and [^{89}Zr]Zr(IV) radiolabelling of DFO derivatised azamacrocycles

4. Synthesis and [^{89}Zr]Zr(IV) radiolabelling of DFO derivatised azamacrocycles

4.1. Introduction

Development of modified DFO-based chelators has been of increasing recent attention. DFT calculations on the Zr(IV) complex of DFO were published by Lewis and co-workers in 2013 showing the hexadentate coordination and indicating the potential for extending this to octadentate.[52] Brechbiel and co-workers studied Zr(IV) complex formation with single molecules of the bidentate hydroxamate, see Figure 67. The results showed that stability constants increased in the order of metal-to-ligand ratio of 1:1 > 1:2 > 1:3 and reached the maximum for 1:4 when it forms an eight coordinate species.[78] In the past few years, there have been several new chelators developed for [^{89}Zr]Zr(IV). In 2014, Mindt and co-workers presented an octadentate bifunctional chelator DFO*.[82] It is a modified DFO molecule with an additional hydroxamic acid moiety so that it would provide octadentate coordination through eight oxygen atoms of four hydroxamic acid groups. The chelator was conjugated to peptide bombesin (BBS) as a model ligand for bifunctional chelator. Radiolabelling with [^{89}Zr]Zr(IV) was performed at room temperature and gave almost 100% yield after 2 hours. Transchelation challenge was assessed in 300- and 3000-fold molar excess of DFO. The results showed that [^{89}Zr]ZrDFO*-BBS remained largely intact after 24 hours. However, the lipophilicity of this species is likely to be too high and so more hydrophilic derivatives could be synthesised.. However, Guus A. M. S. van Dongen and co-workers continued to study DFO*. They prepared DFO*-*p*Phe-NCS as bifunctional chelator and attached to a monoclonal antibody trastuzumab.[83] The *in vitro* study showed superior stability in saline, histidine/sucrose buffer, and human blood serum for 7 days. The *in vivo* experiment used N87 tumour bearing nude mice, and showed that the biodistribution of both [^{89}Zr]ZrDFO*-trastuzumab and [^{89}Zr]ZrDFO-trastuzumab were similar but indicated there may be potential for optimisation of chelator lipophilicity. PET images were obtained at 72 hours post injection and showed similar tumour uptake to [^{89}Zr]ZrDFO-trastuzumab but less bone uptake.

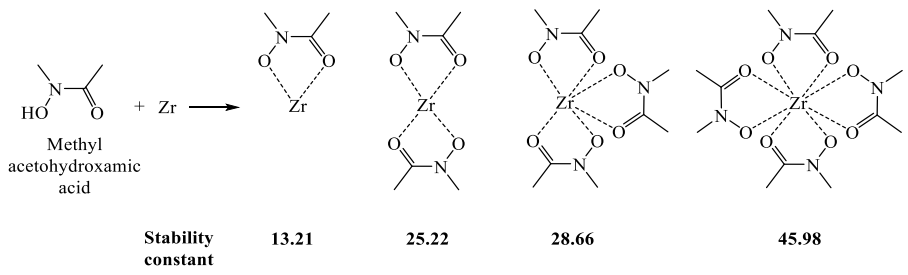

Figure 67 - Stability constants of Zr(IV) complexes of methyl acetohydroxamic acid.[78]

Other DFO analogue chelators have been developed, see Figure 68. For example, desferrioxamine B squaramide ester (H_3DFOSqOEt) was prepared by Donnelly and co-workers.[85] The synthesis of H_3DFOSqOEt was carried out by reacting DFO mesylate and 3,4-diethoxy-3-cyclobutene-1,2-dione in ethanol with DIPEA as base at 50^{o}C for 0.5 hour. As the squaramide ester reacts rapidly with amino groups, the squaramide linker in H_3DFOSq was used for antibody conjugation. The additional advantage of the squaramide linker is that the dione backbone also has the potential to coordinate to Zr(IV) which means H_3DFOSqOEt could offer eight binding sites and improve complex stability. The chelator was conjugated to trastuzumab in a mixture of DMSO and borate buffer solution pH 9.0 at room temperature. The conjugation reaction was successful with no sign of antibody aggregation or precipitation even at monoclonal antibody concentration of 56 mg/mL. [^{89}Zr]Zr(IV) radiolabelling with H_3DFOSq-trastuzumab gave 100% labelling in 30 minutes. It was believed that [^{89}Zr]ZrDFOsq-trastuzumab has a higher radiolabelling efficiency in the short reaction time compared to [^{89}Zr]ZrDFO-*p*Phe-NCS-trastuzumab because it has better solubility in aqueous solution. In terms of the imaging study, [^{89}Zr]ZrDFOsq-trastuzumab showed enhanced imaging quality over [^{89}Zr]ZrDFO-*p*Phe-NCS-trastuzumab. Higher tumour uptake (~ 15% ID/g at 96 hours post administration) and reduced liver (~ 2 *vs* 1.5 to 1 tumour to liver ratio) and bone (~ 4.5 *vs* 3 to 1 tumour to bone ration) uptake were found when using [^{89}Zr]ZrDFOsq-trastuzumab. However, *in vivo* study was performed only up to 96 hours. A full analysis of metal decomplexation *in vivo* after 4 days should be completed.

DFO-HOPO is a DFO derivative modified to be an octadentate chelator. The addition of one hydroxypyridinone moiety to DFO molecule was carried out by Raymond and co-workers in order to produce a low toxicity chelator for tetravalent actinides.[180] It was reported that the complex with Pu(IV) was very stable and potentially useful as a plutonium removal chelating agent. In 2017, this ligand was used for [^{89}Zr]Zr(IV) by Smith and co-workers.[181] The synthesis procedure was adapted from the previous literature by using commercial DFO whilst hydroxamate chloride was synthesised from hydroxypicolinic acid without protection of the *N*-hydroxyl group, see Scheme 19. The radiolabelling with [^{89}Zr]Zr(IV) was carried out at room temperature for 1 hour to give a yield >99% and labelling with a specific activity of 20 MBq/mol. Transchelation was investigated in 100-fold molar excess EDTA, 3200-fold molar excess DFO, and mouse serum. [^{89}Zr]ZrDFO-HOPO was shown to be >99% intact against all three competitors. PET imaging and biodistribution was studied in healthy mice to observe the clearance pathway. It was found that the labelled compound was cleared via both renal and hepatobiliary systems while the positively charged [^{89}Zr]ZrDFO, which had more

hydrophilicity, was mostly cleared through the kidneys. The modification of DFO-HOPO to form a bifunctional chelator is now being investigated by this research group.

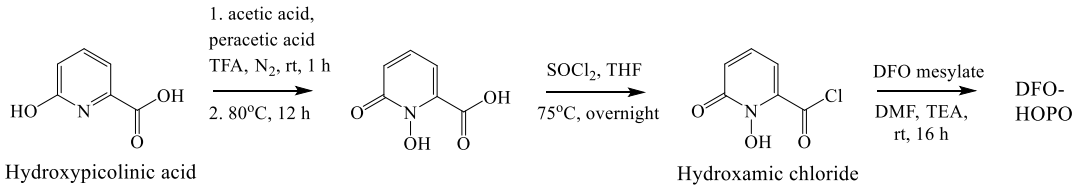

Scheme 19 - Synthesis of DFO-HOPO reported by Smith *et al*. in 2017. [181]

In addition, a linear octadentate siderophore was developed from desferrichrome (DFC), which is a cyclic hydroxamate-containing siderophore, named Orn4-hx. The acyclic Orn4-hx was supposed to provide high synthetic availability, flexibility to modify the number of donor atoms, and feasibility to conjugate to biomolecules.[182] The [^{89}Zr]Zr(IV) radiolabelling reaction was performed at room temperature and gave a quantitative yield within 20 minutes. To radiolabel Orn4-hx conjugated to tratuzumab, the conjugate was incubated for 90 minutes to give a 63 ± 5% yield. However, biodistribution showed bone uptake and liver uptake 7.0 ± 2.2% ID/g and 20.67 ± 1.26% ID/g at 96 hours post injection respectively, which reduced tumour-to-background ratios and would be problematic for further development of this chelator.

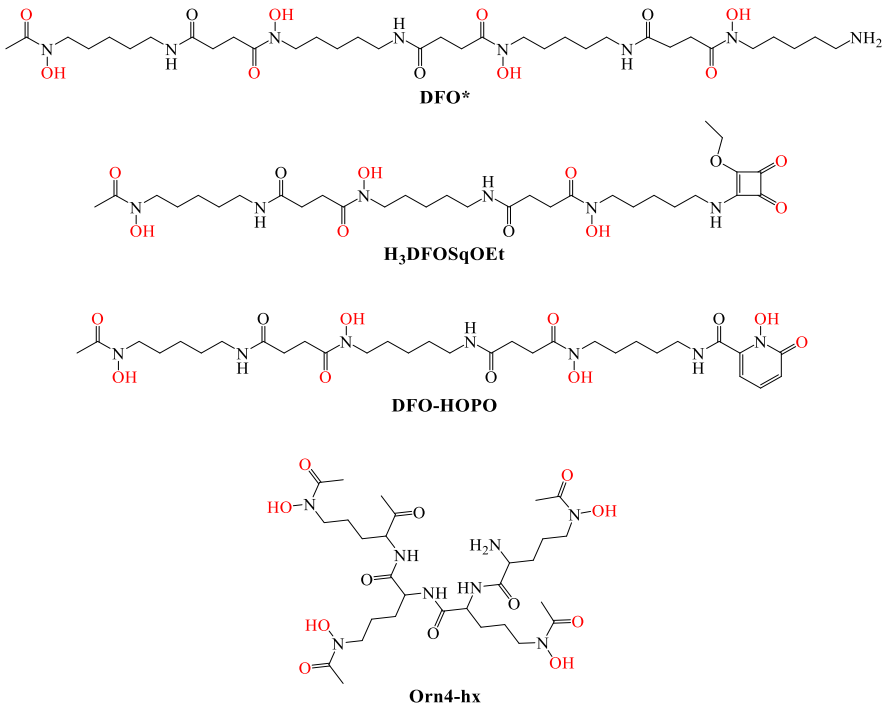

Figure 68 - DFO analogue chelators.

Macrocyclic compounds were labelled with [^{89}Zr]Zr(IV) by Wadas and co-workers as described in chapter 2. Although radiolabelling efficiency was 100% and most of the complexes especially [^{89}Zr]ZrDOTA were stable in competition studies against EDTA, metal ions solution as well as serum, the labelling reactions were performed at 90-95^{o}C which is not suitable for biomolecules.

This study focused on development of a DFO molecule attached onto azamacrocycles; NOTA, DOTA and DOTAGA. NOTA-NHS ester, DOTA-NHS ester and DOTAGA anhydride were reacted with DFO mesylate, see Figure 69. There are a number of reasons that this is of interest. The hybrid chelators all have more than eight donor atoms to bind to zirconium-89 and so could achieve octadentate coordination in different binding modes. It is likely that the metal centre will initially bind to the flexible DFO part of the molecule but this could lead to a two-stage binding process where the metal ion then shifts into the cavity of the macrocycle. This may allow radiolabelling of the macrocycles at lower temperatures. The aim was to synthesise a series of chelators and then proceed rapidly to evaluation of radiolabelling properties. The radiolabelling of these three novel chelators with [^{89}Zr]Zr(IV) was compared with [^{89}Zr]ZrDFO in terms of concentration of the chelator, logD pH 7.4, and stability in EDTA and fetal bovine serum.

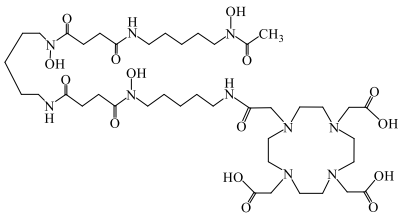

DOTA-DFO (21)

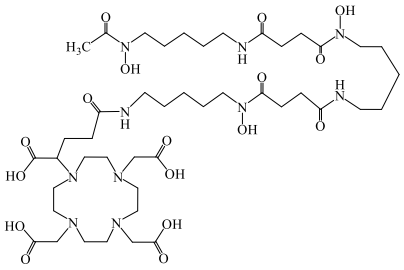

DOTAGA-DFO (22)

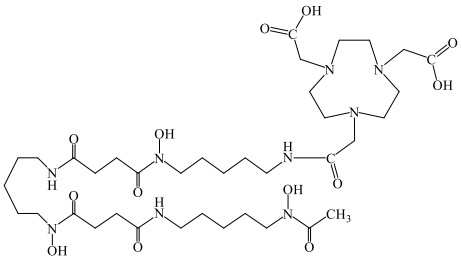

NOTA-DFO (23)

Figure 69 - Macrocyclic-based DFO studied in this work.

4.2. Synthesis of DOTA-DFO (21)

The synthesis of DOTA-DFO was carried out following standard amide bond formation protocols between an acid and an amine. Amide bond formation is shown in Scheme 20.

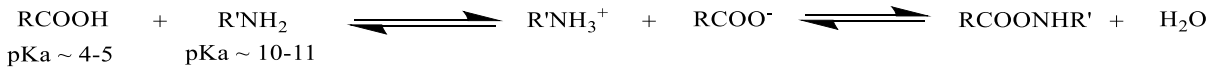

Scheme 20 - Amide bond formation.

To form amide bond, simply reacting the amine and carboxylic acid is a challenge as carboxylate is a poor electrophile. The strategy that is usually applied is the initial conversion of the carboxylic acid to a more reactive group such as acyl chloride, active ester or anhydride.

Acyl chloride or acid chloride is normally prepared by using thionyl chloride ($SOCl_2$) or oxalyl chloride $(COCl)_2$ to convert the acid to the acid chloride. The mechanisms are shown in Scheme 21. Then amide formation is following by coupling with the desired amine.

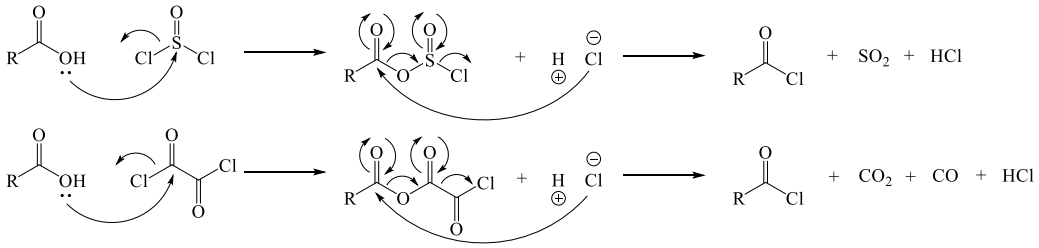

Scheme 21 - Mechanism of acyl chloride formation by using $SOCl_2$ and $(COCl)_2$.

The synthesis of compound **32** was attempted, see Scheme 22. DOTA reacted with $SOCl_2$ in anhydrous DCM. The reaction was performed at room temperature for an hour then evaporated and dried under vacuum overnight. The crude reaction mixture was then dissolved in anhydrous DMF, DFO mesylate was added along with DIPEA as base. However, the desired reaction did not occur as only starting materials DOTA and DFO were found when monitored by MS.

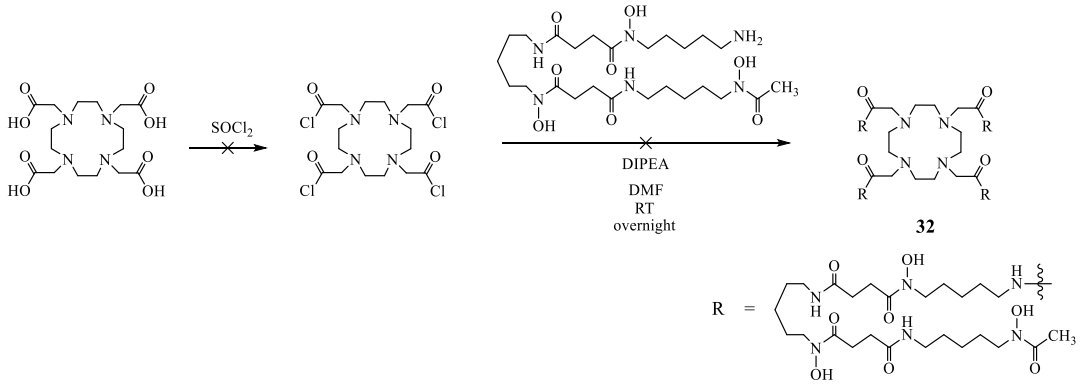

Scheme 22 - Attempt synthesis of DOTA-acyl chloride and DOTA-4DFO (**32**).

Activated esters are generally hydrolysed more easily than alkyl esters but this also means that they can react with amines under mild conditions. To prepare activated esters, different alcohols such as *N*-hydroxysuccinimide (NHS), *p*-nitrophenol, pentafluorophenol and 2,4,5-trichlorophenol can be used in order to increase electrophilicity of the carbonyl group. The preparation of DOTA-NHS activated ester has been completed in one step. DOTA-NHS ester was originally prepared for use in radioimmunotherapy. For example, Pillai and co-workers prepared DOTA-NHS ester for conjugation to form DOTA-lanreotide which was then labelled with ^{177}Lu as a radiolabelled somatostatin analogue.[183] Khorrami and co-workers also synthesised this activated DOTA derivative ester for the study of ^{67}Ga-DOTA-rituximab.[184] Ghannadi-Maragheh and co-workers used the same conditions to produce the DOTA-NHS ester to conjugate to cetuximab which was labelled with ^{170}Tm for treating squamous cell carcinoma.[185] The reaction was generally performed in anhydrous DCM at room temperature using *N,N'*-dicyclohexyl carbodiimide (DCC) as the coupling agent, see Scheme 23.

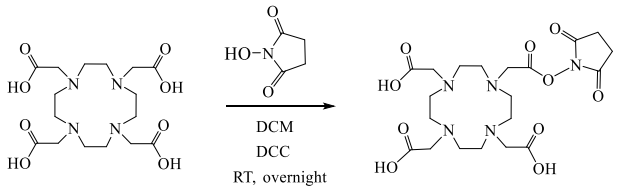

Scheme 23 - Synthesis of DOTA-NHS ester reported by Shirvani-Arani *et al*. in 2012.[185]

The syntheses of four-activated-ester DOTA derivatives were attempted, see Scheme 24. The reaction conditions were modified from the preparation of DOTA-NHS ester reported by Shirvani-Arani *et al.* in 2012[185] by using 4 equiv. of NHS and 4 equiv. of DCC in order to react with all four of carboxylic acid groups. However the desired product was not produced.

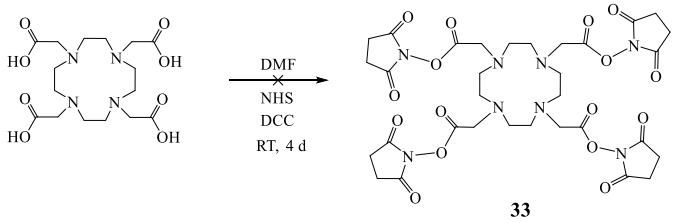

33

Scheme 24 - Attempted synthesis of DOTA-4NHS ester (**33**).

DCC is a common coupling agent used to activate carboxylic acids. It reacts with carboxylic acid and forms O-acylisourea then reacts with amine. Additionally it can react with two molecules of carboxylic acid to form symmetric anhydride which then reacts with amine in the next step. As shown in Scheme 25, this reaction has limitation as only half of carboxylic acid is coupled DCC resulting in low product yield.[186] It also shows that the competing N-acylurea is generated (N-acylurea can react with the amine to give an amide product).[187]

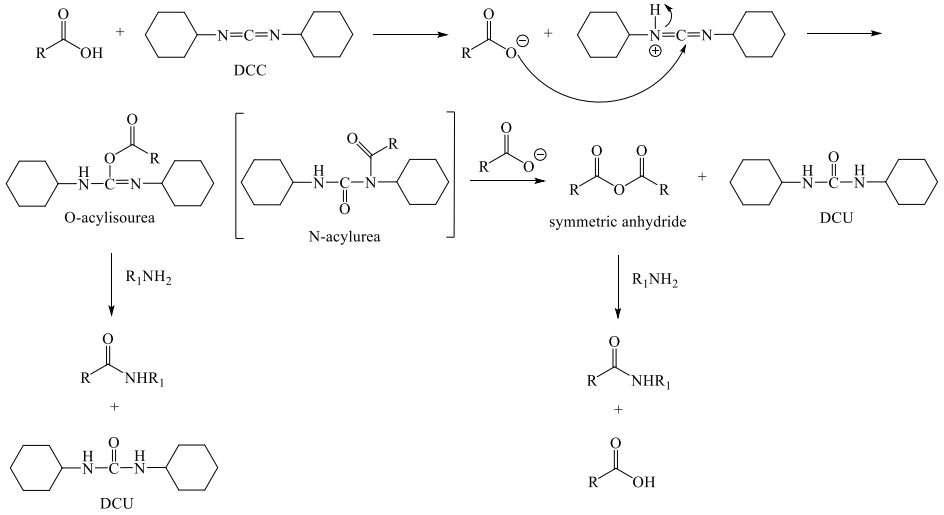

Scheme 25 - Mechanism of active ester preparation by using DCC as coupling agent. [186, 187]

It has been reported that the use of carbodiimide coupling agents fails to yield the desired product when used to form activated esters at multiple sites with DOTA. It was believed that the macrocycle being in a zwitterionic form causes problems for proton transfer to carbodiimide reagents. In 2010, Leon-Rodrıguez and co-workers found that synthesis of several DOTA tetraamide derivatives, which were difficult to prepare, were more successfully prepared using HBTU as coupling agent.[188] The mechanism of carboxylic acid and amine coupling using HBTU as coupling agent is shown in Scheme 26.

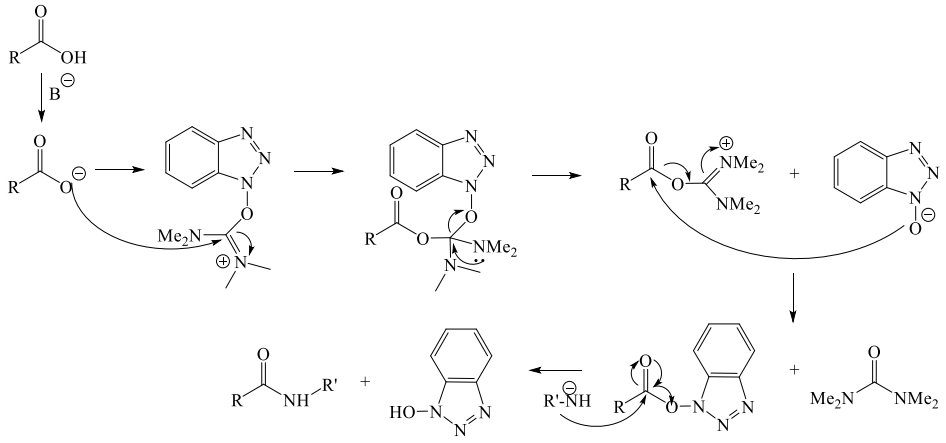

Scheme 26 - Mechanism of carboxylic acid and amine by using HBTU as coupling agent.

Synthesis of DOTA-DFO (**21**) was attempted using DOTA as starting material, HBTU as coupling agent and DIPEA as base in anhydrous DMF. However, the reaction was not successful as the MS of the reaction mixture showed only starting materials were present, see Scheme 27.

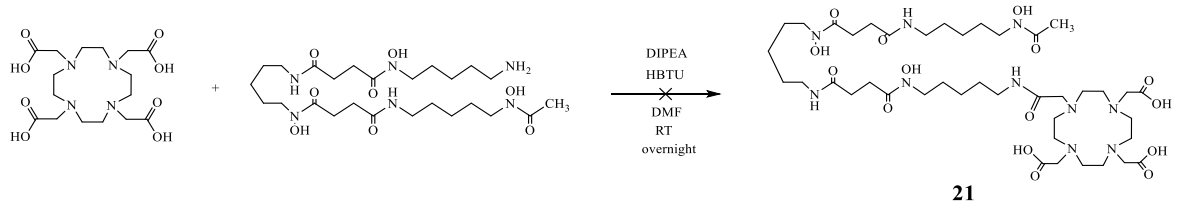

21

Scheme 27 - Attempted synthesis of DOTA-DFO (**21**) by using DOTA as starting material.

Rather than pursuing the multiply functionalised derivative or direct synthesis of the mono-functionalised compound, the commercial DOTA-monoNHS ester was used as the starting material. The reaction was performed by reacting DOTA-NHS ester (0.03 mmol) with DFO mesylate (0.03 mmol) in DMF (1 mL) using DIPEA (0.1 mmol) as base. The reaction was stirred at room temperature overnight under Ar atmosphere then evaporated. The purification was done by semi-preparative-HPLC to give the product in a 44% yield.

4.3. Synthesis of DOTAGA-DFO (22)

DOTAGA is the DOTA derivative containing glutaric acid. It was first synthesised by Maecke and co-workers in 2000.[189] The attachment of the biomolecule onto DOTA derivatives can be performed by conjugation via one acetic pendant arm leading to DOTA-monoamide derivatives, see Figure 70. However, it was found that the complex stability significantly

decreased as reported the kinetic inertness of Ga(III) complex of DO3AM^{Bu} was much lower than GaDOTA complex.[190] C-Functionalised DOTA derivatives were developed to overcome this issue and the DOTAGA derivatives are another approach with a branched pendant arm to retain the four acid groups.

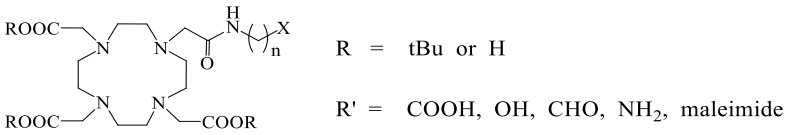

Figure 70 - Examples of DOTA-monoamide derivatives.[191]

The labelling of DOTAGA was reported with various radionuclides such as ^{111}In, ^{90}Y, ^{177}Lu and ^{68}Ga for use in both SPECT and PET.[59, 192] The bioconjugation of DOTAGA can be performed when the acetate arms are protected as esters, while carboxylic acid group on glutaric acid is used to attach biomolecule. Then the deprotection of ester groups is performed; however, the reaction conditions are not compatible with more sensitive biomolecules such as antibodies. Therefore DOTAGA anhydride, see Figure 71, was developed to avoid the deprotection step.

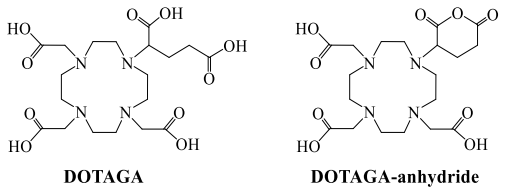

Figure 71 - Structures of DOTAGA and DOTAGA-anhydride.

Denat and co-workers reported the preparation of DOTAGA-anhydride and the reactivity of this molecule with various nucleophiles.[193] They carried out the synthesis of DOTAGA-anhydride in a one-step reaction using DOTAGA as a starting material, see Scheme 28.

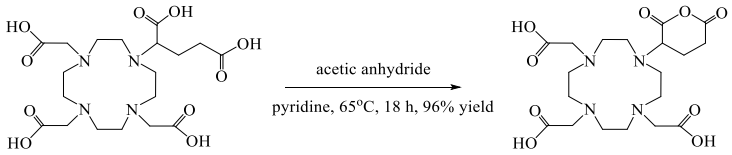

Scheme 28 - Synthesis of DOTAGA-anhydride reported by Denat *et al*. in 2012.[193]

The ring opening reaction of DOTAGA-anhydride was carried out with a variety of precursors, including 4-nitrobenzylamine hydrochloride, 2-aminoethanethiol hydrochloride, ethanol and nitrophenylalanine monoester hydrochloride. All reactions were performed in DMF with triethylamine used as base. After purification by HPLC, the desired products were obtained in 72%, 45%, 35% and 68% yields respectively.

In this research work, DOTAGA-anhydride was reacted with DFO mesylate (1.1 equiv.) in anhydrous DMF under basic conditions. The reaction mixture was stirred at room temperature overnight under Ar atmosphere and then evaporated to dryness. The crude product was purified by semi-preparative HPLC to give the product in a 13.1% yield, see Scheme 29

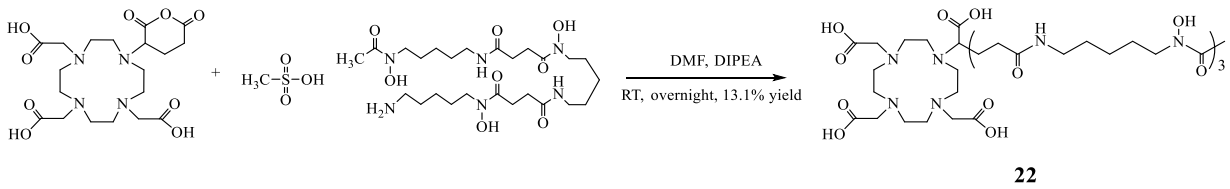

22

Scheme 29 - Synthesis of DOTAGA-DFO (**22**).

It could be argued that the ring opening reaction should lead to two different products as the anhydride group in DOTAGA-anhydride molecule is asymmetric, see Figure 72.

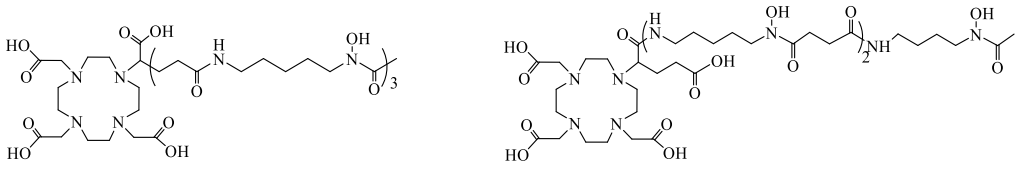

DOTAGA-DFO (22A) **DOTAGA-DFO (22B)**

Figure 72 - Structures of possible DOTAGA-DFO molecules.

The ring opening reaction of DOTAGA-anhydride by a nucleophile was also studied by Denat and co-workers.[193] It was reported that DOTAGA-anhydride was reacted with two equivalents of propylamine in DMF at 50ºC for 2 hours. DFT calculations showed no significant difference between the two isomers. However, the ^{1}H NMR spectrum showed only one product was generated which was isomer **a**, see Figure 73.

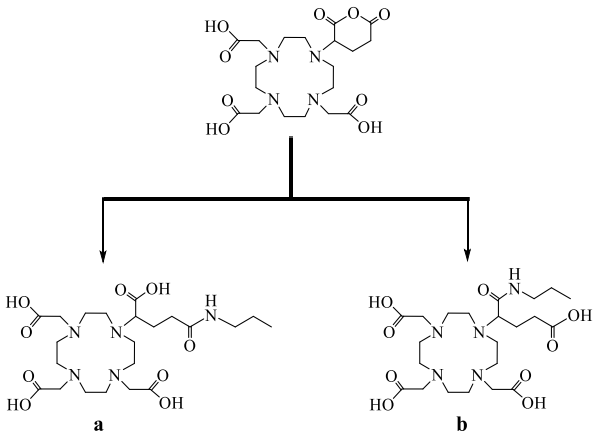

Figure 73 - Two isomers of products from ring opening reaction of DOTAGA-anhydride reported by Denat *et al*. [193]

This was confirmed by comparison with the ^{1}H NMR spectra of compound **a** which had been synthesised by an alternate route (from the coupling reaction of DOTAGA(tBu)$_4$ with propylamine), see Scheme 30.

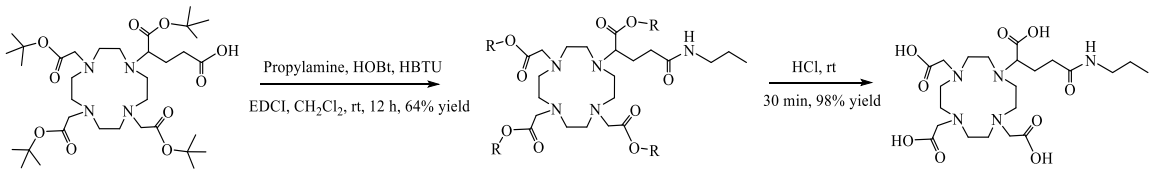

Scheme 30 - Synthesis of isomer **a** from DOTAGA(tBu)$_4$ reported by Denat *et al*. in 2012.[193]

Therefore, it is believed that there was only one isomer for DOTAGA-DFO compound synthesised in this research which is the DOTAGA-DFO **(22A)** structure.

4.4. Synthesis of NOTA-DFO (23)

NOTA is the smallest cyclic molecule in the cyclic polyamino polycarboxylic chelator family.[53] It is 1,4,7-triazacyclononane containing three acetic acid pendants on nitrogen atoms. It was first synthesised by Takahashi and Takamoto in 1977 and then developed into NOTA derivative bifunctional chelators, see Figure 74.

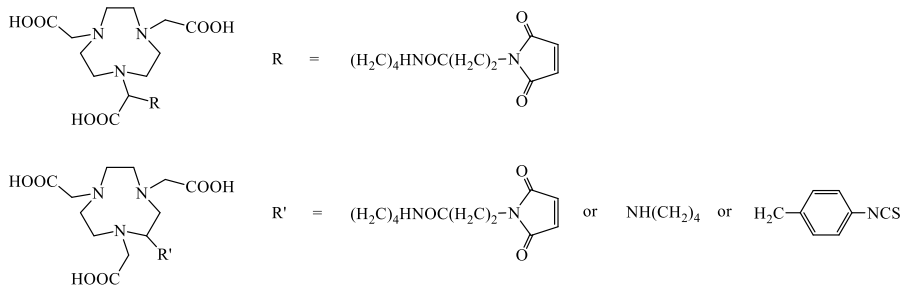

Figure 74 - Examples of NOTA derivative bifunctional chelators.

The NOTA-monoNHS ester has been reported and used to synthesise NOTA-NFB which was labelled with ^{68}Ga as a specific PET imaging agent of CXCR4.[194] ^{68}Ga-NOTA-folate was synthesised by preparation of NOTA-NHS ester from NOTA in the first step then conjugation with γ-hydrazide-folate and radiolabelling with ^{68}Ga to give an agent for detecting folate receptor-positive cancers.[195] The NOTA-NHS ester was also used to prepare a fluorescent/PET bimodal imaging probe. It was reacted with sulfonated zinc phthalocyanine (ZnPc) as fluorescent group and labelled with ^{64}Cu for PET imaging. A preliminary *in vivo* experiment in tumour bearing mice confirmed that the tracer can be used in both PET and fluorescence imaging.[196]

The NOTA-monoNHS ester was used in this study for conjugation with DFO. As with DOTA-DFO (**21**) and DOTAGA-DFO (**22**), the NOTA-NHS ester was reacted with DFO mesylate in DMF at room temperature under an Ar atmosphere. The reaction should be performed in neutral to slightly alkaline conditions. The reaction mixture was stirred overnight, evaporated to dryness and the crude product was purified by semi-preparative HPLC to give the product in a 20% yield.

4.5. Attempted synthesis of NOTA-*n*DFO (25)

Attempts were also made to functionalise multiple arms of the NOTA group. The identified precursor for this reaction was the nitrophenol ester. An attempt was made to react NOTA with 4-nitrophenol to prepare activated phenolic esters. The reaction was a modified method of the route reported by Haberkorn and co-workers in 2005. They synthesised mono activated esters of DOTA with several types of phenolic esters, see Figure 75.[197] The reactions were performed by using DOTA (1.24 mmol) dissolved in water (10 mL), adding a solution of the selected phenol (1.24 mmol) in acetonitrile and then dropwise addition of a solution of DCC (1.24 mmol) in pyridine (8 mL). The reactions were stirred at room temperature for 90 minutes and then evaporated. The residue was added to a solution of 20% acetonitrile in

water and filtered to remove precipitated dicyclohexylurea then lyophilised. The crude products were purified by HPLC.

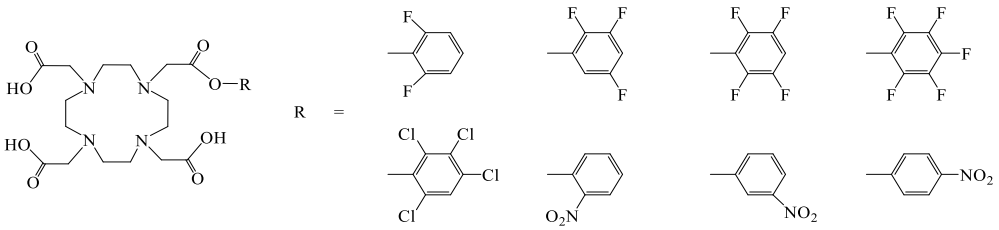

Figure 75 - Mono activated esters of DOTA synthesised by Haberkorn *et al*. in 2005.[197]

In this work, an attempt was made to synthesise the NOTA activated ester with all three arms reacted. NOTA was mixed with 4-nitrophenol (3.3 equiv.) in acetonitrile, using DCC (3.3 equiv.) in pyridine as coupling agent, see Scheme 31.

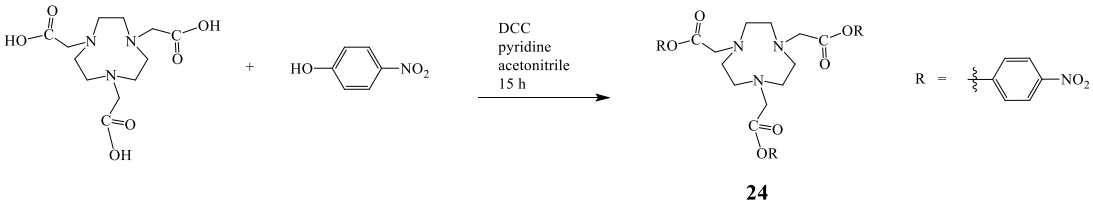

24

Scheme 31 - Synthesis of NOTA-phenyl ester (**24**).

The crude product was analysed by MS and found to be a mixture of 1-, 2- and 3-arm ester products, see Figure 76.

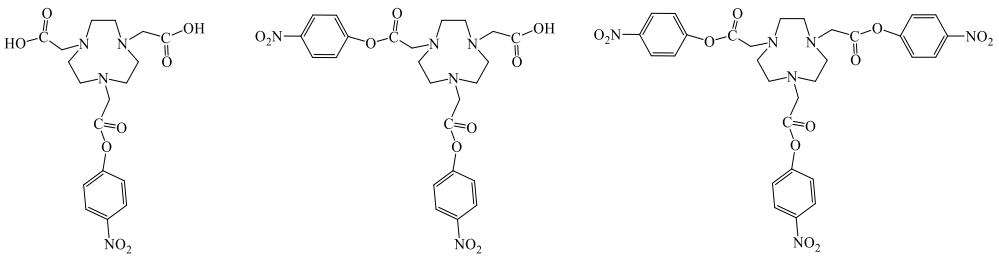

1-arm **24A** **2-arm** **24B** **3-arm** **24C**

Figure 76 - NOTA phenyl ester products.

The crude product was then reacted with DFO mesylate in DMF anhydrous at room temperature under Ar atmosphere and the reaction was monitored by MS, see Scheme 32.

It was considered that a semi-preparative HPLC separation of the products could then be carried out to give sufficient compound for radiolabelling.

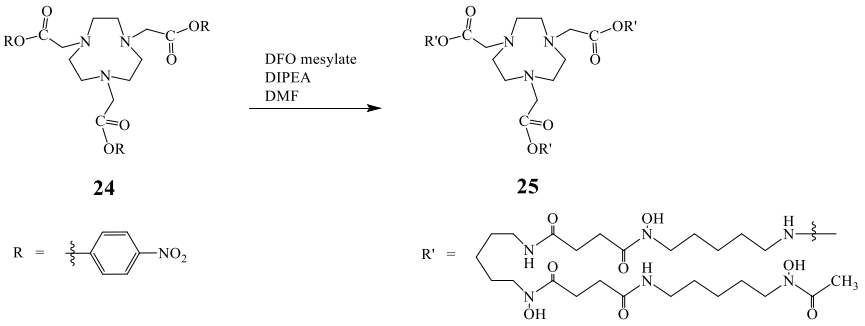

Scheme 32 - Synthesis of NOTA-*n*DFO (**25**).

After leaving the reaction for up to 6 days and monitoring by MS, it was found that the 1-arm and 2-arm products had formed but mass ions were not observed for the 3-arm product, see Figure 77. Azamacrocyclic molecules can be difficult to analyse by MS so further purification and analysis are needed to understand this reaction. It does look promising but unfortunately there was insufficient time to pursue further investigation of the multiple DFO compounds.

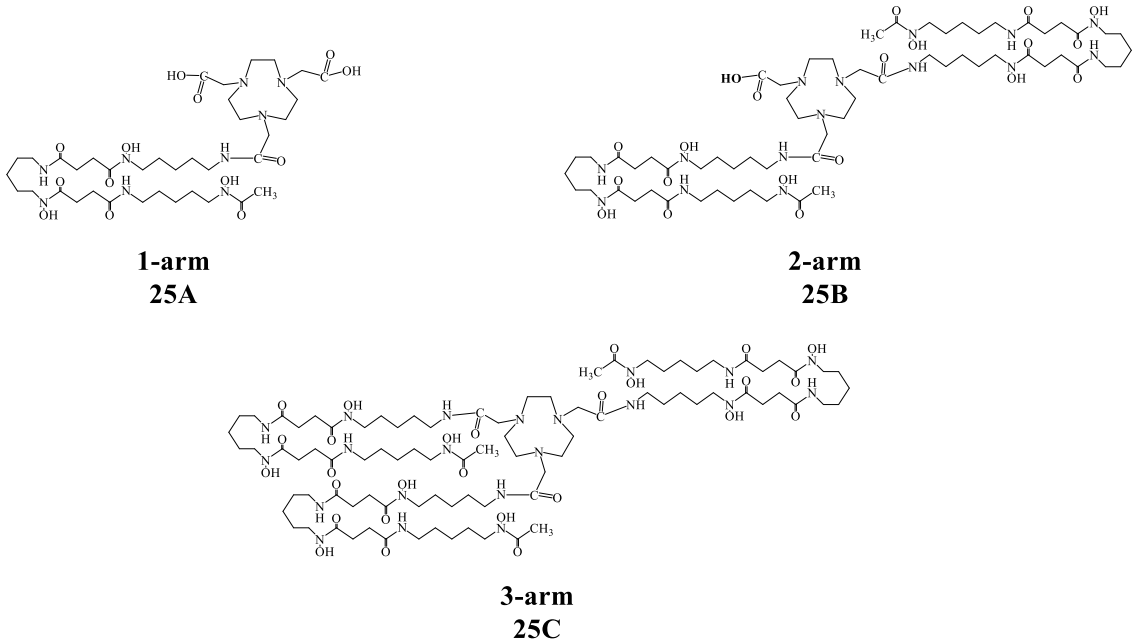

Figure 77 - NOTA-*n*DFO structures.

4.6. [^{89}Zr]Zr(IV) radiolabelling

The three macrocycle-based DFO chelators were radiolabelled with [^{89}Zr]zirconium(IV) oxalate. [^{89}Zr]Zr(IV) in form of oxalate salt was chosen instead of the chloride as it was shown in chapter 2 that the observed labelling yield was 100% at the chelator concentration of 0.56 µM when using [^{89}Zr]zirconium(IV) oxalate while 5 µM was required for [^{89}Zr]zirconium(IV) chloride. [^{89}Zr]zirconium(IV) oxalate was neutralised by 0.5-1 M Cs_2CO_3, with the labelling performed in water at pH 7.0-7.4 at room temperature and analysed by radio-ITLC.

4.6.1. Concentration curve

The chelators were labelled at various concentrations in water, with the [^{89}Zr]Zr(IV) solution adjusted to pH 7.0-7.4, at room temperature for 0.5-2 hours. In 2011 that Blower and co-workers reported labelling experiments to test and compare new chelators, with a series of concentrations compared with a "gold standard" chelator. The compound CP256, which is a tripodal tris(hydroxypyridinone), was labelled with ^{68}Ga at concentrations of 100 nM – 1 mM. A comparison of the chelating efficiency was investigated with the known gallium chelators; DOTA, NOTA and HBED, see Figure 78.[198] The figure shows a trend of radiolabelling efficiency for the chelators. Ferreira and co-workers also made use of a similar radiolabelling study of gallium-68 radiopharmaceuticals.[199] The optimal reaction conditions for each compound were examined with higher temperatures used to improve radiochemical yield and specific activity in some cases.

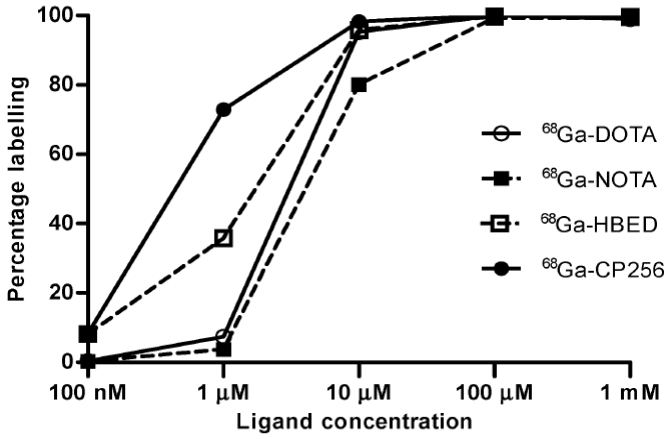

Figure 78 - Radiolabelling yields versus ligand concentrations of ^{68}Ga-chelators reproduced from Blower *et al*. in 2011.[198]

In this work, using the same labelling method that was used for [^{89}Zr]ZrDFO in chapter 2, all three macrocyclic-DFO chelators were dissolved in water, the neutralised [^{89}Zr]Zr(IV) solution (0.5 MBq) was added, pH was adjusted to 7.0-7.4 with 0.5 M Cs_2CO_3 in a total volume of 100 µL, and the reaction was incubated at room temperature. Radio-ITLC was used to analyse the labelling yield at the selected time points.

For [^{89}Zr]Zr**21**, the concentration range was from 0.01 µM to 51.47 µM. At the concentration of 3.43 µM (log[M] = 0.54), the labelling yield was around 76%, while [^{89}Zr]ZrDFO showed quantitative yield. However, it was found that labelling yields increased to 90.0% and reached 97.6% at 1 and 2 hours respectively. The labelling yield was determined at time points up to 2 hours. As [^{89}Zr]Zr(IV) has a half-life of 78.4 hours, after 2 hours reaction time, 98.3% of the original activity remains, see equation 1, which does not make a huge difference on the level of radioactivity in the synthesised compound. Therefore, radiolabelling yields were considered at 2 hours for comparison.

Equation 1

$$A_t = A_0.e^{-\tau t}$$

Where: A_t = Activity at time t, A_0 = Activity at time 0, τ = 0.693 / half-life

The results showed that [^{89}Zr]Zr**21** gave >99% yield at a concentration of 3.43 µM (log[M] = 0.55) and 3% yield at 0.01 µM (log[M] = -2.16), see Figure 79.

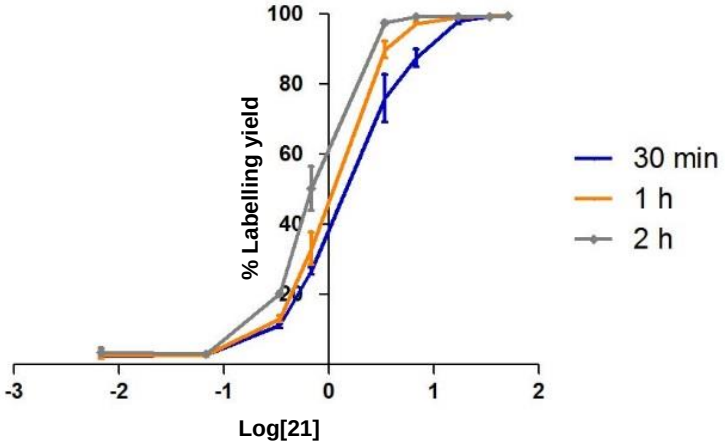

Figure 79 - Concentration curve of [^{89}Zr]Zr**21**.

The other DFO macrocyclic chelators; **22** and **23**, were labelled under the same conditions. The results showed similar trend as [^{89}Zr]Zr**21**, see Figures 80 and 81.

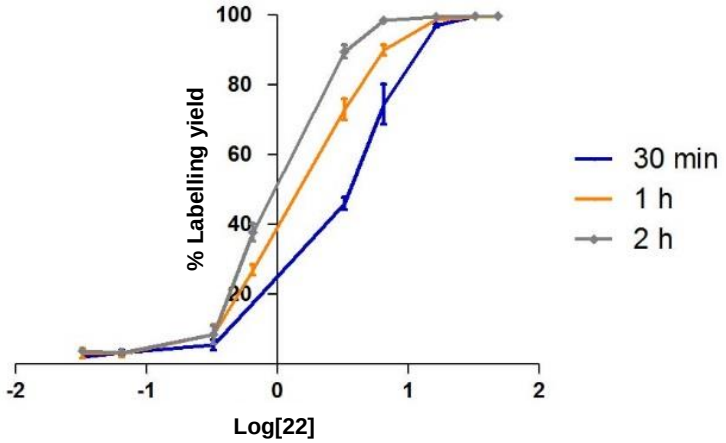

Figure 80 - Concentration curve of [^{89}Zr]Zr**22**.

For [^{89}Zr]Zr**22**, although it showed a 46% labelling yield after incubation for 30 minutes when labelling at concentration of 3.27 µM (log[M] = 0.51), a labelling yield of 90% could be achieved at 2 hours, see Figure 80. Therefore [^{89}Zr]Zr(IV) complexes of **21** and **22** were quite similar and there was not a huge effect of the additional acid group of DOTAGA on the complex formation.

[^{89}Zr]Zr**23** also showed the same trend; however, to reach >90% labelling yield, the concentration of the chelator should not be less than 5.90 µM (log[M] = 0.77), see Figure 81.

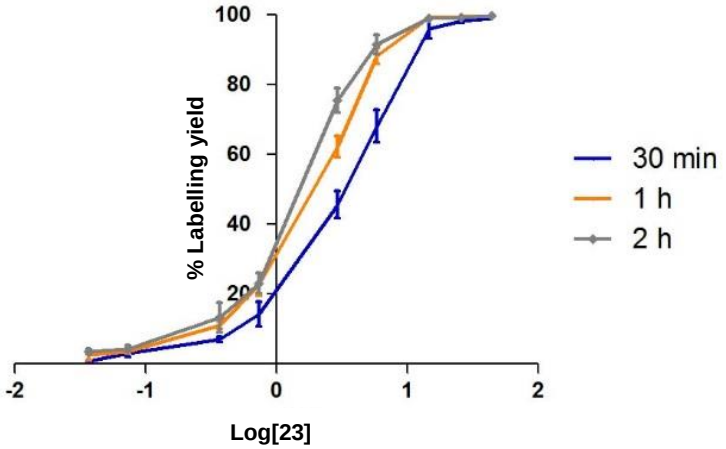

Figure 81 - Concentration curve of [^{89}Zr]Zr**23**.

To compare with [^{89}Zr]ZrDFO, the concentration curves of all labelled compounds were plotted, as shown in Figure 82. As expected, [^{89}Zr]ZrDFO showed the most effective labelling as might be expected for a linear chelator.

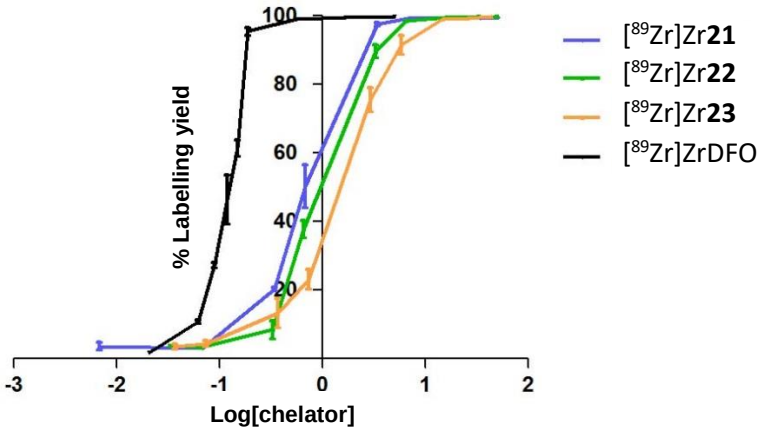

Figure 82 - Radiolabelling yields versus chelator concentrations using optimal conditions compared with control ligand [^{89}Zr]ZrDFO.

4.6.2. EDTA challenge

The novel chelators and DFO were labelled with [^{89}Zr]Zr(IV) and incubated with 100-fold excess of EDTA pH 7 at 37ºC for a period of 7 days in order to investigate the inertness of the complexes toward transchelation. The analysis by radio-ITLC using 10 mM EDTA at pH 6 showed that [^{89}Zr]Zr(IV) complexes stay at the origin while [^{89}Zr]ZrEDTA moves to solvent front. Figure 83 shows % of intact complex plotted against time of incubation with EDTA. All complexes have similar susceptibility to transchelation and remained more than 95% stable for 2 days, then slightly dropped to 90% at 7 days. This result relates to the experiment performed by Deri *et al* in 2014.[88] EDTA stability of [^{89}Zr]ZrDFO in 100-fold excess at pH 7 indicated that ~90% of complex was found at 7 days. It can be concluded that [^{89}Zr]Zr(IV) macrocyclic-DFO chelators have comparable behaviour toward EDTA as [^{89}Zr]ZrDFO with no obvious superiority in this assay.

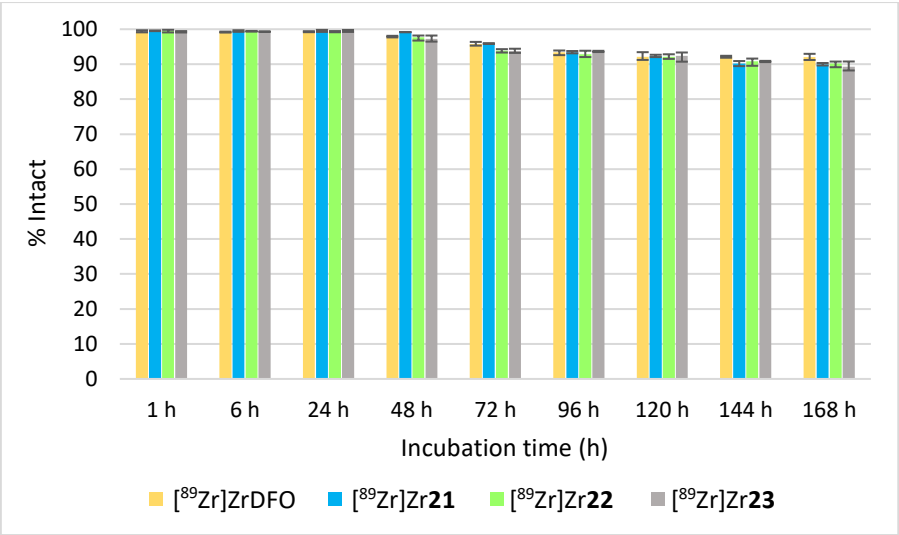

Figure 83 - 100-fold excess EDTA challenge.

4.6.3. Fetal bovine serum stability

Serum stability tests were performed in order to predict *in vivo* stability of the complex. The stability was assessed in fetal bovine serum at 37°C to simulate biological conditions. All [^{89}Zr]Zr(IV) complexes showed high stability with more than 99% of the compound intact after 7 days.

4.6.4. Fe(III) ion competition

Fe(III) ion competition experiments were carried out to evaluate the capability of the complex to resist loss of the label by competition with Fe(III). Dissociation of [^{89}Zr]Zr(IV) from [^{89}Zr]Zr**21** and [^{89}Zr]ZrDFO was observed in the presence of a 30-fold excess of $FeCl_3$ in PBS at pH 7.4 at 37°C and analysed by radio-ITLC as described above. The results showed 87.2 ± 0.6% and 92.4 ± 0.4% (n = 3) stability for [^{89}Zr]Zr**21** and [^{89}Zr]ZrDFO after 1 hour incubation, progressing to an almost quantitative decomplexation of both conjugates within 24 hours (2.2 ± 0.1% and 2.3 ± 0.5% of [^{89}Zr]Zr**21** and [^{89}Zr]ZrDFO remaining, respectively), with a slightly faster decomplexation for [^{89}Zr]Zr**21** for the first 12 hours. Many authors have discussed [^{89}Zr]ZrDFO conjugate stability, however, there are only three reports mentioning [^{89}Zr]ZrDFO stability in presence of the Fe(III) *in vitro*. Ma *et al*. reported that in the presence of the 10-fold excess of Fe(III), [^{89}Zr]ZrDFO complex was 93% intact after 20 min incubation.[94] Deri *et al.* extended the stability study to 7 days and claimed 90.6 ± 4.5%, 48.2 ± 27.0% and 39.1 ± 9.9% stability at 1 hour, 1 day and 1 week incubation time points, respectively.[88] Pandya *et al*. used a 200 fold excess of Fe(III) and found 96.5 ± 0.2%, 76.1 ± 1.3% and 33.9 ± 1.5% stability at 2 hour, 1 day and 1 week incubation time points,

respectively.[108] The Deri *et al.* and Pandya *et al*. results are clearly contradictory for the early time points (1-2 hour and 1 day) and potentially indicate some differences in the experimental protocols that were not reported in the literature. In this work, an intermediate Fe(III) concentration excess was used and found closer agreement with one obtained by Deri *et al*. at 1 hour. Most importantly, the results showed that [^{89}Zr]Zr**21** has a comparable stability in Fe(III) challenge assay to that of [^{89}Zr]ZrDFO, see Figure 84.

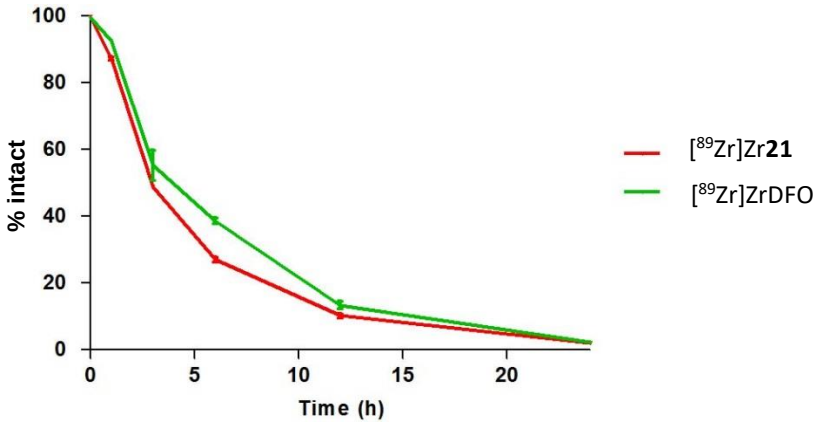

Figure 84 - Fe(III) ion competition of [^{89}Zr]Zr**21** and [^{89}Zr]ZrDFO.

4.6.5. Log D pH 7.4

Determination of distribution coefficient between two immiscible solvents is used to measure the lipophilicity of the compound. Lipophilicity is a major factor which predicts *in vivo* behaviour of compounds such as tissue permeability, absorption, distribution and target affinity. The experiment is performed by adding a small amount of the compound to an organic phase (n-octanol) and an aqueous phase (water or buffer). *N*-Octanol has properties that resemble to lipid membranes; therefore, the distribution of compounds into n-octanol represents the ability of the compounds to diffuse across biological membranes. In this study, PBS at pH 7.4 was used as the aqueous phase. The distribution coefficient was calculated as a ratio of counts in octanol layer to counts in PBS layer using a gamma counter. The results are shown in Table 7.

[^{89}Zr]ZrDFO-macrocycles showed a more hydrophilic character. It is predicted that rapid renal excretion should be the main clearance pathway.

Table 7 - Log D pH 7.4 of the labelled compounds.

[^{89}Zr]Zr(IV) compound	Log D pH 7.4
[^{89}Zr]ZrDFO	-0.52
[^{89}Zr]Zr**21**	-4.09
[^{89}Zr]Zr**22**	-3.96
[^{89}Zr]Zr**23**	-3.35

4.7. Conclusion

Three macrocycle-DFO chelators; DOTA-DFO (**21**), DOTAGA-DFO (**22**) and NOTA-DFO (**23**), were synthesised and radiolabelled with [^{89}Zr]zirconium(IV) oxalate. The radiolabelling efficiency was analysed by radio-ITLC. Labelling reactions were monitored at 30, 60 and 120 minutes, and lipophilicities were reported as log D (pH 7.4). The stability of the complexes was considered in terms of EDTA challenge, fetal bovine serum and Fe(III) ion competition.

EDTA challenge was performed at neutral and biological pH. It showed that the labelled compounds were similarly resistant to transchelation as [^{89}Zr]ZrDFO. The stability in fetal bovine serum was also studied and no degradation and release of [^{89}Zr]Zr(IV) was observed for 7 days. Fe(III) ion competition showed that % intact of [^{89}Zr]Zr**21** was comparable with [^{89}Zr]ZrDFO. The behaviour of [^{89}Zr]Zr**21** *in vivo* needs to be explored by a biodistribution study as part of future work. There does not appear to be any indication of improved stability in comparison to DFO for the novel chelators. It would be of high interest to investigate this *in vivo* but the initial conclusion is that they are behaving in a similar way to DFO. The reduced lipophilicity could be an advantage for many applications as it may improve the clearance rate of the conjugates.

N-Functionalisation of NOTA was attempted by using 4-nitrophenol in order to produce activated ester groups for DFO conjugation The initial reaction was analysed by MS and HPLC and showed that a mixture of 1-, 2- and 3-nitrophenyl arm products were produced. The next step was performed without purification, with the potential for separation of the product mixture after the functionalisation. It showed promising results with one and two arm DFO products detected. These compounds are of interest for further study, particularly those with the presence of two or three pendant DFO arms to wrap around the metal centre.

Chapter 5

Conclusions and future work

5. Conclusions and future work

In this work the synthesis of tetraazamacrocyclic-based chelators **1**, **5**, **9**, **16**, **20**, **21**, **22** and **23** for [^{89}Zr]Zr(IV) radiolabelling is reported. Recently, the one of the areas of interest in positron emission tomography research is the development of chelators for zirconium(IV) with particular focus on octadentate chelators. Various types of chelator based on the tetraazamacrocycles cyclen **1**, **5**, **9**, **16**, **20**, **21** and **22**, cyclam **20**, and TACN **23** were studied. The macrocyclic compounds synthesised in this work were divided into three groups; macrocycle-based chelators with short pendant arms **1**, **5** and **9**, macrocycle-based chelators with long pendant arms **16** and **20** and DFO functionalised macrocycles **21**, **22** and **23**.

5.1.1. Macrocycle-based short pendant arm chelators

In this part of the research work, known chelators were synthesised that had not previously been investigated for their complex formation properties with zirconium. The chelators are based on cyclen functionalised with short pendant arms containing one of phosphonic acid (DOTP) **1**, phosphinic acid (DOTPI) **5** or picolinic acid **9**.

For synthesis of DOTP **1**, there were two strategies previously published for synthesis of this compound; a one-pot synthesis and a multi-step method. The one-pot procedure was attempted using a modified method by heating the cyclen, phosphoric acid and formaldehyde at reflux for up to 48 hours and then the crude product was precipitated by addition of acetone. However, it was believed that the reaction might not be completed as additional peaks assigned to the phosphoric acid starting material were present in the ^{31}P NMR spectrum and two singlets at δ 21.92 and 22.35 which were thought to be a mixture of the product and 3-arm by product. While positive mode MS showed the expected peaks for the product, peaks were also observed for 3-arm and 2-arm compounds that were not thought to be due to fragmentation. However, it was also considered that the issues with the NMR could be complicated by a mixture of protonation states. DOTP is not suitable for purification by silica gel column chromatography and so an alternative procedure where chromatography could be utilised was investigated. The alternative multi-step method was tried by reacting cyclen, paraformaldehyde and triethylphosphite, and the purification was performed using silica gel column chromatography. Then the intermediate was hydrolysed in 6M HCl. ^{31}P NMR was again used to analyse the purity of product and it proved that the multi-step method provided the product in higher purity.

The synthesis of cyclen-based phosphinic acid (DOTPI) chelator **5** was attempted. First of all, the phosphinic acid arm was prepared following the published method and obtained

in a high yield. Then cyclen was *N*-functionalised with the phosphinic acid compound. The reaction was monitored by ^{31}P NMR and MS and the peaks of DOTPI product and the by-product from the *N*-methylation reaction were detected as suggested in the literature. However, the purification was not successful. Ion exchange column chromatography was attempted but ^{1}H NMR showed that the eluted product was not pure and contained phosphinic acid precursor. Purification was also attempted by recrystallisation from methanol and isopropanol as reported for DOTPI and TRAP-Pr; however, crystals were not obtained. Although the compound was not pure, it was still taken forward for a preliminary radiolabelling study to evaluate if DOTPI could be labelled with [^{89}Zr]Zr(IV) and to assess whether it was suitable for further investigation with a pure chelator sample.

Cyclen-based picolinic acid chelators **9** and **16** were of interest as the crystal structure of zirconium(IV) complex with four bidentate picolinate chelators shows the metal centre bound to an O and an N donor from each to give an eight coordinate geometry. It has been shown with other biomedical applications and radiometals that picolinate derivatives offer rapid and stable complex formation and so it is of interest to investigate potentially octadentate chelator systems for complex formation with zirconioum-89. The synthesis of cyclen-based picolinic acid chelator **9** was performed by alkylation of cyclen with the picolinate arm precursor; which was prepared by following a protocol reported in the literature where dimethylpyridine-2,6-dicarboxylate was reduced with sodium borohydride. It was noted that increasing the amount of sodium borohydride reduced the reaction time however both methoxy groups could then be reduced. The alkylation reaction of cyclen was performed using excess of the picolinate precursor and purified by silica gel column chromatography to isolate the pure product.

5.1.2. Radiolabelling of macrocycle-based short pendant arm chelators

Radiolabelling experiments with [^{89}Zr]zirconium(IV) oxalate were carried out with the three compounds synthesised **1**, **5** and **9**. Attempts were made to form the complex of the stable abundant zirconium isotope but issues were encountered with solubility and there were challenges in reproducing literature studies under the same conditions. Generally a mixture of products was produced, and so it was decided to focus the studies on the radiolabelling conditions and the use of zirconium-89 with the low concentrations avoiding many of these issues.. The Zr-DOTA x-ray crystal structure has been published showing that the metal ion sits in the cavity bound the ring N donors and the pendant arms. DOTPI **5** and cyclen-based picolinic acid chelator **9** may form either “in cavity” complexes of this type or could form “out

of cavity complexes where all of the donor atoms come from the pendant arms. This is possible as there sufficient donors on the pendant arms to form an eight coordinate complex without involvement of the ring N-donors. It is worth noting that the analysis conditions use EDTA to complex to the "unbound" zirconium-89 and so the formed complex with the tested chelator must be significantly more stable than the binding to EDTA.

Radiolabelling yields of only 5 - 8% were obtained but it did seem that cyclen-based picolinic acid **9** had some minor advantages over the other chelators and so it was selected for optimisation. This allowed the radiolabelled yield to be increased to 40% after various buffer and pH conditions were tested. The reaction with [^{89}Zr]zirconium(IV) chloride was also tried as during the course of this research work it was reported in the literature that it could be used to successfully radiolabel DOTA, DOTP and DOTAM. The labelling conditions used in this study were varied slightly from the published method as it was found that [^{89}Zr]zirconium(IV) chloride was hydrolysed and formed insoluble species at pH above 6 in water (which remained at the baseline of radio-ITLC). It was believed that acetate buffer would a better option for [^{89}Zr]zirconium(IV) chloride radiolabelling. However, even using the modified conditions, the radiolabelling of DOTPI **5** was not improved, and the labelling yield of DOTP **1** was only 7.5%. The cyclen-based picolinic acid chelator compound **9** showed a slightly better labelling yield with this zirconium-89 precursor which offered suitable condition for labelling the next generation of synthesised chelators where the length of the picolinic acid arm linker was explored.

5.1.3. Macrocycle-based extended pendant arm chelators and their radiolabelling

Cyclen and cyclam azamacrocyclic derivatives **16** and **20**, with a longer linker to the picolinic acid pendant arm, were synthesised. The linker was attached to macrocyclic rings in order to extend the length of the arm and then attach the picolinic acid precursor. The extended picolinic acid arm was designed to allow Zr formation with eight donor atoms from the arms ("out of cavity" binding) and an increase in the flexibility of the chelator to adopt a more optimal geometry around the metal centre. The radiolabelling was performed by using the [^{89}Zr]zirconium(IV) chloride precursor to compare the results with the cyclen-based picolinic acid chelator **9** synthesised previously. However, both cyclen and cyclam-based extended arm picolinic acid chelators had lower labelling yields at all concentrations of the compounds. It was possible that the compounds formed both 1:1 and 1:2 metal-to-ligand complexes and the complexes where the metal centre was bound to multiple chelators (i.e. bidentate/ tridentate/ tetradentate) were not stable to the EDTA challenge from the method for analysis by TLC.

5.1.4. DFO derivatised azamacrocycle chelators and their radiolabelling

A new set of chelators combining azamacrocycle acetic acid pendant arm derivatives with DFO were synthesised by amide bond formation. The primary amine group of DFO was reacted with one or more of the pendant arms of DOTA, DOTAGA or NOTA and the resulting compounds **21**, **22** and **23** were purified by semi-preparative HPLC. The underpinning concept was that a 2-step chelation process may occur where a thermodynamic secondary product forms with the metal ion transferred into the macrocyclic cavity from the initial coordination to DFO which would be the kinetic product. Another alternative is that the zirconium-89 ion may bind to the hexadentate DFO component but gain additional donors for the two remaining coordination sites from the macrocyclic part of the chelator. The novel compounds could be labelled with [^{89}Zr]zirconium(IV) oxalate at room temperature, as was expected. Concentration curves were produced in order to optimise labelling conditions. The results showed that the minimum concentrations, which lead to >90% yield were 3.4, 3.3 and 5.9 μM for DOTA-DFO **21**, DOTAGA-DFO **22** and NOTA-DFO **23** respectively. These concentrations are higher than the one necessary for quantitative chelation of [^{89}Zr]Zr by DFO without the macrocycle present. The stability studies in EDTA and fetal bovine serum showed that the stabilities of the complexes were at least comparable with [^{89}Zr]ZrDFO. The results of [^{89}Zr]Zr**21** challenge with Fe^{3+} ion showed comparable stability to [^{89}Zr]ZrDFO.

5.2. Future work

5.2.1. Zr complex

Both molecular modelling studies and x-ray crystal structural studies of the zirconium(IV) complexes of all of the chelators would provide significant insight into the chelator design and offer better understanding of the radiolabelling results. It may be challenging to grow single crystals of these molecules however modelling studies would still provide useful data for the molecular design step and the selected molecules could be synthesised and radiolabelled in a rapid screen.

5.2.2. Biodistribution study and PET imaging

It would be of high interest to investigate the biodistribution of the [^{89}Zr]Zr**21**, [^{89}Zr]Zr**22** and [^{89}Zr]Zr**23** and also to look at the in vivo stability of these derivatives. This is the key characterisation information that is relevant to the ultimate application. The clearance

pathway and uptake of the labelled compounds will vary with lipophilicity and the nature of this variation will be relevant to future chelator design studies. A key measure of the stability is the release to bone over time. PET imaging in tumour (or other relevant) models of the labelled chelators conjugated to biomolecules such as monoclonal antibodies would be the final evaluation and would only be carried out if sufficient stability is observed *in vivo* for the zirconium-89 complex of the chelator itself.

5.2.3. Development of macrocycle-based multi-DFO compounds

Completion of the synthesis of the NOTA macrocycle functionalised with two and three DFO molecules **25** could be carried out. This synthesis was very promising but there was insufficient time to pursue this and fully investigate the compounds. The experiment carried out showed a mixture of 1-arm and 2-arm products in one of the reactions, see Figure 85. This could easily be purified and properties assessed for the zirconium-89 labelled compound. It would also be relatively easy to access the derivative with three DFO units attached for comparison.

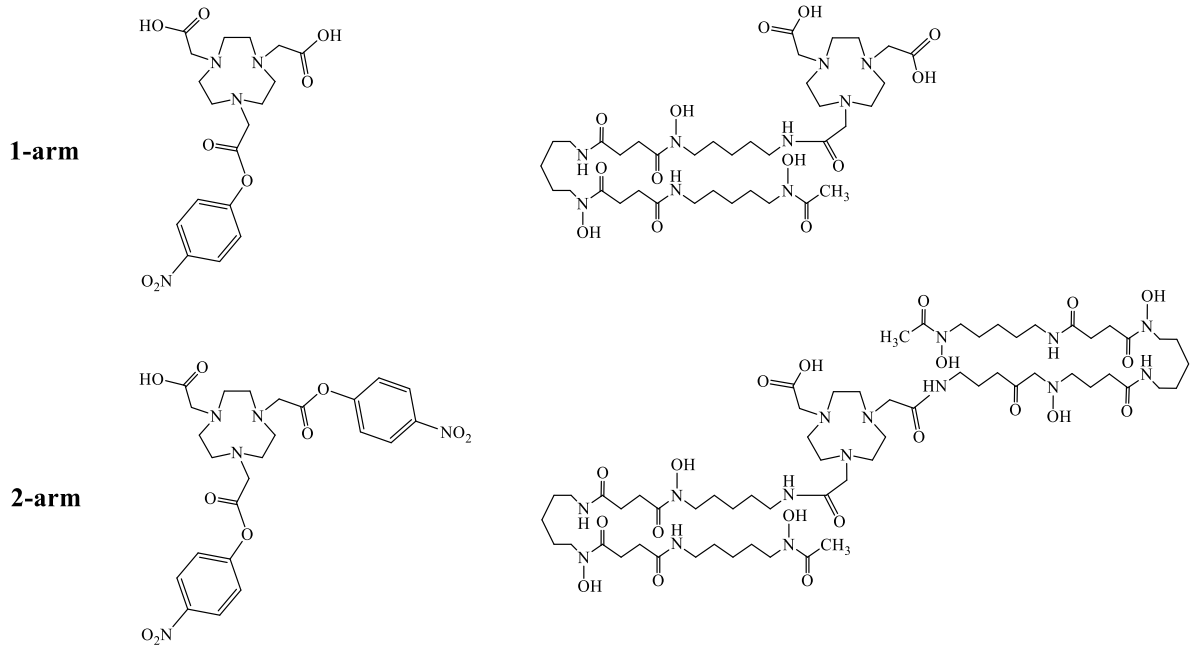

Figure 85 - Structures of NOTA-*n*DFO derivatives.

Chapter 6

Experimental

6. Experimental

6.1. Materials

Chemical reagents and solvents were purchased from Sigma Aldrich, Fisher Scientific, Fluka and VWR International Ltd. When necessary, acetonitrile (CH_3CN) and methanol (MeOH) were dried by using molecular sieves at least 24 hours.[200] NMR solvents were purchased from Fluorochem and Euriso-top. Silica gel (60 A, 35-70 μm) and active neutral alumina 90 (70-230 mesh ASTM) used for column chromatography were purchased from Fluorochem and Merck, respectively.

6.2. [^{89}Zr]Zr(IV)

[^{89}Zr]Zr(IV) in 1.0 M oxalic acid was supplied by Perkin Elmer. It was neutralised by 0.5 - 1.0 M Cs_2CO_3 for radiolabelling. The preparation of [^{89}Zr]zirconium(IV) chloride was performed by using Accell Plus QMA Plus Light cartridge, which was pre-activated by MeCN (6 mL), 0.9% NaCl (10 mL), and water (10 mL). The solution of [^{89}Zr]zirconium(IV) oxalate in 1.0 M oxalic acid was loaded onto the cartridge and washed with water (> 50 mL) to remove oxalic acid and [^{89}Zr]Zr(IV) was eluted with 1.0 M HCl as [^{89}Zr]zirconium(IV) chloride.

6.3. Instrumentation

6.3.1. NMR spectroscopy

The NMR spectroscopy was performed using a Jeol-JNM-LA400 spectrometer at 400 MHz for ^{1}H, 100 MHz for ^{13}C and 100 MHz for ^{31}P spectra the solvents indicated, referenced against standard internal TMS. The chemical shifts (δ) are given in ppm. Splitting pattern are designed as s (singlet), d (doublet), t (triplet), q (quartet), m (multiplet) and br (broad).

6.3.2. Mass spectrometry (MS)

Mass spectrometry was performed using Finnegan MAT 900 XLT system.

6.3.3. Elemental analysis

Elemental analysis was performed using EA1108 CHN analyser.

6.3.4. High performance liquid chromatography (HPLC)

High performance liquid chromatography was carried out using an Agilent 1200 series using a Jupiter 5 μm C18 300A, 150 x 4.6 mm, an ACE 5 C18, 250 x 4.6 mm at 1 mL/min, an ACE 5

C18, 250 x 10 mm at 4.7 mL/min, which was equipped with a UV detector (series G1314A) and a NaI radiodetector. Data was recorded using Lablogic Laura (version 4.1.13.91) software. HPLC conditions were reported for each compound.

6.3.5. Radio-Thin layer chromatography (Radio-TLC)

For [^{89}Zr]Zr(IV) radiolabelling, TLCs were run on ITLC-SG, using 10 mM EDTA pH 6 as mobile phase.

Radio-TLC was carried out using a Lablogic Scan-Ram, equipped with a NaI detector at a speed of 0.1 mm/sec. Data was recorded using Lablogic Laura (version 4.1.7.70) software.

6.3.6. Gamma counter

Radioactive samples were measured using a Perkin Elmer - Wallac wizard 3".

6.4. Synthesis of 1,4,7,10-tetraazacyclododecane-1,4,7,10-tetra(methylenephosphonic acid) DOTP (1)

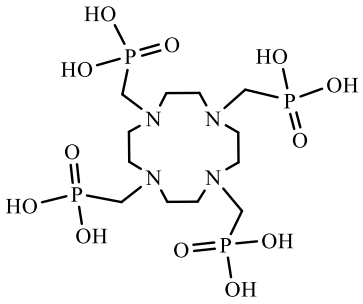

1

One-pot method

The one-pot method was carried out following a modified literature method by Sherry *et al*.[115] A mixture of 1,4,7,10-tetraazacyclododecane (1.4 g, 8.0 mmol), phosphorous acid (2.6 g, 32.0 mmol) dissolved in water (18.0 mL) and concentrated hydrochloric acid (16 mL) was heated to reflux. Formaldehyde (4.8 mL of 37 % solution in water, 64 mmol) was added drop-wise over 1 hour. The reaction conditions were varied in order to improve chemical yields by extending the duration of the reaction from 4 to 48 hours and cooled to room temperature. The mixture was concentrated and diluted with acetone (100 mL) and stirred at 0^{o}C for 3 hours. The precipitate was filtered and dried *in vacuo* for 8 hours to yield an off-white solid (1.3 g, 29%).

^{1}H NMR (D_2O): δ 2.5 - 3.7 (m overlapping, 24H, NCH_2CH_2N, NCH_2P).

^{31}P NMR (D_2O): δ 21.96.

ESI-MS(+): m/z 549.2 $[M+H]^+$.

Multi-step method

Octaethyl ((1,4,7,10-tetraazacyclododecane-1,4,7,10-tetrayl)tetrakis(methylene))tetrakis (phosphonate) **2** (0.8 g, 1.0 mmol) was hydrolysed with 6 M HCl (20 mL) under reflux with N_2[61], for 4 days to obtain the product **1** (0.5 g, 98%).

^{1}H NMR (D_2O): δ 2.5 - 3.6 (m overlapping, 24H, NCH_2CH_2N, NCH_2P).

$^{13}C\{^{1}H\}$ NMR (D_2O): δ 50.75 (NCH_2CH_2); 51.61 - 52.98 (d, J = 138.44 Hz, NCH_2P).

^{31}P NMR (D_2O): δ 18.41.

ESI-MS(+): m/z 549.1 $[M+H]^+$.

6.5. Synthesis of octaethyl ((1,4,7,10-tetraazacyclododecane-1,4,7,10-tetrayl)tetrakis (methylene))tetrakis(phosphonate) (2)

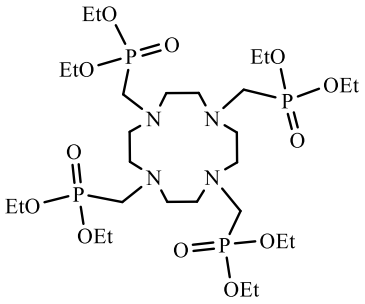

2

The synthesis of octaethyl ((1,4,7,10-tetraazacyclododecane-1,4,7,10-tetrayl)tetrakis (methylene))tetrakis(phosphonate) **2** was performed according to the literature procedure published by Försterová M., *et al.*[118] A mixture of 1,4,7,10-tetraazacyclododecane (1.0 g, 5.8 mmol), paraformaldehyde (0.87 g, 29.0 mmol) and triethyl phosphite (9.8 g, 59.0 mmol, a solvent) were reacted at 40°C for 3 days. The crude product was purified by silica gel column chromatography (150 mL). Triethyl phosphite was eluted with $(C_2H_5)_2O$: MeOH (70:30) and the product was eluted with $(C_2H_5)_2O$: MeOH : NH_4OH (65:30:5)[120] to give a yellow oil (1.1 - 2.4 g, 25 - 53%).

^{1}H NMR ($CDCl_3$): δ 1.27 - 1.30 (t, *J* = 7.07 Hz, 24H, CH_3); 2.80 (s, 16H, NCH_2CH_2N); 2.90 - 2.92 (d, *J* = 8.16 Hz, 8H, NCH_2P); 4.07 - 4.11 (m, 16H, CH_2).

^{13}C{^{1}H} NMR ($CDCl_3$): δ 16.67 (CH_3); 49.97 - 51.50 (d, *J* = 164.14 Hz, NCH_2P); 53.47 (NCH_2CH_2N); 61.74 (CH_2O).

^{31}P NMR ($CDCl_3$): δ 26.61.

ESI-MS(+): m/z 773.4 $[M+H]^+$.

6.6. Synthesis of [2-(tert-butyloxycarbonyl)ethyl]phosphinic acid (3)

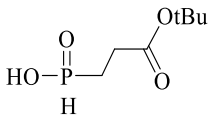

3

The synthesis of the compound **3** was following the literature procedure by Ivan Lukes *et al*. [121] Dry ammonium hypophosphite (12.5 g, 0.15 mol) and hexamethyldisilazane (38.0 g, 0.24 mol) were heated to 105ºC under N_2 atmosphere and stirred, whereupon ammonia gas was observed. After 6 hours the mixture was cooled to room temperature, anhydrous DCM (100 mL) was added and the solution was cooled in an ice bath. Then *tert*-butyl acrylate (14.5 g, 0.11 mol) was added through a syringe and the mixture was stirred for 16 hours at room temperature. Ethanol (250 mL) was added and the reaction mixture was stirred for a while and evaporated to dryness. The crude product was dissolved in $CHCl_3$ (150 mL) and extracted with 3% aq. HCl (2 x 30 mL). The aqueous phases were combined and re-extracted with chloroform (3 x 25 mL). The combined organic extracts were dried over anhydrous Na_2SO_4 and the solvent removed to afford [2-(tert-butyloxycarbonyl)ethyl]phosphinic acid **3** as a colourless, viscous oil (21.1 g, 0.11 mol, 96% yield).

^{1}H NMR ($CDCl_3$): δ 1.39 (s, 9H, CH_3); 1.91 - 1.99 (m, 2H, CH_2); 2.45 - 2.52 (m, 2H, PCH_2).
$^{13}C\{^1H\}$ NMR (1% DCl): δ 24.13 – 25.09 (d, J = 96.39 Hz, CH_2P); 27.19 (CH_2); 28.00 (CH_3); 81.18 (C); 171.05 (CO).
^{31}P NMR ($CDCl_3$): δ 35.47.
ESI-MS(-): m/z 192.6 $[M-H]^-$.

6.7. Synthesis of (2-carboxyethyl)phosphinic acid (4)

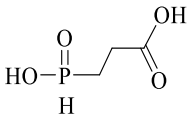

4

The synthesis of the compound **4** was following the literature procedure by Ivan Lukes *et al*.[121] The compound **3** (21.1 g, 0.11 mol) was dissolved in a mixture of EtOH (50 mL) and conc. aq. HCl (50 mL) and heated at reflux for 48 hours. The reaction mixture was then evaporated to remove solvents and volatile components and dried *in vacuo* to yield (2-carboxyethyl) phosphinic acid **4** as a colourless oil which gradually formed a solid when left to stand[121] (15.0 g, 0.11 mol, 100% yield).

^{1}H NMR (1% DCl): δ 1.74 - 1.82 (m, 2H, CH_2); 2.33 - 2.40 (m, 2H, CH_2).

^{13}C{^{1}H} NMR (1% DCl): δ 23.60 - 24.53 (d, J = 93.16 Hz, CH_2P); 25.73 (CH_2); 176.27 (CO).

^{31}P NMR (1% DCl): δ 36.69.

ESI-MS(-): m/z 137.0 $[M-H]^-$.

6.8. Attempted synthesis of 1,4,7,10-tetraazacyclododecane-1,4,7,10-tetra[methyl(2-carboxyethyl) phosphinic acid] (5)

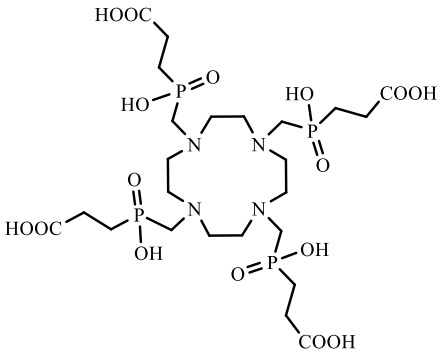

5

The synthesis of the compound **5** was attempted following the modified literature by Notni *et al.*[111] A mixture of 1,4,7,10-tetraazacyclododecane (0.17 g, 1.0 mmol) was added to (2-carboxyethyl)phosphinic acid (1.7 g, 12.3 mmol) in 6 M HCl (10 mL). The reaction was heated to reflux and paraformaldehyde (0.68 g, 22.6 mmol) was added in six portions over 24 hours. The reaction was performed for 72 hours, then evaporated.

The crude product was attempted to purify by column chromatography using Dowex Marathon C H^+-form, column size 10 x 1 cm, and eluted with water. The fractions were analysed by MS. The fractions containing the product were collected and evaporated to give a yellow oil. However, ^{1}H NMR and ^{31}P NMR analysis showed the compound was impure with a yield of less than 20%.

Recrystallisation was attempted. The fractions collected from the ion exchange chromatography was concentrated to remain approximately a volume of 5 mL and added methanol (50 mL) and isopropanol (25 mL). However, after 3 days, crystals had not formed.

ESI-MS(-) : m/z 771.3 $[M-H]^-$, 385.2 $[M-2H]^{2-}$.

^{1}H NMR (1% DCl) and ^{31}P NMR (1% DCl): showed that the compound **5** is not pure.

6.9. Synthesis of methyl 6-(hydroxymethyl)picolinate (6)

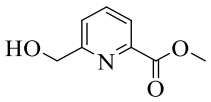

6

The synthesis of the compound **6** was carried out following the literature procedure reported by Rodrıguez-Blas *et al.*, in 2008.[133] Dimethylpyridine-2,6-dicarboxylate (5.8 g, 30.0 mmol) was dissolved in methanol (250 mL) and cooled to 0°C in an ice bath. Sodium borohydride (3.4 g, 89.9 mmol) was added in small portions within 30 min. The reaction was stirred at 0°C for 3 hours. Saturated $NaHCO_3$ solution was added and the MeOH phase was evaporated. The extraction was performed by adding chloroform to the aqueous residue (5 x 70 mL). The organic phases were combined, dried over anhydrous Na_2SO_4 and evaporated to obtain intermediate **6** as white solid (3.41 g, 20.41 mmol, 68% yield).

^{1}H NMR ($CDCl_3$): δ 3.98 (s, 3H, CH_3); 4.85 - 4.86 (d, *J* = 4.63 Hz, 2H, CH_2); 7.52 - 7.53 (d, *J* = 7.57 Hz, 1H, CH); 7.82 - 7.86 (t, *J* = 8.07 Hz, 1H, CH); 8.01 - 8.03 (d, *J* = 7.57 Hz, 1H, CH).
^{13}C{^{1}H} NMR ($CDCl_3$): 52.98 (CH_3); 64.68 (CH_2); 123.95 (CH); 124.11 (CH); 137.79 (CH); 147.10 (CN); 160.20 (CN); 165.64 (s, CO).
ESI-MS(+): m/z 168.2 $[M+H]^+$.

6.10. Synthesis of methyl 6-(chloromethyl)picolinate (7)

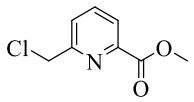

7

The synthesis of the compound **7** was carried out by following the literature procedure reported by Rodrıguez-Blas *et al.* in 2008.[133] Thionyl chloride (15 mL) was added drop-wise to the intermediate product **6** (3.41 g, 20.41 mmol) while stirred at 0°C under N_2 atmosphere. After 2 hours, the mixture was evaporated to remove all volatiles. 1 M $NaHCO_3$ (150 mL) was added to the residue, then extracted with toluene (70 mL x 5). The organic layers were pooled, evaporated and precipitated in $(C_2H_5)_2O$. The product **7** was dried *in vacuo* to gain a pale yellow solid (2.94 g, 15.84 mmol, 77.6% yield).

^{1}H NMR ($CDCl_3$): δ 4.00 (s, 3H, CH_3); 4.77 (s, 2H, CH_2); 7.72 - 7.73 (d, *J* = 7.69 Hz, 1H, CH); 7.87 - 7.91 (t, *J* = 7.70 Hz, 1H, CH); 8.06 - 8.08 (d, *J* = 7.69 Hz, 1H, CH).
^{13}C{^{1}H} NMR ($CDCl_3$): 46.36 (CH_3); 53.19 (CH_2); 124.58 (CH); 126.30 (CH); 138.29 (CH); 147.53 (CN); 157.31 (CN); 165.45 (CO).
ESI-MS(+): m/z 185.8 and 187.8 $[M+H]^+$.

6.11. Synthesis of tetramethyl 6,6',6'',6'''-((1,4,7,10-tetraazacyclododecane-1,4,7,10-tetrayl) tetrakis(methylene))tetrapicolinate (8)

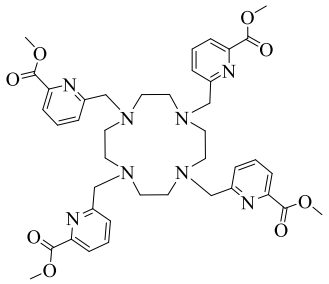

8

The synthesis of the compound **8** was following the literature by Pellet-Rostaing *et al.* in 2015.[134] A mixture of 1,4,7,10-tetraazacyclododecane (0.17 g, 1.0 mmol), 6-chloromethylpyridine-2-carboxylic acid methyl ester (0.93 g, 5.0 mmol) and Cs_2CO_3 (0.81 g, 2.5 mmol) in anhydrous MeCN (10 mL) was heated to 50ºC and stirred under nitrogen for 48 hours, then cooled, filtered and evaporated. The residue was purified by silica gel column chromatography following a procedure modified from that reported by Tripier *et al.* in 2016, eluting with hexane : ethyl acetate (1:3) to remove excess 6-chloromethylpyridine-2-carboxylic acid methyl ester, and with $CHCl_3$: MeOH (8:2) to obtain the product **8** as yellow oil (0.36 g, 0.47 mmol, 47% yield).[201]

^{1}H NMR ($CDCl_3$): δ 2.51 – 3.50 (br m, 16H, NCH_2CH_2N); 3.65 – 3.77 (br m, 8H, CH_2); 3.81 – 3.98 (br m, 12H, CH_3); 7.37 – 7.73 (m, 4H, CH-Ar); 7.75 – 8.06 (m, 8H, CH-Ar).
^{13}C{^{1}H} NMR ($CDCl_3$): δ 52.83 (CH_3); 53.07 (NCH_2CH_2N); 58.29 (CH_2N); 123.77 (CH-Ar); 128.03 (CH-Ar); 137.71 (CH-Ar); 147.00 (C-Ar); 157.51 (C-Ar); 165.51 (CO).
ESI-MS(+) : m/z 769.3 $[M+H]^+$.

6.12. Synthesis of 6,6',6'',6'''-((1,4,7,10-tetraazacyclododecane-1,4,7,10-tetrayl)tetrakis (methylene))tetrapicolinic acid (9)

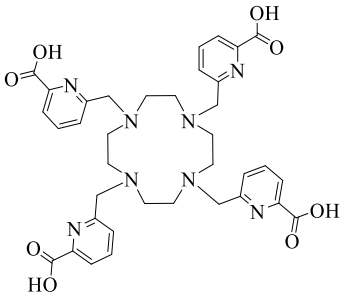

9

8 (0.36 g, 0.47 mmol) was hydrolysed by reflux in 6 M HCl (10 mL) for 48 hour and dried *in vacuo* to yield **9** as brown solid (0.31 g, 0.43 mmol, 93 % yield).[201]

The product was analysed by HPLC using column ACE 5 C18 250 x 4.6 eluted with methanol (A) and 0.2 M ammonium formate pH 3 (B) at the flow rate of 1 mL/min. Gradient – A:B (5:95) at 0 min; (50:50) at 25 min; (5:95) at 26 min and (5:95) at 30 min. The product was eluted at 12:58 minutes.

^{1}H NMR (1% DCl): δ 3.32 (s, 16H, NCH_2CH_2N); 4.18 (s, 8H, CH_2); 7.36 – 7.58 (m, 4H, CH-Ar); 7.73 – 7.89 (m, 8H, CH-Ar).

$^{13}C\{^{1}H\}$ NMR (1% DCl): δ 49.87 (NCH_2CH_2N); 56.81 (CH_2N); 126.30 (CH-Ar); 129.33 (CH-Ar); 142.26 (CH-Ar); 145.02 (C-Ar); 151.34 (C-Ar); 165.25 (CO).

ESI-HRMS(+) : calc. m/z 713.3042 found 713.3038 $[M+H]^+$.

6.13. Synthesis route of benzyl (3-bromopropyl)(methyl)carbamate (10 – 12)

6.13.1. Synthesis of benzyl (3-hydroxypropyl)(methyl)carbamate (10)

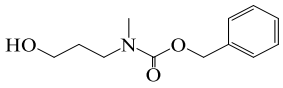

10

A mixture of 3-(methylamino)propan-1-ol (8.94 mg, 100.30 mmol) and TEA (12.0 mL, 120.9 mmol) in DCM anhydrous (100 mL) was stirred at 0^{o}C under Ar atmosphere while added dropwise benzyl chloroformate (17.5 mL, 108.1 mmol). The reaction mixture was stirred at room temperature overnight. The crude product was added DCM (100 mL), washed with water (100 mL x 3), 1 N HCl (100 mL x 3), 10% $NaHCO_3$ (100 mL x 3) and sat. NaCl (100 mL), then dried over $MgSO_4$, filtered, and evaporated to dryness and gained the product as yellow oil (18.04 g, 80.85 mmol, 81% yield).

^{1}H NMR ($CDCl_3$): δ 1.68 – 1.74 (m, 2H, CH_2); 2.91 (s, 3H, CH_3); 3.46 – 3.44 (t, *J* = 5.87 Hz, 2H, CH_2N); 3.53 – 3.57 (t, *J* = 6.56 Hz, 2H, CH_2OH); 5.14 (s, 2H, CH_2O); 7.31 – 7.38 (m, 5H, CH-Ar).
$^{13}C\{^{1}H\}$ NMR ($CDCl_3$): δ 29.78 (CH_2); 34.08 (CH_3N); 45.16 (CH_2N); 58.30 (CH_2OH); 67.50 (CH_2O); 127.94 (CH-Ar); 128.19 (CH-Ar); 128.64 (CH-Ar); 136.71 (C-Ar); 157.64 (CO).
ESI-MS(+): m/z 224.2 $[M+H]^+$.

6.13.2. Synthesis of 3-(((benzyloxy)carbonyl)(methyl)amino)propyl 4-methylbenzene sulfonate (11)

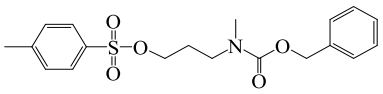

11

A mixture of **10** (18.04 g, 80.85 mmol), TEA (16 mL, 158.3 mmol) and trimethylamine hydrochloride (3.96 g, 41.48 mmol) was dissolved in DCM anhydrous (100 mL) and stirred at 0^{o}C under Ar atmosphere. Small portions of *p*-toluenesulfonyl chloride (24.11 g, 126.47 mmol) were added to the reaction for 30 minutes. The reaction mixture was stirred at 0^{o}C for 2.5 hours and at room temperature for an hour. DCM (100 mL) was added to the reaction then washed with 1 N HCl (150 mL x 3), 10% $NaHCO_3$ (150 mL x 3) and sat. NaCl (150 mL), then dried over $MgSO_4$, filtered, and evaporated to dryness. The crude product was purified by silica gel column eluted with ethyl acetate and hexane (1:3) to remove excess *p*-toluenesulfonyl chloride and moved to ethyl acetate and hexane (1:1) to elute the product (24.18 g, 64.12 mmol, 79% yield).

^{1}H NMR ($CDCl_3$): δ 1.85 – 1.94 (m, 2H, CH_2); 2.44 (s, 3H, CH_3); 2.88 (s, 3H, CH_3N); 3.30 – 3.34 (t, *J* = 6.93 Hz, 2H, CH_2N); 4.02 – 4.05 (t, *J* = 6.51 Hz, 2H, CH_2O); 5.09 (s, 2H, CH_2O); 7.31 – 7.37 (m, 7H, CH-Ar); 7.74 – 7.79 (m, 2H, CH-Ar).
^{13}C{^{1}H} NMR ($CDCl_3$): δ 21.75 (CH_3); 27.31 (CH_2); 35.19 (CH_3N); 46.03 (CH_2N); 67.18 (CH_2O); 68.29 (CH_2O); 127.94 (CH-Ar); 128.00 (CH-Ar); 128.10 (CH-Ar); 128.61 (CH-Ar); 130.00 (C-Ar); 132.95 (C-Ar); 144.98 (CS); 156.18 (CO).
ESI-MS(+): m/z 399.9 $[M+Na]^+$.

6.13.3. Synthesis of benzyl (3-bromopropyl)(methyl)carbamate (12)

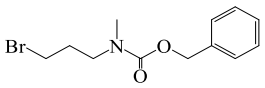

12

The synthesis of **12** was modified from the published method by Perry.[163] The compound **11** (24.18 g, 64.12 mmol) was dissolved in anhydrous acetone (250 mL) and added LiBr (13.42 g, 154.48 mmol). The reaction mixture was stirred at room temperature under Ar atmosphere for 24 hours and evaporated. The crude was dissolved in ethyl acetate (200 mL) and washed with 1 N HCl (150 mL x 3), 10% $NaHCO_3$ (150 mL x 3) and sat. NaCl (150 mL), then dried over $MgSO_4$, filtered and evaporated to dryness to obtain the product as yellow oil (17.75 g, 62.0 mmol, 97% yield).

^{1}H NMR ($CDCl_3$): δ 2.04 – 2.14 (m, 2H, CH_2); 3.35 – 3.38 (t, *J* = 7.03 Hz, 2H, CH_2N); 2.96 (s, 3H, CH_3); 3.41 – 3.44 (t, *J* = 5.93 Hz, 2H, CH_2Br); 5.13 (s, 2H, CH_2O); 7.31 – 7.37 (m, 5H, CH-Ar).
$^{13}C\{^1H\}$ NMR ($CDCl_3$): δ 30.68 (CH_2); 31.31 (CH_2Br); 35.26 (CH_3N); 48.13 (CH_2N); 67.28 (CH_2O); 128.02 (CH-Ar); 128.11 (CH-Ar); 128.59 (CH-Ar); 136.86 (C-Ar); 158.90 (CO).
ESI-MS(+): m/z 308.0 and 310.0 $[M+Na]^+$.

6.14. Synthesis route of 6,6',6'',6'''-((((1,4,7,10-tetraazacyclododecane-1,4,7,10-tetrayl)tetrakis(propane-3,1-diyl))tetrakis(methylazanediyl))tetrakis(methylene)) tetrapicolinic acid (13 – 16)

6.14.1. Synthesis of tetrabenzyl ((1,4,7,10-tetraazacyclododecane-1,4,7,10-tetrayl) tetrakis(propane-3,1-diyl))tetrakis(methylcarbamate) (13)

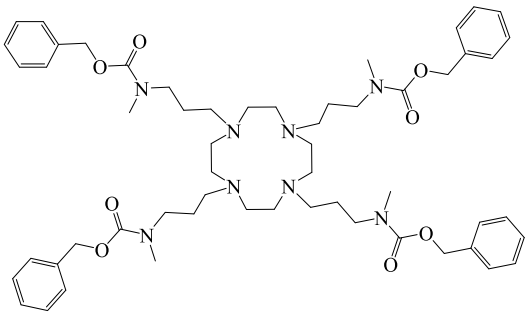

13

A mixture of 1,4,7,10-tetraazacyclododecane (1.04 g, 6.05 mmol) and Cs_2CO_3 (5.20 g, 15.96 mmol) was stirred in anhydrous acetonitrile (200 mL) under Ar atmosphere. To the reaction mixture, **12** (8.64 g, 30.32 mmol) in anhydrous acetonitrile (10 mL) was added dropwise. The reaction was performed at room temperature for 2 days, then filtered and evaporated. The purification was performed by silica gel column chromatography eluting with diethyl ether : methanol : ammonia solution (90:5:5) to gain the product as yellow oil (2.88 g, 2.91 mmol, 48% yield).

^{1}H NMR ($CDCl_3$): δ 1.57 – 1.70 (m, 8H, CH_2); 2.23 – 2.68 (br m, 24H, CH_2N); 2.90 (s, 12H, CH_3N); 3.22 – 3.39 (br m, 8H, CH_2N); 5.11 (s, 8H, CH_2O); 7.25 – 7.42 (m, 20H, CH-Ar).
$^{13}C\{^1H\}$ NMR ($CDCl_3$): δ 25.80 (CH_2); 34.82 (CH_3N); 47.74 (CH_2N); 52.55 (CH_2N); 53.24 (NCH_2CH_2N); 67.02 (CH_2O); 127.89 (CH-Ar); 128.00 (CH-Ar); 128.55 (C-Ar); 137.08 (C-Ar); 156.34 (CO).
ESI-MS(+): m/z 993.0 $[M+H]^+$ and 497.2 $[M+2H]^{2+}$.

6.14.2. Synthesis of 3,3',3'',3'''-(1,4,7,10-tetraazacyclododecane-1,4,7,10-tetrayl)tetrakis (N-methylpropan-1-amine) (14)

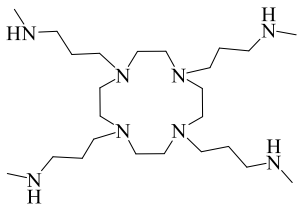

14

13 (2.88 g, 2.91 mmol) was dissolved in methanol (50 mL) and 10% Pd/C (0.58 g, 20% wt.) added. The reaction was performed in a Parr shaker under H_2 overnight, then filtered and evaporated to obtain the product (1.30 g, 2.84 mmol, 98% yield).

^{1}H NMR ($CDCl_3$): δ 1.54 – 1.75 (m, 8H, CH_2); 2.15 – 2.28 (br m, 8H, CH_2N); 2.34 – 2.91 (br m, 36H, CH_2N, CH_3).
$^{13}C\{^1H\}$ NMR ($CDCl_3$): δ 26.92 (CH_2); 36.40 (CH_3N); 45.60 (CH_2N); 52.69 (CH_2N); 58.14 (NCH_2CH_2N).
ESI-MS(+): m/z 457.5 $[M+H]^+$.

6.14.3. Synthesis of tetramethyl 6,6',6'',6'''-((((1,4,7,10-tetraazacyclododecane-1,4,7,10-tetrayl)tetrakis(propane-3,1-diyl))tetrakis(methylazanediyl))tetrakis(methylene)) tetrapicolinate (15)

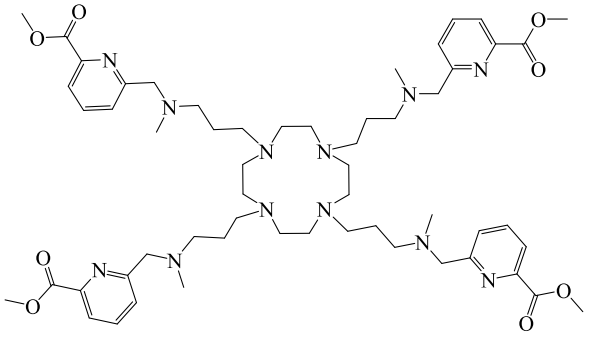

15

A mixture of **14** (0.20 g, 0.44 mmol), 6-chloromethylpyridine-2-carboxylic acid methyl ester **7** (0.44 g, 1.99 mmol) and Cs_2CO_3 (0.35 g, 1.07 mmol) in anhydrous MeCN (20 mL) was stirred under Ar for 1 day, then filtered and evaporated. The crude product was purified by aluminium oxide column eluted with dichloromethane : methanol : triethylamine (99:1:0.1) to remove excess **7** and eluted with dichloromethane : methanol : triethylamine (97:1:0.1) to obtain the product **15** as yellow oil (0.11 g, 0.10 mmol, 23% yield).

^{1}H NMR ($CDCl_3$): δ 1.63 – 1.87 (m, 8H, CH_2); 2.20 (s, 12H, CH_3N); 2.38 – 2.72 (br m, 16H, CH_2N); 2.76 – 2.99 (br m, 16H, NCH_2CH_2N); 3.73 (s, 8H, CH_2N); 3.96 (s, 12H, CH_3O); 7.59 – 7.71 (m, 4H, CH-Ar); 7.76 – 7.84 (m, 4H, CH-Ar); 7.94 – 7.99 (m, 4H, CH-Ar).
^{13}C{^{1}H} NMR ($CDCl_3$): δ 23.35 (CH_2); 42.38 (CH_3N); 45.87 (CH_3O); 50.49 (CH_2N); 52.99 (NCH_2CH_2N); 55.61 (CH_2N); 63.59 (CH_2N); 123.85 (CH-Ar); 126.42 (CH-Ar); 137.64 (CH-Ar); 147.46 (C-Ar); 159.79 (C-Ar); 165.77 (CO).
ESI-MS(+): m/z 1053.7 $[M+H]^+$ and 527.4 $[M+2H]^{2+}$.

6.14.4. Synthesis of 6,6',6'',6'''-((((1,4,7,10-tetraazacyclododecane-1,4,7,10-tetrayl) tetrakis(propane-3,1-diyl))tetrakis(methylazanediyl))tetrakis(methylene))tetrapicolinic acid (16)

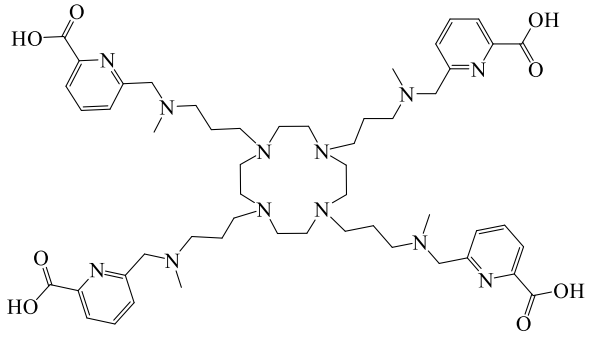

16

The intermediate product **15** (0.11 g, 0.10 mmol) was hydrolysed by reflux in 6 M HCl (10 mL) overnight and dried *in vacuo* to obtain **16** as a brown solid (0.09 g, 0.09 mmol, 89% yield). The product was analysed by HPLC using column ACE 5 C18 250x4.6 eluted with methanol (A) and 0.2 M ammonium formate (B) at the flow rate of 1 mL/min. Gradient – A:B (5:95) at 0 min; (70:30) at 25 min; (5:95) at 26 min and (5:95) at 30 min. The product was eluted at 19.12 minutes.

^{1}H NMR (1% DCl): δ 1.63 – 2.30 (m, 8H, CH_2); 2.66 (s, 12H, CH_3N); 2.86 – 3.46 (br m, 32H, CH_2N); 4.40 (s, 8H, CH_2N); 7.34 – 7.57 (m, 4H, CH-Ar); 7.73 – 7.90 (m, 8H, CH-Ar).
^{13}C{^{1}H} NMR (1% DCl): δ 25.77 (CH_2); 41.19 (CH_3N); 45.43 (CH_2N); 53.75 (NCH_2CH_2N); 59.57 (CH_2N); 63.13 (CH_2N); 125.77 (CH-Ar); 128.61 (CH-Ar); 140.39 (CH-Ar); 146.72 (C-Ar); 149.72 (C-Ar); 167.11 (CO).
ESI-HRMS(+) : calc. m/z 499.3027 found 499.3021 $[M+2H]^{2+}$.

6.15. Synthesis route of 6,6',6'',6'''-((((1,4,8,11-tetraazacyclotetradecane-1,4,8,11-tetrayl) tetrakis(propane-3,1-diyl))tetrakis(methylazanediyl))tetrakis(methylene))tetrapicolinic acid (17 – 20)

6.15.1. Synthesis of tetrabenzyl ((1,4,8,11-tetraazacyclotetradecane-1,4,8,11-tetrayl) tetrakis(propane-3,1-diyl))tetrakis(methylcarbamate) (17)

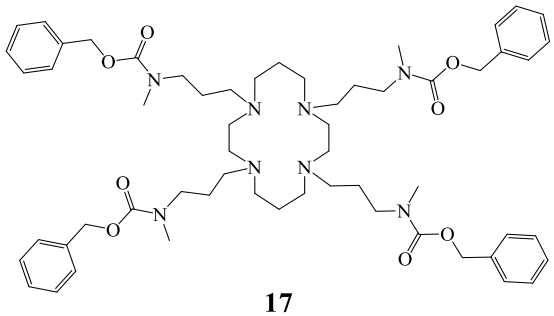

17

A mixture of 1,4,8,11-tetraazacyclotetradecane (1.10 g, 5.50 mmol) and Cs_2CO_3 (5.16 g, 15.84 mmol) was stirred in anhydrous acetonitrile (200 mL) under Ar atmosphere. To the reaction mixture, the compound **12** (8.08 g, 28.35 mmol) in anhydrous acetonitrile (10 mL) was add dropwise. The reaction was performed at room temperature for 2 days, then filtered and evaporated. The purification was performed by silica gel column chromatography eluting with diethyl ether : methanol : ammonia solution (95:2.5:2.5) to gain the product as yellow oil (0.81 g, 0.79 mmol, 14% yield).

^{1}H NMR ($CDCl_3$): δ 1.50 – 1.83 (m, 12H, CH_2); 2.22 – 2.70 (br m, 24H, CH_2N); 2.91 (s, 12H, CH_3N); 3.28 (s, 8H, NCH_2CH_2N); 5.11 (s, 8H, CH_2O); 7.28 – 7.42 (m, 20H, CH-Ar).
$^{13}C\{^1H\}$ NMR ($CDCl_3$): δ 27.90 (CH_2); 30.45 (CH_2); 34.18 (CH_3N); 50.84 (CH_2N); 51.55 (CH_2N); 52.82 (CH_2N); 54.49 (NCH_2CH_2N); 67.02 (CH_2O); 127.86 (CH-Ar); 128.00 (CH-Ar); 128.55 (C-Ar); 131.77 (C-Ar); 156.32 (CO).
ESI-MS(+): m/z 511.6 $[M+2H]^{2+}$.

6.15.2. Synthesis of 3,3',3'',3'''-(1,4,8,11-tetraazacyclotetradecane-1,4,8,11-tetrayl) tetrakis(N-methylpropan-1-amine) (18)

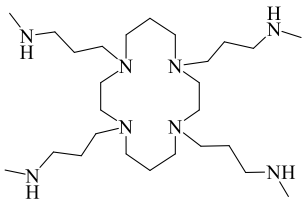

18

The compound **17** (0.80 g, 0.78 mmol) was dissolved in methanol (50 mL) and 10% Pd/C (0.18 g, 20% wt.) added. The reaction was performed using a Parr shaker under H_2 overnight, then filter and evaporated to obtain the product (0.38 g, 0.78 mmol, 100% yield).

^{1}H NMR ($CDCl_3$): δ 1.57 – 1.72 (m, 12H, CH_2); 2.41 – 2.48 (br m, 24H, CH_2N); 2.50 – 2.54 (br m, 8H, CH_2N); 2.60 – 2.71 (br s, 12H, CH_3N).
$^{13}C\{^1H\}$ NMR ($CDCl_3$): δ 23.85 (CH_2); 25.89 (CH_2); 36.08 (CH_3N); 50.08 (CH_2N); 50.53 (CH_2N); 51.17 (CH_2N); 52.47 (NCH_2CH_2N).
ESI-MS(+): m/z 243.7 $[M+2H]^{2+}$.

6.15.3. Synthesis of tetramethyl 6,6',6'',6'''-((((1,4,8,11-tetraazacyclotetradecane-1,4,8,11-tetrayl)tetrakis(propane-3,1-diyl))tetrakis(methylazanediyl))tetrakis(methylene)) tetrapicolinate (19)

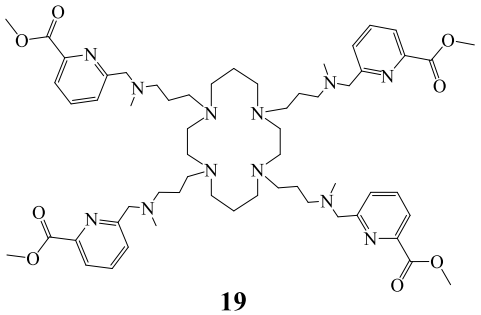

19

A mixture of **18** (0.36 g, 0.74 mmol), 6-chloromethylpyridine-2-carboxylic acid methyl ester **7** (0.75 g, 3.39 mmol) and Cs_2CO_3 (0.64 g, 1.96 mmol) in anhydrous MeCN (35 mL) was stirred under Ar for 1 day, then filtered and evaporated. The crude product was purified by aluminium oxide column chromatography eluted with dichloromethane : methanol : triethylamine (99:1:0.1) to remove excess **7** and dichloromethane : methanol : triethylamine (97:1:0.1) to obtain the product **19** (0.09 g, 0.08 mmol, 11% yield).

^{1}H NMR ($CDCl_3$): δ 1.57 – 1.71 (m, 12H, CH_2); 2.22 (s, 12H, CH_3N); 2.41 – 2.59 (br m, 32H, CH_2N); 3.74 (s, 8H, CH_2N); 3.97 (s, 12H, CH_3O); 7.66 – 7.71 (m, 4H, CH-Ar); 7.77 – 7.82 (m, 4H, CH-Ar); 7.96 – 8.00 (m, 4H, CH-Ar).
^{13}C{^{1}H} NMR ($CDCl_3$): δ 22.33 (CH_2); 36.78 (CH_2); 42.53 (CH_3N); 50.72 (CH_3O); 51.46 (CH_2N); 52.99 (CH_2N); 56.09 (CH_2N); 63.84 (NCH_2CH_2N); 66.47 (CH_2N); 123.65 (CH-Ar); 126.21 (CH-Ar); 137.46 (CH-Ar); 147.34 (C-Ar); 160.79 (C-Ar); 165.99 (CO).
ESI-MS(+): m/z 1081.6 $[M+H]^+$ and 541.3 $[M+2H]^{2+}$.

6.15.4. Synthesis of 6,6',6'',6'''-((((1,4,8,11-tetraazacyclotetradecane-1,4,8,11-tetrayl) tetrakis(propane-3,1-diyl))tetrakis(methylazanediyl))tetrakis(methylene))tetrapicolinic acid (20)

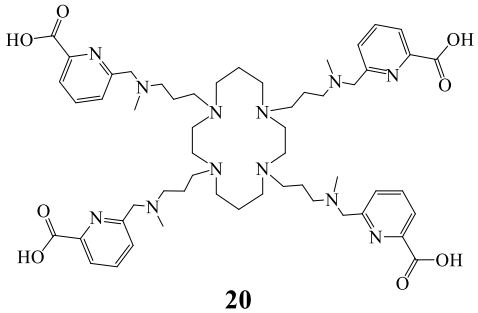

20

The compound **19** (0.09 g, 0.08 mmol) was hydrolysed by reflux in 6 M HCl for 48 hours and dried *in vacuo* to gain **20** as brown solid (0.09 g, 0.08 mmol, 99 % yield).

The product was analysed by HPLC using a reverse phase column (ACE 5 C18 250x4.6) eluted with methanol (A) and 0.2 M ammonium formate (B) at the flow rate of 1 mL/min. Gradient – A:B (5:95) at 0 min; (70:30) at 25 min; (5:95) at 26 min and (5:95) at 30 min. The product was eluted at 21.54 minutes.

^{1}H NMR (1% DCl): δ 1.87 – 2.28 (m, 12H, CH_2); 2.71 (s, 12H, CH_3N); 3.01– 3.55 (br m, 32H, CH_2N); 3.67 (s, 8H, CH_2N); 7.45 – 7.52 (m, 4H, CH-Ar); 7.80 – 7.91 (m, 8H, CH-Ar).

^{13}C{^{1}H} NMR (1% DCl): δ 20.39 (CH_2); 41.58 (CH_3N); 44.80 (CH_2); 45.51 (CH_2N); 48.46 (CH_2N); 53.48 (CH_2N); 53.64 (NCH_2CH_2N); 60.10 (CH_2N); 126.16 (CH-Ar); 128.88 (CH-Ar); 140.80 (CH-Ar); 149.90 (C-Ar); 157.47 (C-Ar); 167.53 (CO).

ESI-HRMS(+) : calc. m/z 513.3184 found 513.3177 $[M+2H]^{2+}$.

6.16. Synthesis of DOTA-DFO (21)

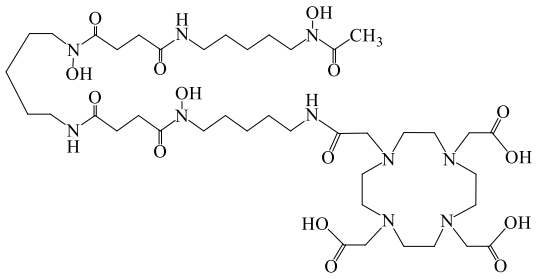

21

The synthesis of the compound **21** was performed by using DOTA-NHS ester (0.02 g, 0.03 mmol) in anhydrous DMF (1 mL) and added DIPEA (18 µL, 0.1 mmol) and DFO mesylate (0.02 g, 0.03 mmol). The reaction mixture was stirred at room temperature under Ar atmosphere overnight and evaporated. The crude product was purified by semi-preparative HPLC using column ACE 5 C18 250x10 eluted with the mixture of acetonitrile with 0.1% TFA (A) and water with 0.1% TFA (B) at the flow rate of 4.7 mL/min. Gradient – A:B (2:98) at 0 min; (40:60) at 25 min; (2:98) at 26 min and (2:98) at 30 min. The product was eluted at 15:13 minutes and lyophilised to gain white powder (0.013 g, 0.013 mmol, 44% yield).

^{1}H NMR (1% DCl): δ 1.05 – 1.19 (m, 6H, CH_2); 1.27 – 1.39 (m, 6H, CH_2); 1.39 – 1.51 (m, 6H, CH_2); 1.95 (s, 3H, CH_3); 2.29 – 2.33 (t, *J* = 6.99 Hz, 4H, CH_2); 2.60 – 2.63 (t, *J* = 6.79 Hz, 4H, CH_2); 2.86 – 3.35 (br m, 22H, CH_2N); 3.36 – 4.01 (br m, 14H, CH_2N).

ESI-HRMS(-) : calc. m/z 945.5262 found 945.5266 $[M-H]^-$.

Elemental analysis for $C_{49}H_{84}F_{12}N_{10}O_{26}$ (**21** + 4TFA + $3H_2O$), calc. C 40.39 H 5.81 N 9.61. Found C 40.25 H 5.45 N 10.00.

6.17. Synthesis of DOTAGA-DFO (22)

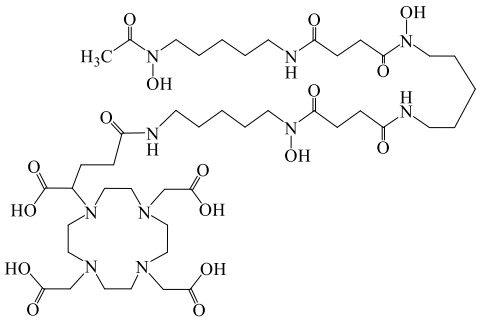

22

The synthesis of the compound **22** was performed by using DOTAGA anhydride (0.02 g, 0.04 mmol) in anhydrous DMF (1 mL) and added DIPEA (29 µL, 0.16 mmol) and DFO mesylate (0.04 g, 0.05 mmol). The reaction mixture was stirred at room temperature under Ar atmosphere overnight and evaporated. The crude product was purified by semi-preparative HPLC using a reverse phase column (ACE 5 C18 250x10) eluted with the mixture of acetonitrile with 0.1% TFA (A) and water with 0.1% TFA (B) at the flow rate of 4.7 mL/min. Gradient – A:B (10:90) at 0 min; (30:70) at 16 min; (10:90) at 17 min and (10:90) at 20 min. The product was eluted at 10.13 minutes and lyophilised to gain white powder (0.005 g, 0.005 mmol, 13% yield).

^{1}H NMR (1% DCl): δ 1.06 – 1.20 (m, 6H, CH_2); 1.28 – 1.38 (m, 6H, CH_2); 1.39 – 1.50 (m, 6H, CH_2); 1.81– 1.92 (m, 4H, CH_2); 1.95 (s, 3H, CH_3); 2.27 – 2.42 (t, *J* = 7.16 Hz, 4H, CH_2); 2.60 – 2.63 (t, *J* = 7.14 Hz, 4H, CH_2); 2.83 (s, 1H, CH); 2.86 – 3.38 (br m, 22H, CH_2N); 3.39 – 4.16 (br m, 12H, CH_2N).

ESI-HRMS(+) : calc. m/z 1019.5619 found 1019.5613 $[M+H]^+$.

6.18. Synthesis of NOTA-DFO (23)

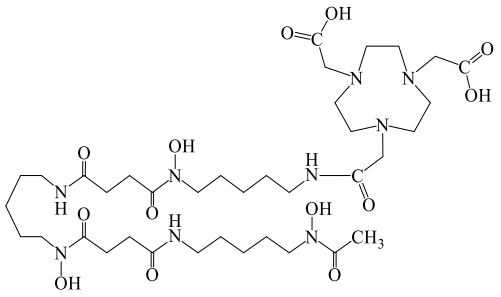

23

The synthesis of NOTA-DFO was performed by using NOTA-NHS ester (0.03 g, 0.05 mmol) in anhydrous DMF (1 mL) and added DIPEA (29 µL, 0.16 mmol) and DFO mesylate (0.04 g, 0.05 mmol). The reaction mixture was stirred at room temperature under Ar atmosphere overnight and evaporated. The crude product was purified by semi-preparative HPLC using a reverse phase column (ACE 5 C18 250x10) eluted with the mixture of acetonitrile with 0.1% TFA (A) and water with 0.1% TFA (B) at the flow rate of 4.7 mL/min. Gradient – A:B (2:98) at 0 min; (30:70) at 20 min; (2:98) at 21 min and (2:98) at 25 min. The product was eluted at 17.54 minutes and lyophilised to gain white powder (0.009 g, 0.01 mmol, 20% yield).

^{1}H NMR (1% DCl): δ 1.04 – 1.20 (m, 6H, CH_2); 1.29 – 1.38 (m, 6H, CH_2); 1.40 – 1.53 (m, 6H, CH_2); 1.95 (s, 3H, CH_3); 2.29 – 2.33 (t, *J* = 7.47 Hz, 4H, CH_2); 2.60 – 2.64 (t, *J* = 7.30 Hz, 4H, CH_2); 2.83 – 3.36 (br m, 18H, CH_2N); 3.39 – 3.85 (br m, 12H, CH_2N).
ESI-HRMS(+) : calc. m/z 846.4931 found 846.4926 $[M+H]^+$.

6.19. Attempted synthesis of NOTA-phenyl ester (24)

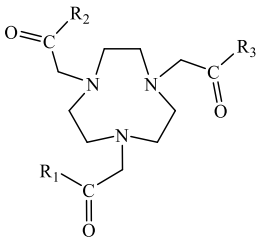

24

24A; R_1 = 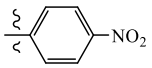 R_2 and R_3 = OH

24B; R_1 and R_2 = 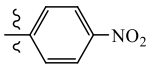 R_3 = OH

24C; R_1, R_2 and R_3 = 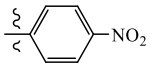

NOTA (0.05 g, 0.17 mmol) in water (5 mL) was added 4-nitrophenol (0.08 g, 0.55 mmol, 3.3 equiv.) in acetonitrile (4 mL) and added dropwise DCC (0.11 g, 0.55 mmol, 3.3 equiv.) in pyridine (4 mL). The reaction mixture was stirred at rt for 15 hours and evaporated, then added 20% acetonitrile in water and filtered of dicyclohexylurea. The filtrate was lyophilised to gain yellow powder (0.065 g). The crude product was analysed by HPLC and MS. ESI-MS(+) found the mixture of 1, 2, 3-arm products.

ESI-MS(+): m/z 425.3 [**24A**+H]$^+$, 546.2 [**24B**+H]$^+$, and 667.1 [**24C**+H]$^+$.

6.20. Attempted synthesis of NOTA-*n*DFO (25)

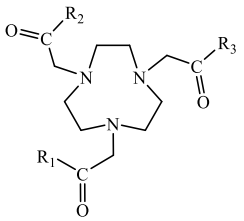

25

25A; R_1 = 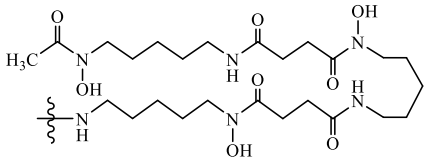 R_2 and R_3 = OH

25B; R_1 and R_2 = 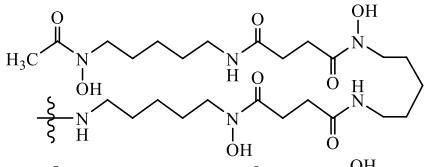 R_3 = OH

25C; R_1, R_2 and R_3 = 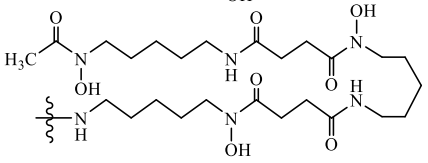

The crude of NOTA-phenyl ester (**24**) (0.026 g) was dissolved in dry DMF (2 mL) and added DFO mesylate (0.13 g, 0.20 mmol) and DIPEA (104 µL, 0.60 mmol). The reaction mixture was stirred at room temperature for 6 days. HPLC and MS were used to analyse the reaction mixture and found unreacted DFO, **25A** and **25B**.

ESI-MS(+): m/z 561.3 $[DFO+H]^+$, 847.4 $[\mathbf{25A}+H]^+$, 694.8 $[\mathbf{25B}+2H]^{2+}$.

6.21. Attempted synthesis of methyl 6-(((3-bromopropyl)amino)methyl)picolinate (26)

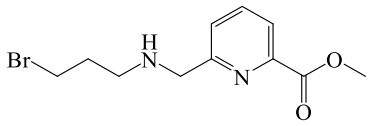

26

7 (0.019 g, 0.10 mmol) was dissolved in acetonitrile (10 mL) and DIPEA added (18 µL, 0.10 mmol). The reaction mixture was stirred at room temperature and added dropwise bromopropylamine hydrochloride (0.028 g, 0.13 mmol) in acetonitrile (10 mL). MS was used to monitored at the reaction; however, after 3 days, only starting materials bromopropylamine (m/z of 138.2 and 140.1 $[M+H]^+$) and **7** (m/z of 186.1 $[\mathbf{7}+H]^+$) were found.

6.22. Attempted synthesis of methyl 6-((4-bromobutoxy)methyl)picolinate (27)

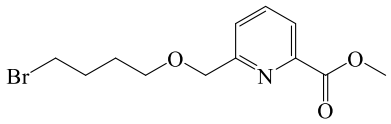

27

The synthesis of compound **27** was modified from the synthesis of bromo acetate derivatives reported by Degrado and co-workers in 2012.[164] The compound **6** (0.33 g, 1.95 mmol) was dissolved in THF anhydrous (20 mL) and cooled to 0^{o}C under N_2. To the reaction, sodium hydride (0.09 g, 2.16 mmol) was added and stirred for 15 minutes. A solution of 1,4-dibromobutane (1.30 g, 6.00 mmol) in THF (5 mL) was added dropwise. The reaction mixture was stirred at 0^{o}C under N_2 for 4 hours and at room temperature overnight. To the reaction mixture was added water (25 mL) and it was extracted with dichloromethane (50 mL x 3). The organic layers were combineded and evaporated. An attempt was made to purify the crude product by silica gel column chromatography eluted with dichloromethane : methanol (99:1); however, the desired product was not isolated.

6.23. Synthesis of methyl 6-(((2-hydroxyethyl)(methyl)amino)methyl)picolinate (28)

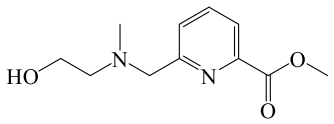

28

7 (3.84 g, 20.75 mmol) was dissolved in anhydrous acetonitrile (100 mL) and K_2CO_3 (1.44 g, 10.39 mmol) and 2-(methylamino)ethan-1-ol (2.37 g, 31.55 mmol) added. The reaction mixture was stirred at 70°C under N_2 overnight, then filtered and evaporated. The crude product was purified by silica gel column chromatography eluted with dichloromethane : methanol (9:1) to obtain the product **28** as yellow oil (1.95 g, 8.70 mmol, 42% yield)

^{1}H NMR ($CDCl_3$): δ 2.33 (s, 3H, CH_3); 2.63 – 2.66 (t, *J* = 4.36 Hz, 2H, CH_2N); 3.63 – 3.65 (t, *J* = 4.91 Hz, 2H, CH_2OH); 3.83 (s, 2H, CH_2N); 3.97 (s, 3H, CH_3); 7.57 - 7.59 (d, *J* = 7.95 Hz, 1H, CH); 7.79 - 7.82 (t, *J* = 7.74 Hz, 1H, CH); 7.99 - 8.01 (d, *J* = 7.32 Hz, 1H, CH).
^{13}C{^{1}H} NMR ($CDCl_3$): δ 42.56 (NCH_3); 53.01 (OCH_3); 58.95 (CH_2N); 59.03 (CH_2N); 63.22 (CH_2O); 123.82 (CH); 126.20 (CH); 137.64 (CH); 147.54 (CN); 159.87 (CN); 165.82 (CO).
ESI-MS(+): m/z 225.0 $[M+H]^+$ and 247.0 $[M+Na]^+$.

6.24. Synthesis of methyl 6-(((2-hydroxyethyl)(methyl)amino)methyl)picolinate (29)

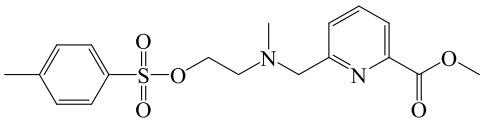

29

28 (1.94 g, 8.69 mmol) was dissolved in dichloromethane anhydrous (100 mL) and triethylamine (2.5 mL, 17.4 mmol) and $Me_3N.HCl$ (0.08 g, 0.08 mmol) added. The reaction mixture was stirred and cooled to 0°C. *p*-Toluenesulfonyl chloride (2.52 g, 13.24 mmol) was added in small portions. The reaction mixture was stirred under N_2 at 0°C for an hour and at room temperature for an hour. Then the reaction mixture was washed with water (100 mL x 3), 5% $NaHCO_3$ (100 mL, x 3) and 1 N HCl (100 mL x 3). The organic phase was dried over Mg_2SO_4, filtered and evaporated to give a yellow oil product (1.63 g, 4.32 mmol, 50% yield).

ESI-MS(+): m/z 379.0 $[M+H]^+$.

6.25. Attempted synthesis of tetramethyl 6,6',6'',6'''-((((1,4,7,10-tetraazacyclododecane-1,4,7,10-tetrayl)tetrakis(ethane-2,1-diyl))tetrakis(methylazanediyl))tetrakis(methylene))tetrapicolinate (30)

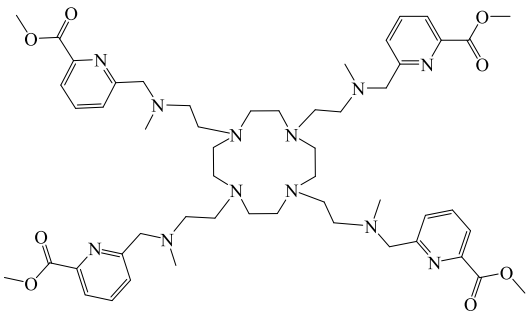

30

A mixture of 1,4,7,10-tetraazacyclododecane (0.11 g, 0.63 mmol) and Cs_2CO_3 (5.28 g, 16.19 mmol) was stirred in anhydrous acetonitrile (25 mL) under an Ar atmosphere. To the reaction mixture, **29** (1.82 g, 4.81 mmol) was added. The reaction mixture was heated to reflux under Ar atmosphere for 2 days. MS was used to analyse the reaction mixture. No product was detected (expected mass of 997.6 $[M+H]^+$ or 499.3 $[M+2H]^{2+}$). The peaks observed indicated the decomposition *p*-TsOH (m/z of 170.7 $[M-H]^-$) and **28** (m/z of 225.3 [**28**+H]$^+$).

6.26. Attempted synthesis of tetramethyl 6,6',6'',6'''-((((1,4,8,11-tetraazacyclotetra decane-1,4,8,11-tetrayl)tetrakis(ethane-2,1-diyl))tetrakis(methylazanediyl))tetrakis (methylene))tetrapicolinate (31)

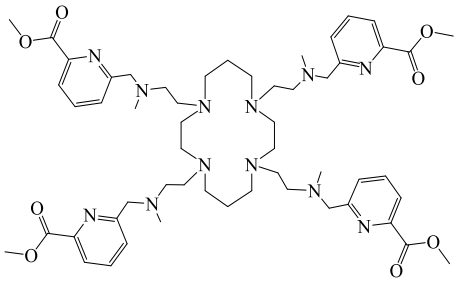

31

A mixture of 11,4,8,11-tetraazacyclotetradecane (0.12 g, 0.62 mmol) and Cs_2CO_3 (5.24 g, 16.07 mmol) was stirred in anhydrous acetonitrile (25 mL) under an Ar atmosphere. To the reaction mixture, **29** (1.82 g, 4.80 mmol) was added. The reaction mixture was heated to reflux under Ar atmosphere for 2 days. MS was used to analyse the reaction mixture. However, it indicated that the desired product was not generated. No product was detected (expected mass of 1025.6 $[M+H]^+$ or 513.3 $[M+2H]^{2+}$). Main peaks observed indicated 1-arm product (m/z of 407.1 $[1\text{-arm}+H]^+$ and the decomposition *p*-TsOH (m/z of 171.0 $[M-H]^-$).

6.27. Attempted synthesis of DOTA-4DFO (32)

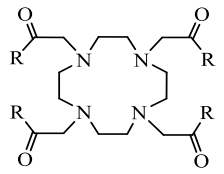

32

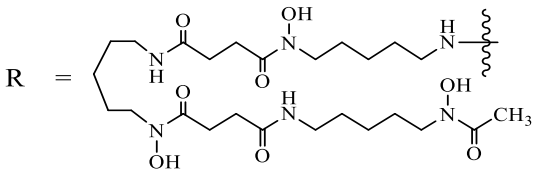

DOTA (0.036 g, 0.09 mmol) in anhydrous dichloromethane (3 mL) was stirred at 0°C under Ar for 10 min. To the reaction, $SOCl_2$ (0.3 mL, 4.1 mmol, 45 equiv.) was added dropwise while the reaction was maintained at 0°C. The reaction mixture was stirred at rt for 1 hour and evaporated and dried on a Schlenk line overnight. The crude compound was dissolved in anhydrous dichloromethane (5 mL) and DFO mesylate was added (0.26 g, 0.40 mmol, 4 equiv.) and DIPEA (159 µL, 0.90 mmol, 10 equiv.). The reaction was stirred at room temperature for 1 day and monitored by MS. However, the MS data indicated that the desired product was not generated. The peaks observed indicated starting materials DOTA (m/z of 405.6 $[DOTA+H]^+$) and DFO (m/z of 561.8 $[DFO+H]^+$).

6.28. Attempted synthesis of DOTA-4NHS ester (33)

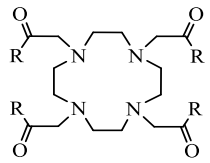

33

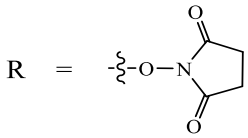

The mixture of DOTA (0.154 g, 0.38 mmol), N-hydroxysuccinimide (0.358 g, 3.11 mmol, 8.2 equiv.) and dicyclohexylcarbodiimide (0.664 g, 3.22 mmol 8.4 equiv.) in anhydrous DMF (10 mL) was stirred at room temperature under Ar for 4 days. MS was used to monitor the reaction; however, the MS data did not show peaks for the desired product. The peak observed indicated starting material DOTA (m/z of 405.5 $[DOTA+H]^+$).

6.29. Attempted synthesis of DOTA-DFO (21) by using DOTA as starting material

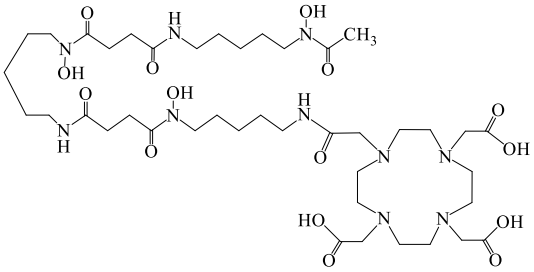

21

To a suspension of DOTA (0.100 g, 0.38 mmol) in anhydrous DMF (5 mL), HBTU (0.021 g, 0.06 mmol) and DIPEA (14 µL, 0.08 mmol) was added. The reaction mixture was stirred at room temperature under Ar atmosphere for 5 minutes. DFO mesylate (0.032 g, 0.05 mmol) was added to the reaction mixture following DIPEA (8 µL, 0.05 mmol). The reaction was stirred at room temperature under Ar overnight. MS was used to monitor the reaction; however, peaks were not observed for the desired product. The peak observed indicated starting material DOTA (m/z of 405.6 $[DOTA+H]^+$).

6.30. [^{89}Zr]Zr(IV) radiolabelling

6.30.1. [^{89}Zr]Zr(IV) radiolabelling of DFO

A solution of DFO in water was labelled with both [^{89}Zr]zirconium(IV) oxalate and [^{89}Zr]zirconium(IV) chloride and adjusted to pH 7 by using 0.5-1.0 M Cs_2CO_3 at room temperature for 30 minutes. Radiolabelling yield was analysed by radio-ITLC. The concentrations of DFO were varied in order to explore concentration effect on labelling yield.

Concentration of DFO (μM)	% Labelling yield (n=3)	
	[^{89}Zr]zirconium(IV) oxalate	[^{89}Zr]zirconium(IV) chloride
0.02	1.76 ± 0.53	19.94 ± 2.15
0.06	10.83 ± 1.00	21.38 ± 6.98
0.09	27.22 ± 1.30	36.10 ± 3.98
0.12	46.43 ± 13.16	39.90 ± 7.86
0.15	61.42 ± 3.59	48.60 ± 5.25
0.19	95.43 ± 1.19	48.71 ± 10.32
0.56	99.11 ± 0.45	53.71 ± 13.09
1.69	99.58 ± 0.20	93.28 ± 11.83
5.07	99.88 ± 0.10	99.66 ± 0.43

6.30.2. [^{89}Zr]Zr(IV) radiolabelling of 1,4,7,10-tetraazacyclododecane-1,4,7,10-tetra(methylenephosphonic acid) (DOTP) (1)

[^{89}Zr]zirconium(IV) oxalate- A solution of **1** (1 mg/mL, 10 µL) was labelled with [^{89}Zr]zirconium(IV) oxalate (3 MBq) in 1 M ammonium acetate buffer at pH 7 (total volume 110 µL), incubated at 95^{o}C for 2 hours. Radio-ITLC showed 5.01 ± 0.23% labelling yield.

[^{89}Zr]zirconium(IV) chloride - A solution of **1** (1 mg/mL, 10 µL) was labelled with [^{89}Zr]zirconium(IV) chloride (0.5 MBq) in water adjusted to pH 6 (total volume 110 µL), incubated at 95^{o}C for 2 hours. Radio-ITLC showed 7.49 ± 2.05% labelling yield.

6.30.3. [^{89}Zr]Zr(IV) radiolabelling of 1,4,7,10-tetraazacyclododecane-1,4,7,10-tetra[methyl(2-carboxyethyl)phosphinic acid] (DOTPI) (5)

[^{89}Zr]zirconium(IV) oxalate- A solution of the compound **5** (1 mg/mL, 10 µL) was labelled with [^{89}Zr]zirconium(IV) oxalate (3 MBq) in 1 M ammonium acetate buffer at pH 7 (total volume 110 µL), incubated at 95^{o}C for 2 hours. Radio-ITLC showed 6.11 ± 2.93% labelling yield.

[^{89}Zr]zirconium(IV) chloride- A solution of the compound **5** (1 mg/mL, 10 µL) was labelled with [^{89}Zr]zirconium(IV) chloride (0.5 MBq) in water adjusted to pH 6 (total volume 110 µL), incubated at 95^{o}C for 2 hours. Radio-ITLC showed 0% labelling.

6.30.4. [^{89}Zr]Zr(IV) radiolabelling of 6,6',6'',6'''-((1,4,7,10-tetraazacyclododecane-1,4,7,10-tetrayl) tetrakis(methylene))tetrapicolinic acid (9)

[^{89}Zr]zirconium(IV) oxalate- A solution of the compound **9** (1 mg/mL, 10 µL) was labelled with [^{89}Zr]zirconium(IV) oxalate (3 MBq) in 1 M ammonium acetate buffer at pH 7 (total volume 110 µL), incubated at 95^{o}C for 2 hours. Radio-ITLC showed 8.42 ± 0.23% labelling yield. The optimisation of radiolabelling of **9** was also tried with other solvents; 0.2 M ammonium acetate buffer at pH 4 or 7, water, and 0.1 M HCl.

Solvent	pH of the reaction	% Labelling yield
1 M acetate buffer	7	8.42 ± 0.23
Water	7	< 5
0.2 M acetate buffer	7	< 5
0.2 M acetate buffer	4	39.80 ± 4.20
0.1 M HCl	2	7.05 ± 0.29

[^{89}Zr]zirconium(IV) chloride- A solution of the compound **9** (1 mg/mL, 10 µL) was labelled with [^{89}Zr]zirconium(IV) chloride (0.5 MBq) in different solvents (total volume 110 µL), incubated at 95ºC for 2 hours.

Solvent	pH of the reaction	% Labelling yield
Water	6	22.3 ± 3.11
0.2 M acetate buffer	4	25.6 ± 1.10
0.2 M acetate buffer	5	22.4 ± 0.51
0.2 M acetate buffer	6	49.3 ± 3.42
0.2 M acetate buffer	7	42.8 ± 4.91

Concentration study

A solution of the compound **9** in 0.2 M ammonium acetate buffer at pH 6.0 was labelled with [^{89}Zr]zirconium(IV) chloride (0.5 MBq) with various concentrations in total volume 110 µL, incubated at 95ºC for 2 hours.

Concentration of **9** (µM)	% Labelling yield (n=3)
1.28	7.54 ± 1.00
6.68	12.49 ± 3.37
12.75	17.26 ± 5.43
33.43	42.93 ± 4.28
66.76	44.74 ± 1.88
133.33	49.28 ± 3.36
227.62	34.86 ± 8.79
334.29	30.89 ± 2.07
667.62	22.55 ± 0.16
1333.33	16.57 ± 1.57

6.30.5. [^{89}Zr]Zr(IV) radiolabelling of 6,6',6'',6'''-((((1,4,7,10-tetraazacyclododecane-1,4,7,10-tetrayl)tetrakis(propane-3,1-diyl))tetrakis(methylazanediyl))tetrakis (methylene)) tetrapicolinic acid (16)

A solution of the compound **16** in 0.2 M ammonium acetate buffer pH 6.0 was labelled with [^{89}Zr]zirconium(IV) chloride (0.5 MBq) with various concentrations in total volume 110 µL, incubated at 95^{o}C for 2 hours.

Concentration of **16** (µM)	% Labelling yield (n=3)
4.76	3.48 ± 0.59
9.52	13.14 ± 2.70
19.14	17.15 ± 5.02
38.19	28.00 ± 7.69
57.33	23.06 ± 1.28
76.38	20.72 ± 2.16
95.50	18.84 ± 1.71
167.14	12.71 ± 1.03
238.76	7.74 ± 1.27
477.52	3.27 ± 0.32

6.30.6. [^{89}Zr]Zr(IV) radiolabelling of 6,6',6'',6'''-((((1,4,8,11-tetraazacyclotetradecane-1,4,8,11-tetrayl)tetrakis(propane-3,1-diyl))tetrakis(methylazanediyl))tetrakis(methylene)) tetrapicolinic acid (20)

A solution of **20** in 0.2 M ammonium acetate buffer at pH 6.0 was labelled with [^{89}Zr]zirconium(IV) chloride (0.5 MBq) with various concentrations in total volume 110 µL, incubated at 95^{o}C for 2 hours.

Concentration of **20** (µM)	% Labelling yield (n=3)
4.64	5.29 ± 0.92
9.29	5.08 ± 2.28
18.58	10.87 ± 4.57
37.16	9.00 ± 7.27
55.73	14.90 ± 3.42
74.31	12.32 ± 2.25
92.89	13.23 ± 4.30
162.55	7.67 ± 2.45
233.22	5.12 ± 0.53
464.43	2.48 ± 0.10

6.30.7. [^{89}Zr]Zr(IV) radiolabelling of DOTA-DFO (21)

A solution of **21** in water was labelled with neutralised [^{89}Zr]zirconium(IV) oxalate and adjusted to pH 7 by using 0.5-1.0 M Cs_2CO_3 at room temperature. Radiolabelling yield was analysed by radio-ITLC at 30, 60 and 120 minutes. Various concentrations of DOTA-DFO were also studied.

Concentration of **21** (μM)	% Labelling yield (n=3)		
	At 30 min	At 60 min	At 120 min
0.01	2.18 ± 0.76	2.66 ± 1.69	3.66 ± 2.07
0.07	2.77 ± 0.42	2.82 ± 1.04	3.06 ± 0.15
0.34	11.19 ± 1.23	13.07 ± 1.58	20.29 ± 0.96
0.69	26.74 ± 1.77	33.12 ± 9.27	50.25 ± 12.28
3.43	76.03 ± 11.26	89.91 ± 4.23	97.57 ± 0.97
6.86	87.57 ± 4.77	97.25 ± 0.81	99.25 ± 0.24
17.16	97.95 ± 1.27	99.01 ± 0.34	99.23 ± 0.19
34.31	99.25 ± 0.09	99.43 ± 0.18	99.27 ± 0.10
51.47	99.26 ± 0.63	99.63 ± 0.31	99.48 ± 0.23

6.30.8. [^{89}Zr]Zr(IV) radiolabelling of DOTAGA-DFO (22)

As with **21**, **22** was radiolabelled with [^{89}Zr]zirconium(IV) oxalate adjusted to pH 7 using 0.5-1.0 M Cs_2CO_3 with the concentration of chelator from 0.033 to 49.042 µM. The reactions were performed at room temperature and analysed at the same time points.

Concentration of **22** (µM)	% Labelling yield (n=3)		
	At 30 min	At 60 min	At 120 min
0.03	2.06 ± 0.81	3.23 ± 1.42	3.89 ± 2.08
0.06	3.19 ± 1.57	3.02 ± 0.99	3.29 ± 0.16
0.33	5.59 ± 3.03	8.60 ± 5.13	8.52 ± 5.20
0.65	17.43 ± 0.33	27.00 ± 1.48	37.79 ± 4.89
3.27	46.06 ± 3.64	73.13 ± 5.61	90.06 ± 1.93
6.54	74.56 ± 11.26	90.05 ± 3.20	98.57 ± 0.13
16.35	97.01 ± 0.95	98.90 ± 0.12	99.48 ± 0.17
32.69	99.88 ± 0.12	99.62 ± 0.16	99.71 ± 0.12
49.04	99.72 ± 0.03	99.78 ± 0.24	99.78 ± 0.17

6.30.9. [^{89}Zr]Zr(IV) radiolabelling of NOTA-DFO (23)

Labelling of **23** was studied in a similar way as **21** and **22**. The compound was radiolabelled with a [^{89}Zr]zirconium(IV) oxalate solution adjusted to pH 7 by addition of 0.5-1.0 M Cs_2CO_3 with the concentration of chelator used in the range from 0.037 to 44.24 µM. The reactions were performed at room temperature and analysed at the same time points.

Concentration of **23** (µM)	% Labelling yield (n=3)		
	At 30 min	At 60 min	At 120 min
0.04	0.76 ± 0.93	2.59 ± 2.93	3.62 ± 1.36
0.07	2.97 ± 1.82	3.62 ± 1.04	4.37 ± 1.60
0.37	7.09 ± 1.48	11.14 ± 2.10	13.28 ± 8.26
0.74	14.31 ± 7.12	22.82 ± 6.28	23.15 ± 5.24
2.95	45.62 ± 7.11	62.33 ± 6.06	75.62 ± 6.76
5.90	68.16 ± 8.61	88.30 ± 4.43	91.47 ± 5.05
14.75	96.10 ± 5.80	99.21 ± 0.47	99.11 ± 0.25
25.81	98.38 ± 0.91	99.55 ± 0.38	99.35 ± 0.40
44.24	99.05 ± 0.81	99.63 ± 0.01	99.69 ± 0.12

6.30.10. Stability study

The compounds were labelled under the conditions below and then split into 20 µL aliquots for stability study experiments.

- DFO 1 mg/mL (5 µL, 5 µg, 0.0077 µmol) was labelled with [^{89}Zr]zirconium(IV) oxalate pH ~7 (31.2 MBq, 90 µL), adjusted to pH ~7 by 0.5 M Cs_2CO_3, total volume 200 µL, conc. 38.1 µM and incubated at rt for 2 hours.
- DOTA-DFO (**21**) 1 mg/mL (10 µL, 10 µg, 0.0068 µmol) was labelled with [^{89}Zr]zirconium(IV) oxalate pH ~7 (31.2 MBq, 90 µL), adjusted to pH ~7 by 0.5 M Cs_2CO_3, total volume 200 µL, conc. 34.3 µM and incubated at rt for 2 hours.
- DOTAGA-DFO (**22**) 1 mg/mL (11 µL, 11 µg, 0.0072 µmol) was labelled with [^{89}Zr]zirconium(IV) oxalate pH ~7 (31.5 MBq, 90 µL), adjusted to pH ~7 by 0.5 M Cs_2CO_3, total volume 200 µL, conc. 35.96 µM, and incubated at rt for 2 hours.
- NOTA-DFO (**23**) 1 mg/mL (9 µL, 9 µg, 0.0066 µmol) was labelled with [^{89}Zr]zirconium(IV) oxalate pH ~7 (31.3 MBq, 90 µL), adjusted to pH ~7 by 0.5 M Cs_2CO_3, total volume 200 µL, conc. 33.18 µM and incubated at rt for 2 hours.

6.30.10.1. EDTA stability challenge of the radiolabelled compounds

To each aliquot 1 mM EDTA at pH 7 (100 µL, 0.1 µmol) was added, the tube was incubated at 37ºC and analysed for the % remaining intact over 7 days.

EDTA 1/100 mol ratio	% intact			
Time (h)	[^{89}Zr]ZrDFO	[^{89}Zr]Zr**21**	[^{89}Zr]Zr**22**	[^{89}Zr]Zr**23**
1	99.28 ± 0.40	99.53 ± 0.12	99.51 ± 0.43	99.27 ± 0.21
6	99.25 ± 0.21	99.51 ± 0.25	99.43 ± 0.12	99.32 ± 0.11
24	99.26 ± 0.17	99.47 ± 0.31	99.25 ± 0.22	99.49 ± 0.30
48	97.85 ± 0.26	99.17 ± 0.02	97.70 ± 0.94	97.28 ± 0.82
72	95.79 ± 0.58	95.92 ± 0.18	93.83 ± 0.50	93.73 ± 0.69
96	93.35 ± 0.76	93.40 ± 0.37	92.87 ± 0.98	93.64 ± 0.23
120	92.11 ± 1.32	92.30 ± 0.39	92.06 ± 0.77	92.35 ± 1.63
144	92.07 ± 0.33	90.18 ± 0.74	90.81 ± 1.27	90.81 ± 0.21
168	92.01 ± 0.41	89.93 ± 0.29	90.17 ± 1.04	89.23 ± 1.54

6.30.10.2. Fetal bovine serum stability challenge of radiolabelled compounds

180 µL of fetal bovine serum was added to each aliquot and incubated at 37ºC. The reactions were analysed for the % remaining intact over 7 days.

Bovine serum 1/10 vol.	% intact			
Time (h)	[^{89}Zr]ZrDFO	[^{89}Zr]Zr**21**	[^{89}Zr]Zr**22**	[^{89}Zr]Zr**23**
1	99.50 ± 0.13	99.68 ± 0.14	99.36 ± 0.06	99.41 ± 0.23
6	99.36 ± 0.38	99.42 ± 0.38	99.46 ± 0.40	99.45 ± 0.18
24	99.24 ± 0.23	99.33 ± 0.46	99.25 ± 0.06	99.42 ± 0.31
48	99.28 ± 0.38	99.32 ± 0.44	99.41 ± 0.07	99.26 ± 0.01
72	99.36 ± 0.18	99.43 ± 0.08	99.20 ± 0.06	99.26 ± 0.23
96	99.20 ± 0.21	99.35 ± 0.16	99.26 ± 0.14	99.32 ± 0.38
120	99.26 ± 0.26	99.34 ± 0.20	99.22 ± 0.09	99.32 ± 0.16
144	99.21 ± 0.10	99.29 ± 0.03	99.06 ± 0.07	99.30 ± 0.11
168	99.37 ± 0.19	99.16 ± 0.12	99.09 ± 0.24	99.31 ± 0.03

6.30.10.3. Fe(III) ion competition

To 20 µL x 3 of each [^{89}Zr]ZrDFO and [^{89}Zr]Zr**21** was added a 30 fold excess of competing iron(III) ions (1 mM $FeCl_3$ solution in PBS (20 µL)) and the solution was incubated at 37ºC.

Time (h)	% intact	
	[^{89}Zr]ZrDFO	[^{89}Zr]Zr**21**
0	99.54 ± 0.50	99.75 ± 0.20
1	92.45 ± 0.67	87.22 ± 0.93
3	55.18 ± 8.61	48.72 ± 0.15
6	38.61 ± 1.67	27.00 ± 1.59
12	13.41 ± 2.06	10.27 ± 1.27
24	2.29 ± 0.79	2.15 ± 0.22
48	0.77 ± 0.32	0.54 ± 0.05
72	0.82 ± 0.51	0.44 ± 0.10
96	0.62 ± 0.29	0.37 ± 0.28

6.30.11. Log D pH 7.4

6 µL of [^{89}Zr]Zr(IV) compound was added to octanol (500 µL) and PBS (500 µL). The mixture was vortexed for 5 min and centrifuged for 5 min. The top layer (octanol) 100 µL and bottom layer (PBS) 5 µL were separated counted using the gamma counter.

Log D pH 7.4 = Log (count octanol layer/count PBS layer x 20)

[^{89}Zr]Zr(IV) compound	Log D pH 7.4
[^{89}Zr]ZrDFO	-0.52
[^{89}Zr]Zr**21**	-4.09
[^{89}Zr]Zr**22**	-3.96
[^{89}Zr]Zr**23**	-3.35

References

1. J. K. Willmann, N. van Bruggen, L. M. Dinkelborg and S. S. Gambhir, *Nat. Rev. Drug Discov.*, 2008, **7**, 591-607.
2. D.-E. Lee, H. Koo, I.-C. Sun, J. H. Ryu, K. Kim and I. C. Kwon, *Chem. Soc. Rev.*, 2012, **41**, 2656-2672.
3. L. W. Goldman, *J. Nucl. Med. Technol.*, 2007, **35**, 115-128.
4. D. J. Brenner and E. J. Hall, *New Engl. J. Med.*, 2007, **357**, 2277-2284.
5. Vijayalaxmi, M. Fatahi and O. Speck, *Mutat. Res. - Rev. Mutat. Res.*, 2015, **764**, 51-63.
6. B. Bybel, R. C. Brunken, F. P. DiFilippo, D. R. Neumann, G. Wu and M. D. Cerqueira, *Radiographics*, 2008, **28**, 1097-1113.
7. N. C. Gupta, D. J. Esterbrooks, D. E. Hilleman and S. M. Mohiuddin, *J. Am. Coll. Cardiol.*, 1992, **19**, 248-257.
8. I. Matsunari, G. Böning, S. I. Ziegler, I. Kosa, S. G. Nekolla, E. P. Ficaro and M. Schwaiger, *J. Nucl. Cardiol.*, 1998, **5**, 48-55.
9. M. J. Manyak, G. H. Hinkle, J. O. Olsen, R. P. Chiaccherini, A. W. Partin, S. Piantadosi, J. K. Burgers, J. H. Texter, C. E. Neal, J. A. Libertino, G. L. Wright Jr and R. T. Maguire, *Urology*, 1999, **54**, 1058-1063.
10. R. ter Heine, R. Lange, O. B. Breukels, H. J. Bloemendal, R. G. Rummenie, A. M. Wakker, H. de Graaf, F. J. Beekman, M. M. L. van der Westerlaken, M. M. Malingré, J. P. M. Wielders, L. van den Berg, N. H. Hendrikse and J. M. H. de Klerk, *Int. J. Pharm.*, 2014, **465**, 317-324.
11. D. L. Nosco and J. A. Beaty-Nosco, *Coord. Chem. Rev.*, 1999, **184**, 91-123.
12. S. Banerjee, M. R. Ambikalmajan Pillai and N. Ramamoorthy, *Semin. Nucl. Med.*, 2001, **31**, 260-277.
13. T. J. Wadas, E. H. Wong, G. R. Weisman and C. J. Anderson, *Chem. Rev.*, 2010, **110**, 2858-2902.
14. I. Verel, G. W. M. Visser and G. A. van Dongen, *J. Nucl. Med.*, 2005, **46**, 164S-171S.
15. S. Reddy and M. K. Robinson, *Semin. Nucl. Med.*, 2010, **40**, 182-189.
16. T. F. Massoud and S. S. Gambhir, *Genes Dev.*, 2003, **17**, 545-580.
17. T. Beyer, D. W. Townsend, T. Brun, P. E. Kinahan, M. Charron, R. Roddy, J. Jerin, J. Young, L. Byars and R. Nutt, *J. Nucl. Med.*, 2000, **41**, 1369-1379.
18. B. J. Pichler, H. F. Wehrl, A. Kolb and M. S. Judenhofer, *Semin. Nucl. Med.*, 2008, **38**, 199-208.
19. M. S. Judenhofer and S. R. Cherry, *Semin. Nucl. Med.*, 2013, **43**, 19-29.
20. K. Gariani, J. Gariani, G. Amzalag, B. M. A. Delattre, O. Ratib and V. Garibotto, *Obes. Res. Clin. Pract.*, 2015, **9**, 613-617.
21. J. A. K. Blokland, P. Trindev, M. P. M. Stokkel and E. K. J. Pauwels, *Eur. J. Radiol.*, 2002, **44**, 70-75.
22. E. L. Cole, M. N. Stewart, R. Littich, R. Hoareau and P. J. H. Scott, *Curr. Top. Med. Chem.*, 2014, **14**, 875-900.
23. J. S. Stehouwer and M. M. Goodman, *PET Clin.*, 2009, **4**, 101-128.
24. F. Rösch, *Curr Radiopharm.*, 2012, **5**, 202-211.
25. S. R. Banerjee and M. G. Pomper, *Appl. Radiat. Isot.*, 2013, **76**, 2-13.
26. E. W. Price and C. Orvig, *Chem. Soc. Rev.*, 2014, **43**, 260-290.
27. I. A. E. AGENCY, *Cyclotron Produced Radionuclides: Physical Characteristics and Production Methods*, INTERNATIONAL ATOMIC ENERGY AGENCY, Vienna, 2009.
28. M. Lubberink and H. Herzog, *Eur. J. Nucl. Med. Mol. Imag.*, 2011, **38**, 10-18.
29. Z. Li and P. S. Conti, *Adv. Drug Del. Rev.*, 2010, **62**, 1031-1051.
30. A. J. Amoroso, I. A. Fallis and S. J. A. Pope, *Coord. Chem. Rev.*, 2017, **340**, 198-219.
31. O. F. Ikotun and S. E. Lapi, *Future Med. Chem.*, 2011, **3**, 599-621.
32. B. M. Zeglis and J. S. Lewis, *Dalton Trans.*, 2011, **40**, 6168-6195.
33. H. G. Keen, B. A. Dekker, L. Disley, D. Hastings, S. Lyons, A. J. Reader, P. Ottewell, A. Watson and J. Zweit, *Nucl. Med. Biol.*, 2005, **32**, 395-402.

34. B. Dekker, H. Keen, D. Shaw, L. Disley, D. Hastings, J. Hadfield, A. Reader, D. Allan, P. Julyan, A. Watson and J. Zweit, *Nucl. Med. Biol.*, 2005, **32**, 403-413.
35. Z. K. Hohn A., Schaub E., Hirzel W., Schubiger P. A., Schibli R., *Q. J. Nucl. Med. Mol. Imaging*, 2008, **52**, 145-150.
36. A. L. M. Wooten, E.; Schweitzer, G. D.; Lawrence, L. A.; Mebrahtu, E.; Lewis, B. C.; Lapi, S. E., *Appli. Sci.*, 2013, **3**, 593-613.
37. T. Olafsen and A. M. Wu, *Semin. Nucl. Med.*, 2010, **40**, 167-181.
38. S. M. Knowles and A. M. Wu, *J. Clin. Oncol.*, 2012, **30**, 3884-3892.
39. D. E. Milenic, E. D. Brady and M. W. Brechbiel, *Nat. Rev. Drug Discov.*, 2004, **3**, 488-499.
40. K. E. McCabe and A. M. Wu, *Cancer Biother. Radiopharm.*, 2010, **25**, 253-261.
41. G. A. M. S. van Dongen, G. W. M. Visser, M. N. Lub-de Hooge, E. G. de Vries and L. R. Perk, *Oncologist*, 2007, **12**, 1379-1389.
42. Y. Z. Patt, L. M. Lamki, J. Shanken, J. M. Jessup, C. Charnsangavej, J. A. Ajani, B. Levin, B. Merchant, C. Halverson and J. L. Murray, *J. Clin. Oncol.*, 1990, **8**, 1246-1254.
43. R. Schoffelen, W. T. A. van der Graaf, R. M. Sharkey, G. M. Franssen, W. J. McBride, C.-H. Chang, D. L. Bos, D. M. Goldenberg, W. J. G. Oyen and O. C. Boerman, *J. Nucl. Med.*, 2012, **53**, 1926-1932.
44. H. Kim, T. R. Chaudhuri, D. J. Buchsbaum, D. Wang and K. R. Zinn, *Mol. Cancer Ther.*, 2007, **6**, 866-875.
45. M. D'Huyvetter, C. Xavier, V. Caveliers, T. Lahoutte, S. Muyldermans and N. Devoogdt, *Expert Opin. Drug Deliv.*, 2014, **11**, 1939-1954.
46. I. H. Song, T. S. Lee, K. I. Kim, Y. J. Lee, J. H. Kang, C. W. Choi and S. M. Lim, *J. Nucl. Med.*, 2014, **55**, 1091.
47. I. Verel, G. M. Visser, M. W. D. Vosjan, R. Finn, R. Boellaard and G. M. S. van Dongen, *Eur. J. Nucl. Med. Mol. Imag.*, 2004, **31**, 1645-1652.
48. S. Martin, R. O'Donnell, D. Kukis, C. Abbey, H. McKnight, J. Sutcliffe and J. Tuscano, *Mol. Imag. Biol.*, 2009, **11**, 79-87.
49. A. A. Shukla, L. S. Wolfe, S. S. Mostafa and C. Norman, *Bioeng. Transl. Med.*, 2017, **2**, 58-69.
50. L. E. Lamberts, S. P. Williams, A. G. T. T. v. Scheltinga, M. N. L.-d. Hooge, C. P. Schröder, J. A. Gietema, A. H. Brouwers and E. G. E. d. Vries, *J. Clin. Oncol.*, 2015, **33**, 1491-1504.
51. Y. H. Zhang, H.; Cai, W., *Curr Radiopharm.*, 2011, **4**, 131-139.
52. M. A. Deri, B. M. Zeglis, L. C. Francesconi and J. S. Lewis, *Nucl. Med. Biol.*, 2013, **40**, 3-14.
53. L. Lattuada, A. Barge, G. Cravotto, G. B. Giovenzana and L. Tei, *Chem. Soc. Rev.*, 2011, **40**, 3019-3049.
54. M. W. Brechbiel, *Q. J. Nucl. Med. Mol. Imaging*, 2008, **52**, 166-173.
55. T. J. Wadas, E. H. Wong, G. R. Weisman and C. J. Anderson, *Curr. Pharm. Des.*, 2007, **13**, 3-16.
56. S. Liu and D. S. Edwards, *Bioconjugate Chem.*, 2001, **12**, 7-34.
57. J. Seemann, B. P. Waldron, F. Roesch and D. Parker, *ChemMedChem*, 2015, **10**, 1019-1026.
58. L. F. Lindoy, *The Chemistry of Macrocyclic Ligand Complexes*, Cambridge University Press, 1990.
59. M. Jamous, U. Haberkorn and W. Mier, *Molecules*, 2013, **18**, 3379.
60. R. E. Mewis and S. J. Archibald, *Coord. Chem. Rev.*, 2010, **254**, 1686-1712.
61. R. Ferdani, D. J. Stigers, A. L. Fiamengo, L. Wei, B. T. Y. Li, J. A. Golen, A. L. Rheingold, G. R. Weisman, E. H. Wong and C. J. Anderson, *Dalton Trans.*, 2012, **41**, 1938-1950.
62. F. C. J. van de Watering, M. Rijpkema, L. Perk, U. Brinkmann, W. J. G. Oyen and O. C. Boerman, *Biomed. Res. Int.*, 2014, **2014**, 13.
63. G. Fischer, U. Seibold, R. Schirrmacher, B. Wängler and C. Wängler, *Molecules*, 2013, **18**, 6469-6490.
64. J. R. Osborne, D. A. Green, D. E. Spratt, S. Lyashchenko, S. B. Fareedy, B. D. Robinson, B. J. Beattie, M. Jain, J. S. Lewis, P. Christos, S. M. Larson, N. H. Bander and D. S. Scherr, *J. Urol.*, 2014, **191**, 1439-1445.
65. D. J. Vugts and G. A. M. S. van Dongen, *Drug Discov. Today Technol.*, 2011, **8**, e53-e61.
66. W. E. Meijs, H. J. Haisma, R. P. Klok, F. B. van Gog, E. Kievit, H. M. Pinedo and J. D. M. Herscheid, *J. Nucl. Med.*, 1997, **38**, 112-118.

67. I. Verel, G. W. M. Visser, R. Boellaard, M. Stigter-van Walsum, G. B. Snow and G. A. M. S. van Dongen, *J. Nucl. Med.*, 2003, **44**, 1271-1281.
68. I. Verel, G. W. M. Visser, R. Boellaard, O. C. Boerman, J. van Eerd, G. B. Snow, A. A. Lammertsma and G. A. M. S. van Dongen, *J. Nucl. Med.*, 2003, **44**, 1663-1670.
69. S. Bhattacharyya, K. Kurdziel, L. Wei, L. Riffle, G. Kaur, G. C. Hill, P. M. Jacobs, J. L. Tatum, J. H. Doroshow and J. D. Kalen, *Nucl. Med. Biol.*, 2013, **40**, 451-457.
70. J. N. Tinianow, H. S. Gill, A. Ogasawara, J. E. Flores, A. N. Vanderbilt, E. Luis, R. Vandlen, M. Darwish, J. R. Junutula, S.-P. Williams and J. Marik, *Nucl. Med. Biol.*, 2010, **37**, 289-297.
71. B. Baur, L. Miller, E. Andreolli, H. Machulla, S. Reske, M. Lindén and C. Solbach, *J. Nucl. Med.*, 2014, **55**, 1231.
72. L. Karmani, D. Labar, V. Valembois, V. Bouchat, P. G. Nagaswaran, A. Bol, J. Gillart, P. Levêque, C. Bouzin, D. Bonifazi, C. Michiels, O. Feron, V. Grégoire, S. Lucas, T. V. Borght and B. Gallez, *Contrast Media Mol. Imaging*, 2013, **8**, 402-408.
73. L. Miller, G. Winter, B. Baur, B. Witulla, C. Solbach, S. Reske and M. Linden, *Nanoscale*, 2014, **6**, 4928-4935.
74. C. Pérez-Medina, D. Abdel-Atti, J. Tang, Y. Zhao, Z. A. Fayad, J. S. Lewis, W. J. M. Mulder and T. Reiner, *Nat. Commun.*, 2016, **7**, 11838.
75. J. P. Holland, V. Divilov, N. H. Bander, P. M. Smith-Jones, S. M. Larson and J. S. Lewis, *J. Nucl. Med.*, 2010, **51**, 1293-1300.
76. T. H. Oude Munnink, M. A. d. Korte, W. B. Nagengast, H. Timmer-Bosscha, C. P. Schröder, J. R. d. Jong, G. A. M. S. v. Dongen, M. R. Jensen, C. Quadt, M. N. L.-d. Hooge and E. G. E. d. Vries, *Eur. J. Cancer*, 2010, **46**, 678-684.
77. T. K. G. Nayak, K.; Milenic, D. E.; Brechbiel, M. W., *J. Nucl. Med.*, 2012, **53**, 113-120.
78. F. Guerard, Y.-S. Lee, R. Tripier, L. P. Szajek, J. R. Deschamps and M. W. Brechbiel, *Chem. Commun.*, 2013, **49**, 1002-1004.
79. J. P. Holland and N. Vasdev, *Dalton Trans.*, 2014, **43**, 9872-9884.
80. W. E. Meijs, J. D. M. Herscheid, H. J. Haisma and H. M. Pinedo, *Int. J. Rad. Appl. Instrum. A*, 1992, **43**, 1443-1447.
81. F. Guérard, Y.-S. Lee and M. W. Brechbiel, *Chem. Eur. J.*, 2014, **20**, 5584-5591.
82. M. Patra, A. Bauman, C. Mari, C. A. Fischer, O. Blacque, D. Haussinger, G. Gasser and T. L. Mindt, *Chem. Commun.*, 2014, **50**, 11523-11525.
83. D. J. Vugts, C. Klaver, C. Sewing, A. J. Poot, K. Adamzek, S. Huegli, C. Mari, G. W. M. Visser, I. E. Valverde, G. Gasser, T. L. Mindt and G. A. M. S. van Dongen, *Eur. J. Nucl. Med. Mol. Imag.*, 2017, **44**, 286-295.
84. C. Zhai, D. Summer, C. Rangger, G. M. Franssen, P. Laverman, H. Haas, M. Petrik, R. Haubner and C. Decristoforo, *Mol. Pharm.*, 2015, **12**, 2142-2150.
85. S. E. Rudd, P. Roselt, C. Cullinane, R. J. Hicks and P. S. Donnelly, *Chem. Commun.*, 2016, **52**, 11889-11892.
86. J. Rousseau, Z. Zhang, G. M. Dias, C. Zhang, N. Colpo, F. Bénard and K.-S. Lin, *Bioorg. Med. Chem. Lett.*, 2017, **27**, 708-712.
87. E. Boros, J. P. Holland, N. Kenton, N. Rotile and P. Caravan, *ChemPlusChem*, 2016, **81**, 274-281.
88. M. A. Deri, S. Ponnala, B. M. Zeglis, G. Pohl, J. J. Dannenberg, J. S. Lewis and L. C. Francesconi, *J. Med. Chem.*, 2014, **57**, 4849-4860.
89. A. E. V. Gorden, J. Xu, K. N. Raymond and P. Durbin, *Chem. Rev.*, 2003, **103**, 4207-4282.
90. R. Burgada, T. Bailly, J. P. Noël, J. M. Gomis, A. Valleix, E. Ansoborlo, M. H. Hengé-Napoli, F. Paquet and P. Gourmelon, *J. Labelled Compd. Radiopharmaceut.*, 2001, **44**, 13-19.
91. B. P. Burke, J. Seemann and S. J. Archibald, *Chapter Seven - Advanced Chelator Design for Metal Complexes in Imaging Applications: Radiopharmaceuticals, Protein Targeting, and Conjugation*, Academic Press, 2016.
92. M. A. Deri, S. Ponnala, P. Kozlowski, B. P. Burton-Pye, H. T. Cicek, C. Hu, J. S. Lewis and L. C. Francesconi, *Bioconjugate Chem.*, 2015, **26**, 2579-2591.
93. J. N.Tinianow, D. N. Pandya, S. L. Pailloux, A. Ogasawara, A. N. Vanderbilt, H. S. Gill, S.-P. Williams, T. J. Wadas, D. Magda and J. Marik, *Theranostics*, 2016, **6**, 511-521.

94. M. T. Ma, L. K. Meszaros, B. M. Paterson, D. J. Berry, M. S. Cooper, Y. Ma, R. C. Hider and P. J. Blower, *Dalton Trans.*, 2015, **44**, 4884-4900.
95. C. Buchwalder, C. Rodriguez-Rodriguez, P. Schaffer, S. K. Karagiozov, K. Saatchi and U. O. Hafeli, *Dalton Trans.*, 2017, **46**, 9654-9663.
96. D. N. Pandya, S. Pailloux, D. Tatum, D. Magda and T. J. Wadas, *Chem. Commun.*, 2015, **51**, 2301-2303.
97. M. A. Deri, Ph.D. Dissertations & Theses, City University of New York, 2015.
98. E. W. Price, J. F. Cawthray, G. A. Bailey, C. L. Ferreira, E. Boros, M. J. Adam and C. Orvig, *J. Am. Chem. Soc.*, 2012, **134**, 8670-8683.
99. E. W. Price, B. M. Zeglis, J. S. Lewis, M. J. Adam and C. Orvig, *Dalton Trans.*, 2014, **43**, 119-131.
100. A. Chaudhary and E. Rawat, *Int. J. Inorg. Chem.*, 2014, **2014**, 30.
101. H. Braband, S. Imstepf, M. Benz, B. Spingler and R. Alberto, *Inorg. Chem.*, 2012, **51**, 4051-4057.
102. J. Šimeček, M. Schulz, J. Notni, J. Plutnar, V. Kubíček, J. Havlíčková and P. Hermann, *Inorg. Chem.*, 2012, **51**, 577-590.
103. B. P. Burke and S. J. Archibald, *Annu. Rep. Prog. Chem., Sect. A*, 2013, **109**, 232-253.
104. M. Gaspar, R. Grazina, A. Bodor, E. Farkas and M. Amelia Santos, *J. Chem. Soc., Dalton Trans.*, 1999, 799-806.
105. R. Laforest, S. E. Lapi, R. Oyama, R. Bose, A. Tabchy, B. V. Marquez-Nostra, J. Burkemper, B. D. Wright, J. Frye, S. Frye, B. A. Siegel and F. Dehdashti, *Mol. Imag. Biol.*, 2016, **18**, 952-959.
106. L. G. Alves, F. Hild, R. F. Munha, L. F. Veiros, S. Dagorne and A. M. Martins, *Dalton Trans.*, 2012, **41**, 14288-14298.
107. L. G. Alves, F. Madeira, R. F. Munha, S. Barroso, L. F. Veiros and A. M. Martins, *Dalton Trans.*, 2015, **44**, 1441-1455.
108. D. N. Pandya, N. Bhatt, H. Yuan, C. S. Day, B. M. Ehrmann, M. Wright, U. Bierbach and T. J. Wadas, *Chem. Sci.*, 2017, **8**, 2309-2314.
109. S. Heskamp, R. Raavé, O. Boerman, M. Rijpkema, V. Goncalves and F. Denat, *Bioconjugate Chem.*, 2017, **28**, 2211-2223.
110. E. W. Price, K. J. Edwards, K. E. Carnazza, S. D. Carlin, B. M. Zeglis, M. J. Adam, C. Orvig and J. S. Lewis, *Nucl. Med. Biol.*, 2016, **43**, 566-576.
111. J. Šimeček, P. Hermann, J. Havlíčková, E. Herdtweck, T. G. Kapp, N. Engelbogen, H. Kessler, H.-J. Wester and J. Notni, *Chem. Eur. J.*, 2013, **19**, 7748-7757.
112. A. Anichini, L. Fabbrizzi, P. Paoletti and R. Clay, *J. Chem. Soc., Chem. Commun.*, 1977, 244-245.
113. D. W. Swinkels, G. I. Tesser, J. P. M. van Duynhoven and C. W. Hilbers, *Recl. Trav. Chim. Pays-Bas*, 1991, **110**, 124-128.
114. A. Dean Sherry, C. F. G. C. Geraldes and W. P. Cacheris, *Inorg. Chim. Acta*, 1987, **139**, 137-139.
115. I. Lazar, D. C. Hrncir, W. D. Kim, G. E. Kiefer and A. D. Sherry, *Inorg. Chem.*, 1992, **31**, 4422-4424.
116. Z. Kotková, G. A. Pereira, K. Djanashvili, J. Kotek, J. Rudovský, P. Hermann, L. Vander Elst, R. N. Muller, C. F. G. C. Geraldes, I. Lukeš and J. A. Peters, *Eur. J. Inorg. Chem.*, 2009, **2009**, 119-136.
117. K. Bazakas and I. Lukes, *J. Chem. Soc., Dalton Trans.*, 1995, 1133-1137.
118. M. Försterová, Z. Jandurová, F. Marques, L. Gano, P. Lubal, J. Vaněk, P. Hermann and I. Santos, *J. Inorg. Biochem.*, 2008, **102**, 1531-1540.
119. J. L. W. Griffin, P. V. Coveney, A. Whiting and R. Davey, *J. Chem. Soc., Perkin Trans. 2*, 1999, 1973-1981.
120. X. Li, S. Zhang, P. Zhao, Z. Kovacs and A. D. Sherry, *Inorg. Chem.*, 2001, **40**, 6572-6579.
121. J. Notni, P. Hermann, J. Havlíčková, J. Kotek, V. Kubíček, J. Plutnar, N. Loktionova, P. J. Riss, F. Rösch and I. Lukeš, *Chem. Eur. J.*, 2010, **16**, 7174-7185.
122. J. Notni, K. Pohle and H.-J. Wester, *EJNMMI Res.*, 2012, **2**, 28.
123. J. Notni, J. Šimeček and H.-J. Wester, *ChemMedChem*, 2014, **9**, 1107-1115.

124. J. Simecek, H.-J. Wester and J. Notni, *Dalton Trans.*, 2012, **41**, 13803-13806.
125. J. Šimeček, O. Zemek, P. Hermann, H.-J. Wester and J. Notni, *ChemMedChem*, 2012, **7**, 1375-1378.
126. J. Notni, J. Šimeček, P. Hermann and H.-J. Wester, *Chem. Eur. J.*, 2011, **17**, 14718-14722.
127. J. Notni, K. Pohle and H.-J. Wester, *Nucl. Med. Biol.*, 2013, **40**, 33-41.
128. R. S. Grant, S. E. Coggan and G. A. Smythe, *Int. J. Tryptophan Res.*, 2009, **2**, 71-79.
129. Z. G. Aliev, L. O. Atovmyan, E. A. Saratovskikh, V. I. Krinichnii and V. G. Kartsev, *Bull. Acad. Sci. USSR, Div. Chem. Sci.*, 1988, **37**, 2246-2252.
130. E. W. Price, C. L. Ferreira, M. J. Adam and C. Orvig, *Can. J. Chem.*, 2014, **92**, 695-705.
131. E. Molnár, N. Camus, V. Patinec, G. A. Rolla, M. Botta, G. Tircsó, F. K. Kálmán, T. Fodor, R. Tripier and C. Platas-Iglesias, *Inorg. Chem.*, 2014, **53**, 5136-5149.
132. M. Steyn, H. G. Visser, A. Roodta and T. J. Muller, *Acta Crystallogr. E*, 2011, **E67**, m1240-m1241.
133. M. Mato-Iglesias, A. Roca-Sabio, Z. Palinkas, D. Esteban-Gomez, C. Platas-Iglesias, É. Tóth, A. De Blas and T. Rodríguez-Blas, *Inorg. Chem.*, 2008, **47**, 7840-7851.
134. S. Gracia, G. Arrachart, C. Marie, S. Chapron, M. Miguirditchian and S. Pellet-Rostaing, *Tetrahedron*, 2015, **71**, 5321-5336.
135. N. B. Bhatt, D. N. Pandya, J. Xu, D. Tatum, D. Magda and T. J. Wadas, *PLoS One*, 2017, **12**, e0178767.
136. T. J. Ferris, P. Charoenphun, L. K. Meszaros, G. E. D. Mullen, P. J. Blower and M. J. Went, *Dalton Trans.*, 2014, **43**, 14851-14857.
137. F. Guerard, M. Beyler, Y. S. Lee, R. Tripier, J. F. Gestin and M. W. Brechbiel, *Dalton Trans.*, 2017, **46**, 4749-4758.
138. M. Lin, U. Mukhopadhyay, G. J. Waligorski, J. A. Balatoni and C. González-Lepera, *Appl. Radiat. Isot.*, 2016, **107**, 317-322.
139. J. P. Holland, Y. Sheh and J. S. Lewis, *Nucl. Med. Biol.*, 2009, **36**, 729-739.
140. D. S. Abou, T. Ku and P. M. Smith-Jones, *Nucl. Med. Biol.*, 2011, **38**, 675-681.
141. A. Cohen and E. Schwartz, *J. Pediatr.*, 1978, **92**, 643-647.
142. W.-J. Zhang, H. Wei and B. Frei, *Exp. Biol. Med.*, 2010, **235**, 633-641.
143. A. Butler and R. M. Theisen, *Coord. Chem. Rev.*, 2010, **254**, 288-296.
144. M. Petrik, C. Zhai, H. Haas and C. Decristoforo, *Clin. Transl. Imaging.*, 2017, **5**, 15-27.
145. J. R. Pollack and J. B. Neilands, *Biochem. Biophys. Res. Commun.*, 1970, **38**, 989-992.
146. H.-P. Fiedler, P. Krastel, J. Müller, K. Gebhardt and A. Zeeck, *FEMS Microbiol. Lett.*, 2001, **196**, 147-151.
147. L. D. Loomis and K. N. Raymond, *Inorg. Chem.*, 1991, **30**, 906-911.
148. K. N. Raymond, E. A. Dertz and S. S. Kim, *Proc. Natl. Acad. Sci. U. S. A.*, 2003, **100**, 3584-3588.
149. M. A. Esteves, M. C. T. Vaz, M. L. S. S. Goncalves, E. Farkas and M. A. Santos, *J. Chem. Soc., Dalton Trans.*, 1995, 2565-2573.
150. P. Comba, U. Jermilova, C. Orvig, B. O. Patrick, C. F. Ramogida, K. Rück, C. Schneider and M. Starke, *Chem. Eur. J.*, 2017, **23**, 15945-15956.
151. M. Bonnaud, P. Fleurat-Lessard, G. W. Severin, A. T. I. Jensen, F. Boschetti and F. Denat, *Proceedings of European Molecular Imaging Meeting (EMIM)*, 2015.
152. K. Dhingra Verma, A. Mishra, J. Engelmann, M. Beyerlein, M. E. Maier and N. K. Logothetis, *ChemPlusChem*, 2012, **77**, 758-769.
153. V. Pavan Kumar, M. Somi Reddy, M. Narender, K. Surendra, Y. V. D. Nageswar and K. Rama Rao, *Tetrahedron Lett.*, 2006, **47**, 6393-6396.
154. M. Bodanszky and A. Bodanszky, *Protecting Groups*, Springer Berlin Heidelberg, Berlin, Heidelberg, 1984.
155. P. G. M. Wuts and T. W. Greene, *Protection for the Amino Group*, John Wiley & Sons, Inc., Hoboken, NJ, USA, 2006.
156. E. A. Papageorgiou, M. J. Gaunt, J.-q. Yu and J. B. Spencer, *Org. Lett.*, 2000, **2**, 1049-1051.
157. Z. Wang, *Bergmann-Zervas Peptide Synthesis*, John Wiley & Sons, Inc., 2010.
158. M. Bergmann and L. Zervas, *Ber. Dtsch. Chem. Ges.*, 1932, **65**, 1192-1201.
159. R. Ding, Y. He, X. Wang, J. Xu, Y. Chen, M. Feng and C. Qi, *Molecules*, 2011, **16**, 5665.

160. J. M. Van der Eijk, R. J. M. Nolte and J. W. Zwikker, *J. Org. Chem.*, 1980, **45**, 547-548.
161. G. W. Kabalka, M. Varma, R. S. Varma, P. C. Srivastava and F. F. Knapp, *J. Org. Chem.*, 1986, **51**, 2386-2388.
162. B. Das, V. S. Reddy and M. R. Reddy, *Tetrahedron Lett.*, 2004, **45**, 6717-6719.
163. M. C. Perry, X. Cui, M. T. Powell, D.-R. Hou, J. H. Reibenspies and K. Burgess, *J. Am. Chem. Soc.*, 2003, **125**, 113-123.
164. M. K. Pandey, A. P. Belanger, S. Wang and T. R. DeGrado, *J. Med. Chem.*, 2012, **55**, 10674-10684.
165. A. V. Dale, G. I. An, D. N. Pandya, Y. S. Ha, N. Bhatt, N. Soni, H. Lee, H. Ahn, S. Sarkar, W. Lee, P. T. Huynh, J. Y. Kim, M.-R. Gwon, S. H. Kim, J. G. Park, Y.-R. Yoon and J. Yoo, *Inorg. Chem.*, 2015, **54**, 8177-8186.
166. S. Brandes, S. Lacour, F. Denat, P. Pullumbi and R. Guilard, *J. Chem. Soc., Perkin Trans. 1*, 1998, 639-642.
167. J. O. Springborg, Carl Erik; Søtofte, Inger, *Acta Chem. Scand.*, 1995, **49**, 555-563.
168. A. Ingham, M. Rodopoulos, K. Coulter, T. Rodopoulos, S. Subramanian and A. McAuley, *Coord. Chem. Rev.*, 2002, **233**, 255-271.
169. A. Rodríguez-Rodríguez, D. Esteban-Gómez, A. de Blas, T. Rodríguez-Blas, M. Fekete, M. Botta, R. Tripier and C. Platas-Iglesias, *Inorg. Chem.*, 2012, **51**, 2509-2521.
170. A. M. Nonat, C. Gateau, P. H. Fries, L. Helm and M. Mazzanti, *Eur. J. Inorg. Chem.*, 2012, **2012**, 2049-2061.
171. C. Platas-Iglesias, M. Mato-Iglesias, K. Djanashvili, R. N. Muller, L. V. Elst, J. A. Peters, A. de Blas and T. Rodríguez-Blas, *Chem. Eur. J.*, 2004, **10**, 3579-3590.
172. N. Chatterton, C. Gateau, M. Mazzanti, J. Pecaut, A. Borel, L. Helm and A. Merbach, *Dalton Trans.*, 2005, 1129-1135.
173. E. Boros, C. L. Ferreira, J. F. Cawthray, E. W. Price, B. O. Patrick, D. W. Wester, M. J. Adam and C. Orvig, *J. Am. Chem. Soc.*, 2010, **132**, 15726-15733.
174. D. M. Weekes, C. F. Ramogida, M. d. G. Jaraquemada-Peláez, B. O. Patrick, C. Apte, T. I. Kostelnik, J. F. Cawthray, L. Murphy and C. Orvig, *Inorg. Chem.*, 2016, **55**, 12544-12558.
175. A. Nonat, P. H. Fries, J. Pécaut and M. Mazzanti, *Chem. Eur. J.*, 2007, **13**, 8489-8506.
176. T. Das, S. Chakraborty, P. R. Unni, S. Banerjee, G. Samuel, H. D. Sarma, M. Venkatesh and M. R. A. Pillai, *Appl. Radiat. Isot.*, 2002, **57**, 177-184.
177. B. Mathew, S. Chakraborty, T. Das, H. D. Sarma, S. Banerjee, G. Samuel, M. Venkatesh and M. R. A. Pillai, *Appl. Radiat. Isot.*, 2004, **60**, 635-642.
178. A. Egli, R. Alberto, L. Tannahill, R. Schibli, U. Abram, A. Schaffland, R. Waibel, D. Tourwé, L. Jeannin, K. Iterbeke and P. A. Schubiger, *J. Nucl. Med.*, 1999, **40**, 1913-1917.
179. W. Tieu, T. Lifa, A. Katsifis and R. Codd, *Inorg. Chem.*, 2017, **56**, 3719-3728.
180. D. L. White, P. W. Durbin, N. Jeung and K. N. Raymond, *J. Med. Chem.*, 1988, **31**, 11-18.
181. L. Allott, C. Da Pieve, J. Meyers, T. Spinks, D. M. Ciobota, G. Kramer-Marek and G. Smith, *Chem. Commun.*, 2017, **53**, 8529-8532.
182. C. J. Adams, J. J. Wilson and E. Boros, *Mol. Pharm.*, 2017, **14**, 2831-2842.
183. S. Banerjee, T. Das, S. Chakraborty, G. Samuel, A. Korde, S. Srivastava, M. Venkatesh and M. R. A. Pillai, *Nucl. Med. Biol.*, 2004, **31**, 753-759.
184. A. R. Jalilian, L. Mirsadeghi, R. Haji-Hosseini and A. Khorrami, *Radiochim. Acta*, 2008, **96**, 167-174.
185. S. Shirvani-Arani, A. Bahrami-Samani, A. R. Jalilian, A. Shirvani-Arani and M. Ghannadi-Maragheh, *J. Labelled Compd. Radiopharmaceut.*, 2012, **55**, 103-107.
186. C. A. G. N. Montalbetti and V. Falque, *Tetrahedron*, 2005, **61**, 10827-10852.
187. K.-L. Wei, C.-H. Wu, W.-H. Huang, J.-J. Lin and S. A. Dai, *Macromolecules*, 2006, **39**, 12-14.
188. L. M. De León-Rodríguez, S. Viswanathan and A. D. Sherry, *Contrast Media Mol. Imaging*, 2010, **5**, 121-125.
189. K.-P. Eisenwiener, P. Powell and H. R. Mäcke, *Bioorg. Med. Chem. Lett.*, 2000, **10**, 2133-2135.
190. V. Kubíček, J. Havlíčková, J. Kotek, G. Tircsó, P. Hermann, É. Tóth and I. Lukeš, *Inorg. Chem.*, 2010, **49**, 10960-10969.
191. A. Barge, L. Tei, D. Upadhyaya, F. Fedeli, L. Beltrami, R. Stefania, S. Aime and G. Cravotto, *Org. Biomol. Chem.*, 2008, **6**, 1176-1184.

192. M. Weineisen, M. Schottelius, J. Simecek, R. P. Baum, A. Yildiz, S. Beykan, H. R. Kulkarni, M. Lassmann, I. Klette, M. Eiber, M. Schwaiger and H.-J. Wester, *J. Nucl. Med.*, 2015, **56**, 1169-1176.
193. C. Bernhard, M. Moreau, D. Lhenry, C. Goze, F. Boschetti, Y. Rousselin, F. Brunotte and F. Denat, *Chem. Eur. J.*, 2012, **18**, 7834-7841.
194. Z. Wang, M. Zhang, L. Wang, S. Wang, F. Kang, G. Li, O. Jacobson, G. Niu, W. Yang, J. Wang and X. Chen, *Theranostics*, 2015, **5**, 882-889.
195. I. Aljammaz, B. Al-Otaibi, N. Al-Hokbany, S. Amer and S. Okarvi, *Anticancer Res.*, 2014, **34**, 6547-6556.
196. E. Ranyuk, R. Lebel, Y. Bérubé-Lauzière, K. Klarskov, R. Lecomte, J. E. van Lier and B. Guérin, *Bioconjugate Chem.*, 2013, **24**, 1624-1633.
197. W. Mier, J. Hoffend, S. Krämer, J. Schuhmacher, W. E. Hull, M. Eisenhut and U. Haberkorn, *Bioconjugate Chem.*, 2005, **16**, 237-240.
198. D. J. Berry, Y. Ma, J. R. Ballinger, R. Tavare, A. Koers, K. Sunassee, T. Zhou, S. Nawaz, G. E. D. Mullen, R. C. Hider and P. J. Blower, *Chem. Commun.*, 2011, **47**, 7068-7070.
199. C. L. Ferreira, E. Lamsa, M. Woods, Y. Duan, P. Fernando, C. Bensimon, M. Kordos, K. Guenther, P. Jurek and G. E. Kiefer, *Bioconjugate Chem.*, 2010, **21**, 531-536.
200. D. B. G. Williams and M. Lawton, *J. Org. Chem.*, 2010, **75**, 8351-8354.
201. L. M. P. Lima, Z. Halime, R. Marion, N. Camus, R. Delgado, C. Platas-Iglesias and R. Tripier, *Inorg. Chem.*, 2014, **53**, 5269-5279.

Appendix

A. HPLC of the compound 9

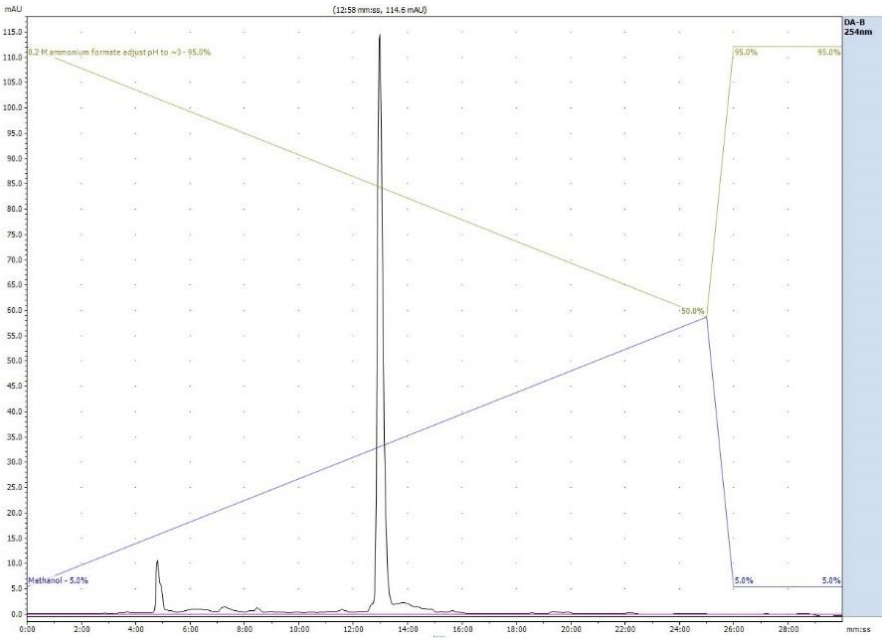

B. HPLC of the compound 16

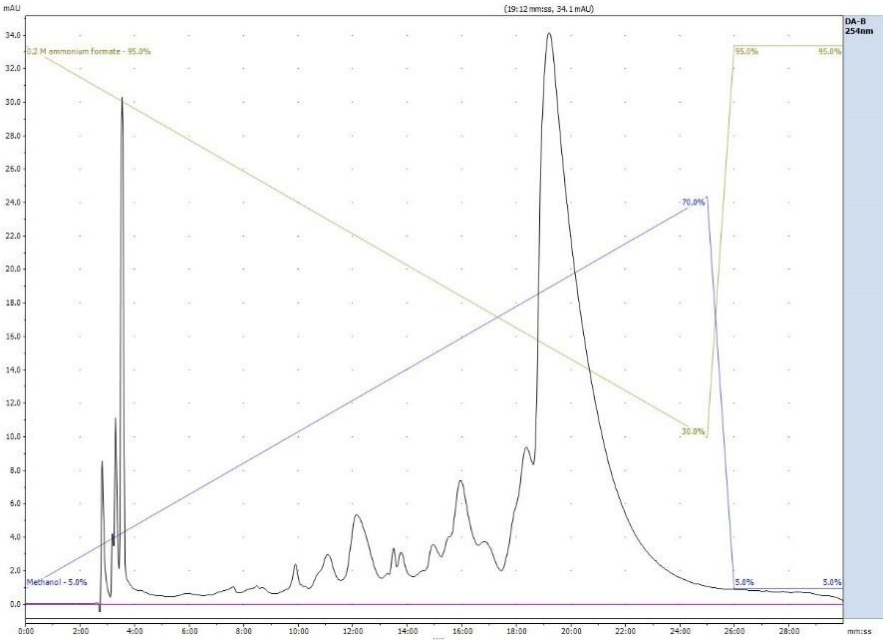

C. HPLC of the compound 20

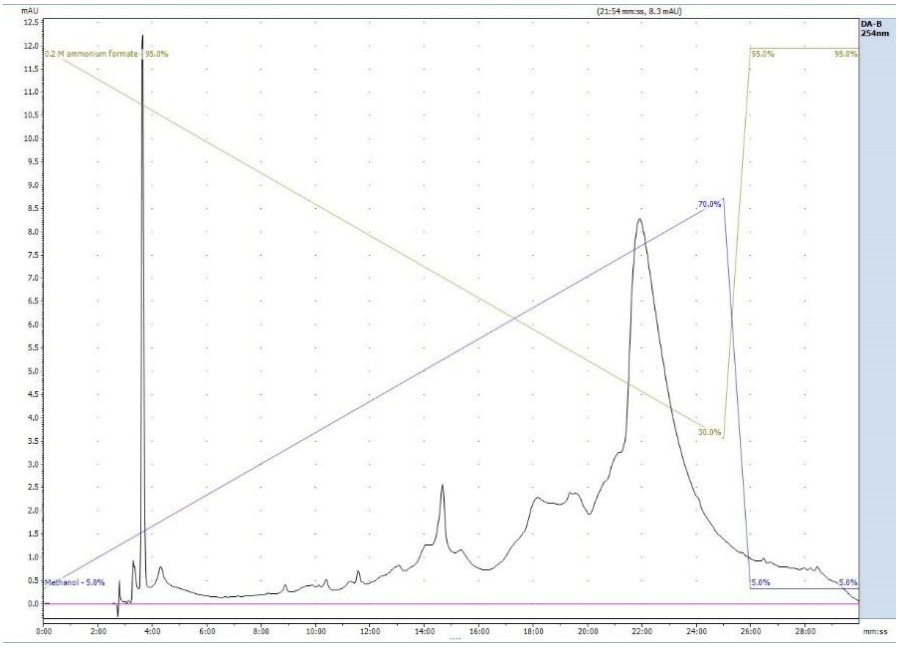

D. HPLC of the compound 21

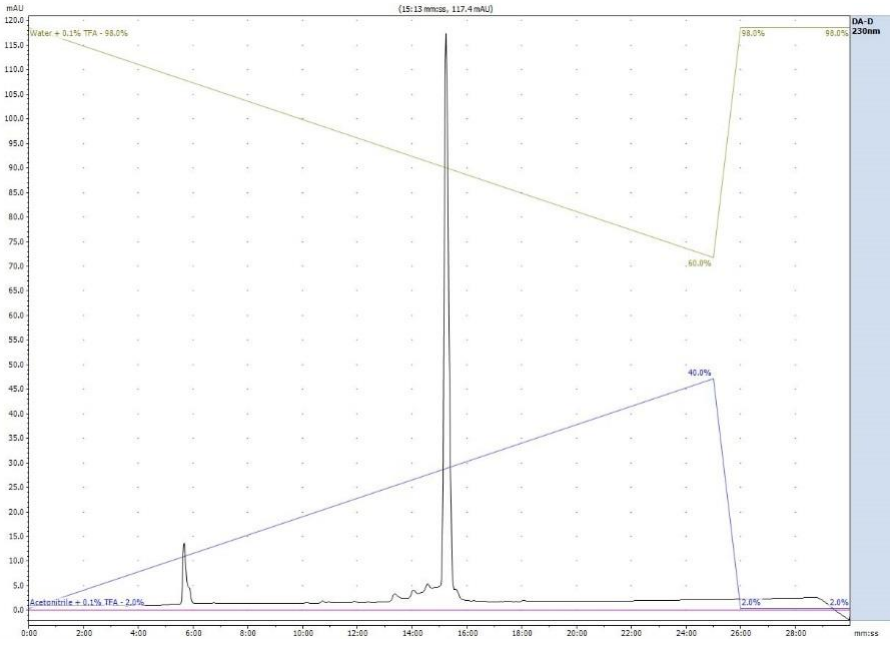

E. HPLC of the compound 22

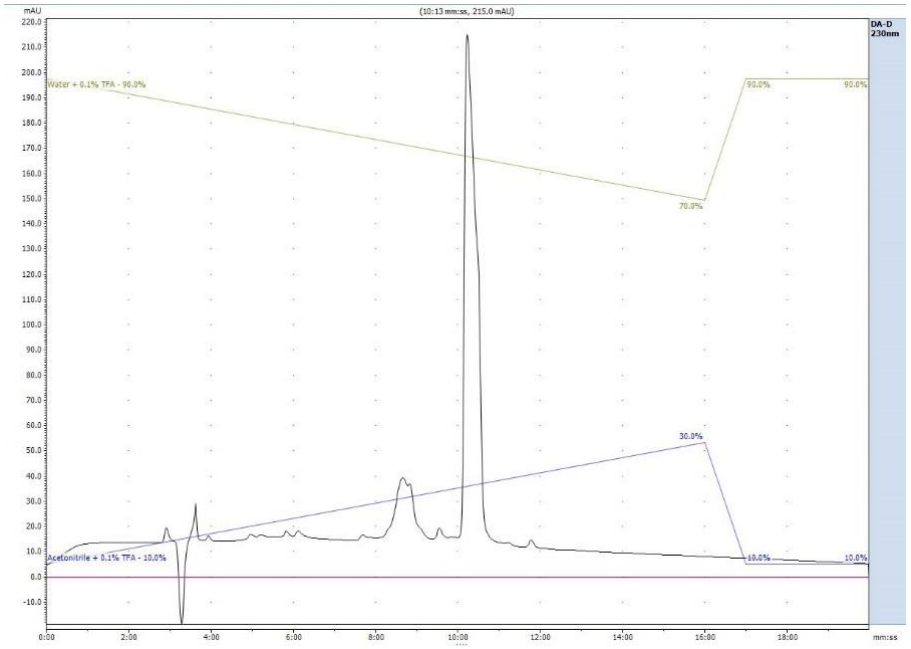

F. HPLC of the compound 23